THE

LONDON, EDINBURGH, AND DUBLIN

PHILOSOPHICAL MAGAZINE

AND

JOURNAL OF SCIENCE.

[SEVENTH SERIES.]

MAY 1935.

LXXI. *Factors influencing the Cataphoresis of Small Particles in Water.* *By* C. L. S. GILFORD, *B.Sc.**

1. *Introduction.*

THE first theoretical explanation of the electro-kinetic and electro-capillary phenomena was given by Helmholtz[1], who showed that both could be explained if it were assumed that a double layer of electricity existed at the boundary between the two substances involved. Considering the case of endosmosis in a uniform cylindrical capillary, he arrived at the following equation :

$$v = \frac{\zeta \mathrm{HD}}{4\pi\eta},$$

where

ζ = P.D. between the layers,
H = electric field,
D = dielectric constant,
η = viscosity of the water,

and he argued further that the cataphoretic velocity of a suspended particle should also be given by this expression (with the sign reversed), irrespective of its size or shape. The value of ζ can only be determined

* Communicated by Prof. J. A. Crowther, M.A., Sc.D., F.Inst.P. Thesis presented for the Degree of M.Sc. in the University of Reading.

by calculation from measurements of these phenomena, but all the other factors in the equation may be studied independently. As a result of experiments by many workers this equation has been found to be inadequate. Mooney[2] and McTaggart[3] have verified the relationship with H, Freundlich[4] with η, on the assumption that small changes in temperature do not affect the other variables appreciably, and Smoluchowski has pointed out that the insertion of the dielectric constant D, gives values of ζ comparable with the Nernst P.D. usually denoted by ϵ, even though it was generally considered that such an essentially macroscopic constant could not be used where thicknesses of water of the order of a few hundred molecular diameters were being considered.

It is, however, in experiments on the variation of velocity with shape and size that we meet with divergences from the Helmholtz equation. Alty[6], working with air-bubbles in water, and Mooney[7], using oil-drops, both found appreciable variations of velocity with diameter, whereas according to Helmholtz's theory, there should be no variation of velocity with size, provided that the value of ζ is constant.

The theory of Helmholtz was later modified by the work of Debye and Hückel[8], [9]. Assuming that the presence of the particle had no effect on the direction of the electric field in the immediate neighbourhood, they found that, although $v = \frac{1}{4\pi} \frac{\zeta HD}{\eta}$ was correct for endosmosis in a cylindrical tube or the cataphoresis of a cylindrical particle, in the case of a sphere the constant $\frac{1}{4\pi}$ should be replaced by $\frac{1}{6\pi}$.

Henry[10] pointed out that the assumption that the external field is unaffected by the presence of the particle is only justified when the conductivities of the two media are equal. He gave the full theory of the effect, taking general values, μ, μ', for the conductivities of the particle and liquid respectively, and treated in particular the cases of a sphere and of an infinite cylinder with its axis parallel to and at right angles to the electric field. The values of the constant factor in particular cases are given below :

	$\mu<<\mu'$.	$\mu=\mu'$.	$\mu>>\mu'$.
(1) Cylinder (lengthwise)..	$\frac{1}{4\pi}$	$\frac{1}{4\pi}$	$\frac{1}{4\pi}$
(2) Sphere	$\frac{1}{4\pi}$	$\frac{1}{6\pi}$	0
(3) Cylinder (transverse)..	$\frac{1}{4\pi}$	$\frac{1}{8\pi}$	0

The first vertical column corresponds to Helmholtz's assumptions, the second to those of Debye and Hückel. In the third column we have a conducting particle in an insulating medium. The surface of the particle will be an equipotential, and the lines of force will enter it perpendicularly at all points. The cataphoretic velocity will therefore be zero, except in the case of the cylinder (1), where there is theoretically no flow of electric current between liquid and particle.

This paper describes experiments to examine the various special cases for which the constant factors have been arrived at theoretically, and to discriminate between the sets of assumptions involved.

2. *Apparatus* (fig. 1).

The cell used consisted of an uniform cylindrical glass tube 35 cm. long and about 1·3 cm. internal diameter. At about its mid-point a flat was ground, using a fine carborundum wheel, and a hole about $1\frac{1}{2}$ mm. in diameter was bored in the centre of this flat. The grinding was then continued until the boundaries of the hole were less than 0·2 mm. thick, and a small cover-slip window was then cemented over the hole, using black cellulose enamel as the cement. The tube was supported inside a thin-walled brass tube. Accurate location was ensured by waxing to the upper end of the glass cell a brass ring of the same diameter as the inside of the brass tube, carrying a pin which engaged with a V-notch on the latter. The lower end of the brass tube carried three adjusting screws by which its axis could be made to coincide with that of the glass cell. The brass tube was carried on supports which allowed movements and rotations in all directions, and mounted inside a thermostat. This was a double-walled structure of sheet metal. It was provided with a door in the front, also double-

walled, and water was circulated through both door and case by means of a small centrifugal pump contained in a separate compartment which also contained a heating coil. A thermo-regulator utilizing the expansion of benzene, with mercury contacts, was placed in the water

Fig. 1.

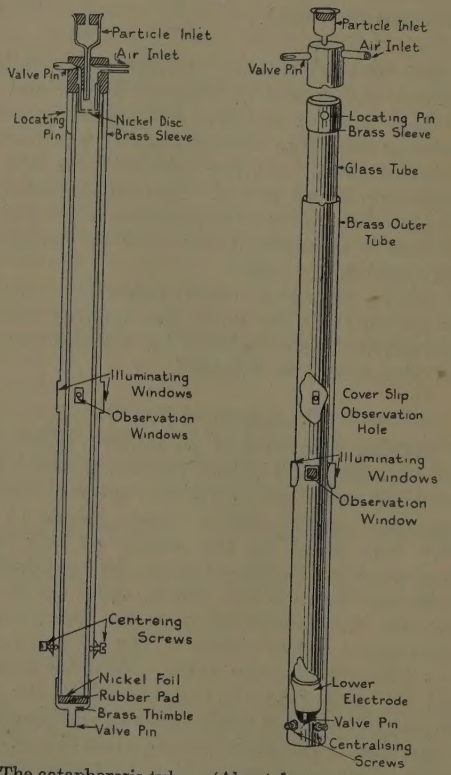

The cataphoresis tube. (About ½ natural size.)

in the double-walled case, and, in conjunction with an Isenthal relay, provided temperature-control to 1/20° C. A sensitive thermometer was used for temperature measurements.

The electrodes were of nickel. The lower end of the cell was ground square and closed by its electrode.

This comprised a piece of nickel foil compressed between the ground face and a rubber disk inside a brass thimble which was waxed on to the tube. A tongue of foil was bent round the rubber and made contact with the outer thimble, which was provided with a valve-pin. The upper electrode was pierced by three holes, at the centre, and at two positions in line with the tube window and distant $\frac{r}{\sqrt{2}}$ from the axis. The electrode contained a hollow space for the introduction of particles in suspension, and an arrangement of tubes allowed pure air to be bubbled past the suspension during introduction in order to prevent contamination by carbon dioxide.

Illumination was effected by a 100-watt lamp and a simple lens system through glass windows cemented into the sides of the thermostat case. A small mirror mounted on the tube-supports provided back-illumination when required, but for most of the work the particles were illuminated transversely. A grid of fine scratches was made on the tube opposite to the cover-slip window, which enabled the tube to be aligned with accuracy.

A hole cut in the door permitted the introduction of the objective of a travelling microscope. Distances parallel to the axis of the cell were measured by means of a vertical eyepiece scale, and distances from the axis were measured by means of the traverse scale (moving in a direction parallel to the line joining the window to the axis of the cell).

The cell was connected in series with the 200-volt D.C. mains and a moving-coil galvanometer. A reversing key enabled the field to be applied in either direction, and a voltmeter was connected across the cell for measurements of the total potential difference. All voltage measurements were reduced by the amount of the back-E.M.F., approximately $1\frac{1}{2}$ volts. This arrangement enabled the conductivity of the suspension to be measured at frequent intervals during the progress of the experiment. A still of the type described by Bourdillon[11] was used for preparing the conductivity water used throughout.

3. *Experimental Procedure.*

After filling with the suspension to be used, the tube was accurately lined up and the thermostat door finally

closed. The system was then left for a few hours to attain a steady state.

The microscope was then focussed on the front of the tube window and the traverse scale read ; if the microscope was now screwed forward until the reading of the scale had increased by an amount equal to the apparent distance, with water in the tube, of the axis from the window, then the microscope would be set to observe particles at the axis of the tube. This apparent distance was known from calculation, and also from direct measurements on the full tube.

The microscope was then advanced from its position with the window at the focal plane to any convenient distance in the direction of the tube. When a particle appeared in a suitable part of the field of view, the current through the tube was switched on. The time taken by the particle to traverse one or two large divisions of the eyepiece scale was measured, using a 1/10th sec. stop-watch, with the current first in one direction and then in the other. Since for most of the substances used the velocity was not quite independent of the size of the particle, observations were confined to those having a diameter of approximately half a scale-division (about $1{\cdot}57\times10^{-3}$ cm.).

Since the velocity is closely proportional to the force on a particle, the velocities in the two cases will be

$$V_A = V_x + V_g + u,$$
$$V_B = -V_x + V_g + u,$$

and hence

$$V_x = \tfrac{1}{2}(V_A - V_B),$$

where V_A and V_B are the observed velocities, V_x is the required component due to the electric field, and u the constant speed due to gravity and to convection and other currents in the tube.

The calculated values of V_x were plotted for every particle observed against the square of its distance from the axis of the tube.

4. *The Theory of the Cylindrical Tube.*

The velocity of a particle at any point in the tube is the sum of the following components :—

(1) Velocities due to gravity, convection currents, etc. : which are eliminated in the experiments as described in the last section.

(2) The cataphoretic velocity of the particle.

(3) The velocity of return flow of the surrounding liquid, due to endosmosis at the walls of the tube.

The flow of liquid being necessarily symmetrical about the axis, we may write down the condition for steady flow of a coaxial hollow cylinder of liquid, thus :

$$\frac{d^2y}{dr^2} = \frac{1}{\eta}\left(\frac{dp}{dl}\right),$$

where r is the radius of the cylindrical shell, y its velocity, η the viscosity, and $\frac{dp}{dl}$ the longitudinal pressure gradient in the tube.

On integrating this equation, and inserting the correct integration constants at both stages, we have

$$Y = V + E\left(1 - \frac{2r^2}{R^2}\right),$$

where Y is the actual velocity of the particle due to (2) and (3), V is its cataphoretic velocity, and E is the velocity of endosmosis at the walls of the tube. R is the internal radius of the cell.

It will be noticed that where r is equal to $R/\sqrt{2}$, $Y = V$, *i. e.*, there is no component due to (3).

Now

$$r^2 = \frac{R^2}{2E}(E + V - Y),$$

which is of the form

$$r^2 = k(A - Y),$$

where A is the sum of the cataphoretic and endosmotic velocities. If, therefore, Y be plotted against r^2, the result should be a straight line intercepting the Y-axis at a value of Y equal to A, *i. e.*, the sum of the endosmosis and the cataphoresis, and meeting the line $2r^2 = R^2$ at a value of Y equal to the cataphoretic velocity.

This is confirmed by most of the curves obtained, of which fig. 2 is an example.

5. *The Importance of considering Endosmosis in the Cylindrical Tube.*

Several experimenters have assumed that for velocity determinations taking only a short time it is unnecessary to take endosmosis into account for particles far from the walls of the tube, since, they argue, a considerable time is likely to elapse before these particles are affected by

Fig. 2.

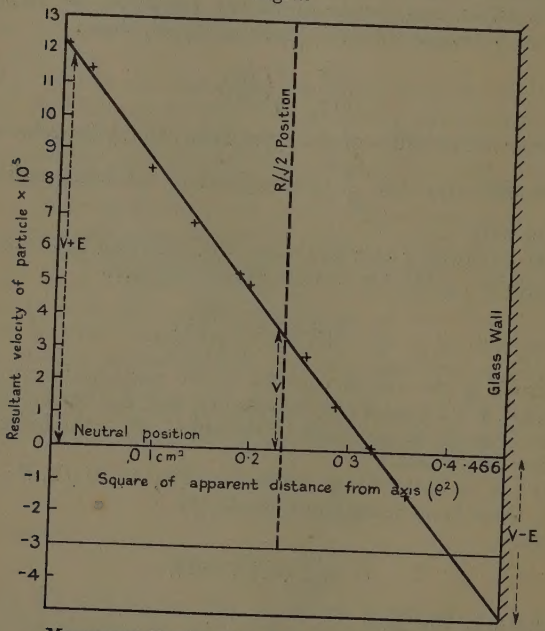

Manganese dioxide 25° C. $3{\cdot}53 \times 10^{-6}$ conductivity.
Normal relation between velocity and axial distance.

the movements of masses of liquid near to the walls of the tube. This is not, however, borne out by experiments which I made with the object of testing this point, and which indicate that this interval of time is very small indeed. Working with a tube of 1·3 cm. diameter, the speed of the particles was observed to change as the effects of endosmosis made themselves felt; but the speed was

invariably observed to reach a constant value within a few seconds of the current being started or reversed. That this constant velocity is compounded of cataphoresis and endosmosis is amply evident from the slope of the line shown in fig. 2, and from the agreement to be seen later with the expected behaviour when systematic errors arise (figs. 4 and 5).

Thus the U-tube method of Burton[14], and its developments by Lachs and Gestel[15] and others, must be regarded with caution, though it is true that in these experiments results were obtained which agree closely with the results of other methods.

Fig. 3.

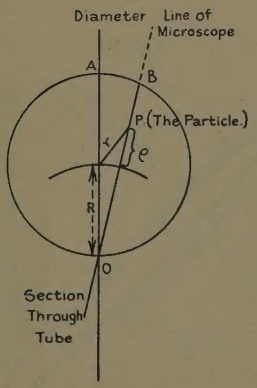

6. *Error in Alignment* (fig. 3).

Several systematic errors alter the simple form of the curve in fig. 2.

(1) Error in alignment :—

Let θ be the angle AOB, ρ the assumed distance from the axis, r=the real distance. Then

$$OP = R + \rho.$$

The equation for the velocity is

$$r^2 = k(A - y).$$

Now
$$\begin{aligned} r^2 &= (R+\rho)^2 + R^2 - 2R(R+\rho)\cos\theta \\ &= \rho^2 + 2R(R+\rho)(1-\cos\theta) \\ &= \rho^2 + R\theta^2(R+\rho), \end{aligned}$$

neglecting $\theta^4/4$!. Whence

$$y=A-\frac{1}{k}\{\rho^2+R\theta^2(R+\rho)\}.$$

Now, where $\rho=0$,

$$y=A-\frac{R^2\theta^2}{k};$$

then

$$\frac{dy}{d(\rho^2)}=\frac{1}{2\rho}\cdot\frac{dy}{d\rho}=\frac{1}{k}\left(1\pm\frac{R\theta^2}{2\rho}\right).$$

Suppose, now, that ρ^2 has a small value, h; then

$$\frac{dy}{d(\rho^2)}=\pm\frac{R\theta^2}{2k\sqrt{h}}, \text{ i.e., } \propto \frac{1}{h}.$$

Fig. 4.

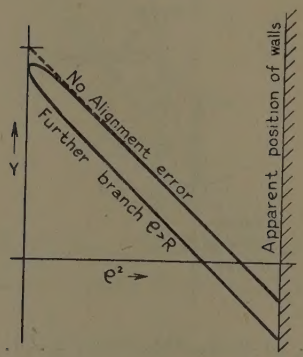

Alignment error.

Integrating, $y=\pm\log\rho^2+$constant. Thus the curve is of the form shown in fig. 4. Fig. 5 is an example of this type. True values of the cataphoresis and endosmosis may be obtained from such a curve by consideration of the ideal line from which it is a departure.

7. *Error in calculating the Position of the Axis.*

With the notation of the last section, let $\rho=r-\delta$, where δ is a small error. Then the equation of the tube is

$$(r+\delta)^2=k(A-y).$$

The gradient of the curve at any point is

$$\frac{dy}{d\delta^2} = -\frac{1}{k}\left(1 \pm \frac{\delta}{\rho}\right).$$

Thus the curve produced is of a similar type to the alignment-error curve, but lies partly above the ideal coincident pair of straight lines, and partly below.

Fig. 5.

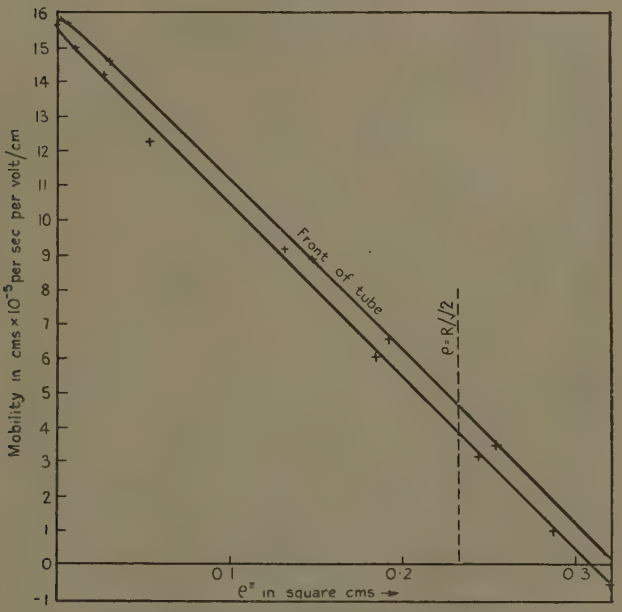

Antimony 18·5° C. $1{\cdot}25 \times 10^{-6}$ conductivity.
Relation distorted by incorrect alignment.

8. *The Effect of the Window.*

The plane window used for observing the particles also causes a slight error in two ways :—

(*a*) By accumulation of small quantities of foreign substance round its edges.

(*b*) By a local increase in the value of the radius of the tube.

These two effects, taken together, produce curves such as that shown in fig. 6. With this type of curve it is the straight branch (back of the tube) which is used in calculating the mobilities.

Fig. 6.

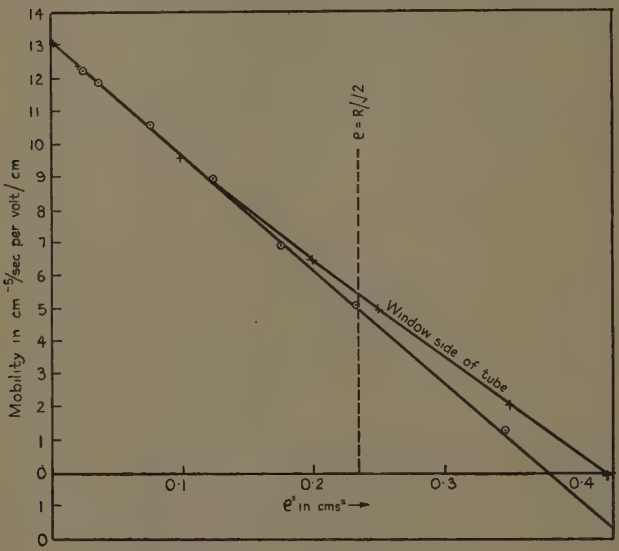

Sugar carbon 21·7° C., $1{\cdot}38 \times 10^{-6}$ ohm^{-1} cm.$^{-1}$.
Relation distorted by the effect of the window.

9. *The Variation of Velocity with Temperature.*

It has already been noted (section 1) that Freundlich has quoted results showing that electro-kinetic velocities only vary with temperature in so far as the viscosity of the liquid phase varies. Some experiments were made to verify this in order to make sure that, within the range of temperature covered by these experiments, results at different temperatures could be compared directly, merely by multiplying the velocities by the viscosities corresponding to the respective temperatures at which the velocity determinations were made.

The method of experiment was to determine the value of the endosmosis of the glass tube at two different

temperatures, the conductivity remaining constant as far as possible. The unavoidable differences in conductivity were corrected for by interpolation from results at different conductivities at the standard temperature, 15° C. The results are shown in the following table :—

Set.	Quantity.	Conductivity in 10^{-6} cm.$^{-1}$ ohm^{-1}.	Temperature, °C.	Viscosity, η.	Velocity, v.	$\eta \times v$.
1.	Endosmosis of glass.	4·35	15·0	·01142	$6{\cdot}65 \times 10^{-5}$	$7{\cdot}59 \times 10^{-7}$
			22·7	·00943	$8{\cdot}2 \times 10^{-5}$	$7{\cdot}73 \times 10^{-7}$
2.	Endosmosis of glass.	1·34	15·0	·01142	$5{\cdot}05 \times 10^{-5}$	$5{\cdot}76 \times 10^{-7}$
			17·3	·1076	$5{\cdot}35 \times 10^{-5}$	$5{\cdot}77 \times 10^{-7}$
3.	Endosmosis of glass.	3·53	15·0	·01142	$7{\cdot}2 \times 10^{-5}$	$8{\cdot}2_3 \times 10^{-7}$
			25·0	·00893	$9{\cdot}0 \times 10^{-5}$	$8{\cdot}0_4 \times 10^{-7}$
4.	From Freundlich ...		11·0	·01282	$19{\cdot}6 \times 10^{-5}$	$25{\cdot}1 \times 10^{-7}$
			21·0	·00992	$25{\cdot}2 \times 10^{-5}$	$25{\cdot}2 \times 10^{-7}$

The differences between the pairs of figures in the last column are in every case well within the limits of experimental error, and, moreover, the products show no tendency to be systematically greater at either the lower or the higher temperature.

The agreement between the pairs of products is thus sufficiently close to justify the conclusion that the temperature variation depends only on the variation of viscosity. This result will be used in all subsequent work.

10. *The Variation of Velocity with Diameter.*

A few experiments were also made to test the relation between velocity and diameter in the case of clove-oil drops (see next section). The diameter of a drop was measured by time-determinations. The electric current was turned on so as to oppose the motion of the drop past the microscope (if the velocity under the influence of gravity and tube-currents was not small enough without such opposition), and the time taken for the whole drop to cross a scale-line was recorded. The time taken by the drop to cover the length of the scale at the

same speed was also measured, and hence the diameter calculated. Drops at or close to the axis were chosen, and their velocities measured as described in section 3. Curves were then drawn connecting the axial velocity with the diameter of the drop. These curves were similar in every way to the curves given by Mooney[7] for oil-drops, and indicated that, though the velocities of minute drops were more than 10 per cent. lower, the velocities of drops from $\frac{1}{4}$ to $\frac{3}{4}$ of a scale-division in diameter (about 0·7 to $2{\cdot}2.10^{-3}$ cm.) were constant to within two or three per cent. As already stated, observation was confined to particles or drops having a diameter of $\frac{1}{2}$ scale-division in other experiments, and it seems that no appreciable error should arise from taking particles of slightly different diameter from the exact half scale-division.

11. *Determination of the Conductivity-Variation of the Endosmosis of the Glass Tube.*

It has already been shown that in order to obtain a value for the cataphoretic mobility of any particular substance it is necessary to subtract the endosmotic mobility of the glass from the total velocity of a particle at the axis. The two quantities can, of course, be obtained from a single traverse across the tube, but if the endosmosis of the tube is already known for the particular conditions of conductivity and temperature, only axial readings are needed, and, moreover, the velocity is sensibly constant over an appreciable area surrounding the point on the axis which is under observation.

Preliminary determinations of the endosmosis of the tube were therefore made in water of conductivity ranging from 0·8 to 10 times 10^{-6} ohm^{-1} cm.$^{-1}$, using an emulsion of clove-oil. Drops of clove-oil were chosen on account of their uniformity, chemical inactivity, insolubility, density so near to that of water ; clove-oil readily breaks up into a fine emulsion, and is readily soluble in alcohol, so that the tube may be thoroughly washed out between experiments. Additional check calibrations were also made with solids in order to ensure that the clove-oil was not in any way altering the characteristics of the glass surface or of the water. The results are shown in fig. 7. The upper curve is the axial mobility of clove-oil

in the tube, and the lower one is the endosmosis. This curve shows a marked resemblance to the curve obtained by Miss Newton[5] for paraffin drops, having a maximum for a conductivity of about $3{\cdot}25 \times 10^{-6}$ ohm^{-1} cm.$^{-1}$.

12. *Note on the Cataphoresis of Beeswax.*

Miss Newton[5] found in experiments upon waxes that one of them, beeswax, showed no cataphoretic velocity when in the form of irregular particles, a result which was totally at variance with those obtained with

Fig. 7.

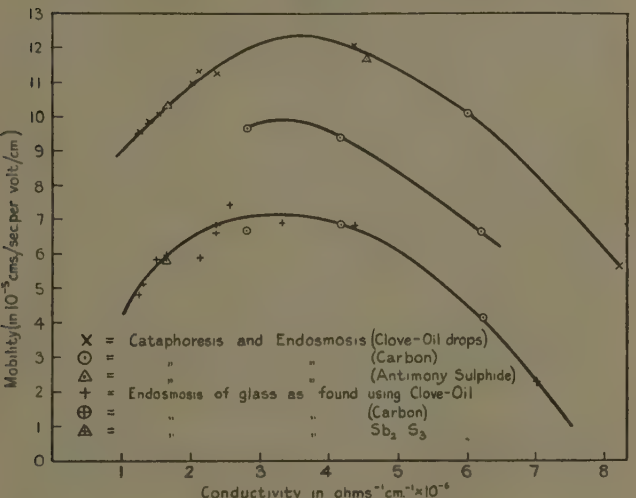
Mobility (in 10^{-5} cms./sec per volt/cm.)
Conductivity in ohms^{-1}cm.$^{-1}$ $\times 10^{-6}$
X = Cataphoresis and Endosmosis (Clove-Oil drops)
⊙ = " " (Carbon)
△ = " " (Antimony Sulphide)
+ = Endosmosis of glass as found using Clove-Oil
⊕ = " " (Carbon)
⧋ = " " Sb_2S_3

Various substances at 15° C.

the rest. I repeated the measurements in water of about the same conductivity (4×10^{-6} ohm^{-1} cm.$^{-1}$), but obtained the value $2{\cdot}0 \times 10^{-4}$ for the cataphoresis of this substance at 15° C.

This is in good agreement with the average value of $2{\cdot}2 \times 10^{-4}$ which she obtained with the other waxes.

13. *The Influence of the Conductivity of the Particle upon Velocity: the Behaviour of Good Conductors.*

The Helmholtz theory, which regards the outer charge layer as undeformable and of negligible thickness,

requires that, if the conductivity of the suspended particle is large, its velocity shall be vanishingly small. For in this case, since the surface of a conductor is an equipotential, there is no tangential component of the electrical forces on any point of the electrical double layer, and hence no relative movement.

Regarding the outer sheet as a diffuse space-charge, however, the case is more complicated, since we are here dealing with a deformable double layer which may vary in thickness over the surface of the particle. The boundary of this space-charge may be considered to be defined by the positions in which the electrical forces on an ion become negligible in comparison with the inter-molecular forces. When no field is applied, the distribution of force round the central particle is radially symmetrical, and in consequence the boundary of the space-charge will be a sphere (if for the moment we are dealing with a spherical particle). Outside this sphere the electrical forces are negligible, and therefore, the preponderance of one sign over the other is no longer appreciable.

Now suppose we apply a uniform field to the system, say from left to right. Let us say that the central charge is positive. The central particle now experiences a force to the right and the ions of the atmosphere a force to the left. As soon as the particle commences to move to the right it experiences an opposing force due to the attraction of the surplus atmospheric ions on its left, and if the system were merely an elastic assembly of bound charges there would be no resultant steady motion, provided, of course, that the field were insufficiently strong to disrupt the system.

If, however, we suppose that the particle were fixed in position, the space-charge round it would tend to assume a position in which there is an excess of ions on the right of the particle. For we have defined the space-charge boundary as being the surface at which the electrical forces become negligible in comparison with the forces due to the kinetic agitation of the molecules, and this is further from the centre of the particle on the right than it is on the left, since the action of the applied field is to reinforce the field of attraction on the right and diminish it on the left. At all points within the space-charge the ion-density is a function of the potential

energy (Boltzmann), and thus it follows that there will be an excess to the right of the particle. The two cases are represented in fig. 8.

In the first case, represented by (*b*), as soon as the field is applied the particle commences to move to the right. The negative atmosphere, under the influence of the applied field and of the inter-molecular forces, proceeds relatively slowly to take up its equilibrium form about the particle (represented by (*c*)), and the particle finally reaches a steady velocity towards the right which is mainly determined by the speed with which the boundaries of the atmosphere travel towards the position which they would occupy if the particle were stationary. In this case the relaxation force opposes the electrophoretic force.

Fig. 8.

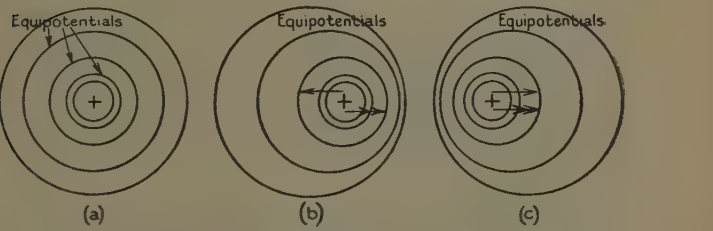

The distortion of the space-charge by an applied field.
(*a*) No field. (*b*) Movable particle fixed charges.
(*c*) Fixed particle movable charges.

These sketches are diagrammatic only, and are not intended to be strictly accurate.
→ indicates direction of applied field.
→→ indicates direction of relaxation force on the particle.

If, however, the particle is held stationary, the space-charge takes the form represented in (*c*), and exerts a force towards the right on the particle, *i. e.*, even if, as in the case of a conductor, the total force when the field is applied is zero; as soon as the space-charge takes up its new configuration it will start to exert a force on the particle, and produce motion in the same direction as that expected, having regard to the direction of the field and the sign of the charge on the particle.

Thus the particle moves through the liquid under the action of two forces :—

(1) The direct attraction, modified by the shielding effect of the space-charge.

(2) A force due to the time of relaxation of the atmosphere, which may either oppose or reinforce (1).

H. H. Paine gives this relaxation force as

$$\frac{\mathrm{E}^2\mathrm{K}}{6\mathrm{D}k\mathrm{T}} \cdot \frac{1}{1+b\mathrm{K}} \rho v,$$

where E is the central charge, k Boltzmann's constant, D the dielectric constant of the liquid, T the absolute temperature, ρ the friction constant of the ions, v the velocity, b the radius of the particle, and K the reciprocal of the mean double-layer thickness. He then gives the velocity of cataphoresis by the equation

$$v = \frac{\mathrm{XE}}{6\pi\eta b}\left[1 - \frac{b\mathrm{K}}{1+b\mathrm{K}} - \frac{a}{b} \cdot \frac{\mathrm{E}^2\mathrm{K}}{6\mathrm{D}k\mathrm{T}(1+b\mathrm{K})}\right].$$

The first two terms represent the ordinary electro-kinetic effect—Stokes's law modified by a shielding term due to the effect of the outer layer. If, for instance, $\mathrm{K}=0$, representing a simple charged particle without a surrounding space-charge layer, then Stokes's law is obeyed accurately.

For a conducting particle, however, the equation cannot be considered to hold accurately, since in its derivation it was assumed that the applied field was everywhere undistorted by the presence of the particle, whereas it is clear that the presence of a good conductor will cause considerable distortion in the field. From the simple reasoning given at the beginning of this section, in short, the ordinary electro-kinetic effect, as represented by the first two terms of Paine's equation, will be zero.

So long as there is a continuous electric field through the outer layer, however, the relaxation force will still be present (though of slightly smaller value for a conductor, since the field forces on individual ions in the space-charge will in general be at an angle with the direction of the applied field, instead of directly along, as assumed by Debye and Hückel).

We have, in fact, the condition of a stationary particle, as shown in (*c*) of fig. 8, which will now be acted upon solely by a relaxation force in the same direction as that in which the central particle would move if not surrounded by a space-charge.

The velocity attained will be of the order

$$\frac{XE}{6\pi\eta b} \times \frac{a}{b} \frac{E^2K}{6Dk\Gamma(1+bK)},$$

as given by Paine's equation. Putting $E=eb/a$, since there is no great change of layer potential with size, and capacity is proportional to the radius, and making Kb large in comparison with 1 (for a thin double layer), this velocity is of the same order as the Stokes's law velocity, $\frac{XE}{6\pi\eta b}$. We thus conclude that, owing to the presence of a relaxation force, a conductor will in general show a cataphoretic velocity comparable with the velocities of other substances.

The disagreement between these conclusions and those of Henry (see section 1) may be explained by the fact that he assumes implicitly, in the course of his paper, that the distribution of potential in the neighbourhood of the space-charge is unaffected by the presence of the applied field. But as we have seen, the applied field causes a distortion of the space-charge and of its equipotential surfaces. This assumption is, in fact, equivalent to neglecting the important effect of the relaxation force.

The behaviour of non-conductors and of particles of which the conductivity is about the same as that of the surrounding liquid no doubt follows the predictions of Helmholtz and of Debye and Hückel. This remains for experimental verification. Henry's equations provide a link between these two cases which may be perfectly valid for bodies which are not good conductors, even if it be eventually found to fail for the case of conductors. This will be further discussed in section 16.

14. *Investigation of Good Conductors.*

Experiments on the cataphoreseis of the following good or partial conductors were carried out :—

(1) Graphite.
(2) Sugar carbon.
(3) Antimony.
(4) Antimony sulphide.
(5) Manganese dioxide.

The conductivity of the water used was in all experiments between 1 and 4×10^{-6} ohm^{-1} cm.$^{-1}$. In every case the particles used were of an irregular shape, being prepared by pulverization. In preparing experimental substances every care was taken to ensure that the particles did not form adhering layers of air, oxides, or other impurities. Numerous experimenters have shown that colloidal solutions of all the metals exhibit electrokinetic effects, but it may be remarked that all particles produced by electric-arc disruption will be highly oxidized, and will in most cases present insulating surfaces. It was, therefore, necessary to find conductors which could be finely enough divided without recourse to such methods. All the substances chosen were readily reduced to a sufficiently fine powder by crushing in an agate mortar. A lump of the substance was placed in the mortar under a covering of conductivity water and thoroughly powdered. The suspension thus obtained was allowed to settle and the top layer drawn off and used for the experiments. This process may be expected to give particles of irregular shape, and consequently we should expect, if there is any variation of velocity with shape, that the actual velocities of individual particles would show small variations from the mean value. Results seemed to show that this variation for the particles used was slight, at any rate in comparison with other errors, even though for particles of widely different shape (*e. g.*, needle-shaped and spherical), there is a considerable difference in velocity, as will be seen from the results obtained with antimony oxide later. The graphite was selected from a lump of the naturally occurring mineral and yielded poor results. The sugar carbon was prepared by the ignition of pure cane sugar in a crucible, and was disintegrated by throwing the red-hot residue into cold conductivity water. The other substances mentioned were all prepared from lumps of A.R. chemicals.

Attempts were also made to prepare suspensions of other metals by filing under water, or grinding with a fine emery wheel. These attempts failed because the particles thus obtained were too large, and, moreover, tended to oxidize when in the water. Attempts to produce mercury drops also failed, though, of course, Millikan has succeeded in producing mercury drops small enough to fall very slowly through air.

15. *Results with Conductors.*

The principal results obtained with the five conductors listed are shown in the following table. The values V are all of the cataphoretic mobility in 10^{-4} c.g.s. units at 15° C. The conductivity Γ is given in 10^{-6} ohm^{-1} cm.$^{-1}$.

These results show that every conductor, or partial conductor, which has yet been examined possesses a cataphoretic velocity which is not zero, and which does not approach zero as a limiting value at any particular conductivity of the water.

Graphite.		Sugar carbon.		Antimony, Sb.		Antimony sulphide, Sb_2S_3.		Manganese dioxide.	
Γ.	V.	Γ.	V.	Γ.	V.	Γ.	V.	Γ.	V.
—	—	1·16	3·81	1·25	3·82	—	—	1·49	0·37
—	—	1·38	3·86*	1·40	3·66	—	—	1·94	1·4
—	—	-	—	1·67	4·46	—	—	2·65	1·74
2·8	3·0	—	—	—	—	4·55	5·2	3·53	2·69
4·3	2·6	—	—	—	—	9·5	−0·4†	—	—
6·4	2·5	—	—	—	—	—	—	—	—

* *cf.* Lachs and Gestel, 3·87 at about 10^{-6} conductivity and 15° C.
† All values except this one are +ve.

It is true that in two of the conductors investigated, viz., Sb_2S_3 and MnO_2, the velocity evidently reaches a zero value for a particular value of the conductivity (this is clear if the results at various conductivities are plotted on squared paper), but these are merely points at which the velocity changes sign as the conductivity changes by a finite amount. It is important to note that the velocity does not in any case tend to zero as a limit at any particular limiting value of the conductivity of the water, as, for example, when the conductivity becomes very large or very small.

This change of sign has been noticed in many substances, and Smoluchowski [13] has explained it by drawing a distinction between the Nernst P.D., which is the total

drop of potential between the interior of the solid and the free liquid, and the electro-kinetic potential, which is the effective P.D. between the *movable* ionic charge in the liquid and the *fixed* charge, a part of which consists of ions in that part of the liquid which adheres to the solid surface. The full explanation need not be given here. It is sufficient to say that many substances exhibit cataphoretic velocities of different sign at different conductivities. The conductors investigated did not show behaviour in any way peculiar to themselves. (In this connexion reference may be made to Miss Newton's results[5] on the change of sign when the conductivity is artificially raised by the introduction of thorium nitrate.)

16. *The Influence of Shape on Speed.*

Experiments were made upon needle-shaped crystals of antimony oxide moving in, and at right angles to, the direction of their axis. Regarding the crystals as long ellipsoids, with one principal axis much longer than the other two, it was proved, by integration of an equation given by Lamb for ellipsoids moving slowly through a viscous fluid, that the speed of a crystal under electro-kinetic forces will be substantially the same whether it be transverse to the motion or within a small angle of this position. For a crystal moving longitudinally the velocity may be expected to change rapidly for small variations from the exact direction. Therefore, in observing crystals in the two positions, care was taken to select crystals which were as nearly as possible parallel to the direction of motion, whereas more latitude was allowed in selecting crystals about the exact right-angle position. The direction of the field being vertical, these two cases will be henceforth spoken of as the vertical and horizontal cases respectively.

The crystals were prepared by heating the oxide to a bright red-heat in a covered crucible. On cooling slowly the surface of the oxide powder was found to be covered with a mat of long needle-shaped crystals, many of which were as much as a hundred times as long as thick. Crystals of suitable thickness were picked out by mechanical means and suspended in conductivity water in the tube. Although this substance is slightly

soluble in water (forming a weak acid), this effect was small enough not to interfere with the conductivity of the suspension, and the crystals showed no diminution in size.

Observations were made on both the horizontal and vertical positions, as already noted. Some latitude was allowed in the position of the "horizontal" crystals, but care had to be taken to ensure that the "vertical" crystals were not only vertical in the field of the microscope, but also in focus over their whole length, *i. e.*, entirely in the focal plane, which was itself vertical.

Results for the two positions were plotted with distinctive marks on squared paper and values of the cataphoresis deduced for both the vertical and horizontal positions separately.

Now Henry's paper[10] gives

$$V_T = \frac{2\mu}{\mu+\mu'} \cdot \frac{DX\zeta}{8\pi\eta}$$

for the transverse cylinder, and

$$V_L = \frac{DX\zeta}{4\pi\eta}$$

for the vertical case, μ being the conductivity of the cylinder, μ' that of the water. Hence

$$\frac{V_L}{V_T} = \frac{\mu'+\mu}{\mu},$$

and thus we have a direct test of Henry's equations provided that we know the values of μ and μ'.

In view of the results already given for good conductors, the $\frac{\mu+\mu'}{\mu}$ term can hardly be expected to apply for all values of μ and μ', but since Henry's equations are in agreement with those given by Debye and Hückel for $\mu=\mu'$, and by Helmholtz for $\mu\to\infty$, it is possible that the equations are correct over this range, even though they fail, apparently, for good conductors.

This experiment gave approximately parallel lines on squared paper for the two positions of the crystals indicating mobilities of $2{\cdot}7\times10^{-4}$ for the vertical and $1{\cdot}5\times10^{-4}$ for the horizontal position in water at 15° C. and of $1{\cdot}19\times10^{-6}$ ohm^{-1} cm.$^{-1}$.

Now

$$\frac{V_L}{V_T}=\frac{\mu+\mu'}{\mu};$$

$$\therefore \quad \mu'=\mu.\frac{V_L-V_T}{V_T}.$$

Substituting the values for V_L and V_T in this equation, we have

$$\mu'=1{\cdot}19\times\frac{1{\cdot}4}{1{\cdot}9}=0{\cdot}86\times10^{-6}\ \text{ohm}^{-1}\ \text{cm.}^{-1}.$$

Hence the specific resistance is $1{\cdot}14\times10^{6}$ ohm cm.

Attempts were made to check this value, since no figures could be found in the International Critical Tables. Measurements on the compressed powder were tried, but gave variable results, which were only able to indicate with certainty that the specific resistance of the crystals was less than 4×10^{7} ohms. Further work on the conductivity of the crystals themselves, unfortunately, had to be brought to a close before they gave reliable results, difficulty being experienced in making contact with the minute faces of the crystals. Accurate values of the conductivities of crystals of this substance would shed a very clear light on the accuracy and applicability of the $\frac{\mu+\mu'}{\mu}$ term at conductivities of the same order as that of the water used in the foregoing experiments. In making observations on these needle-shaped crystals due allowance must be made for the following :—

(*a*) A needle-shaped crystal, being prismatic rather than circular in section, will have electrical and hydrodynamic properties slightly different from those of the simple forms which have been examined mathematically.

(*b*) End-effects.

(*c*) The electrical conductivity of the material will vary according to the direction in which it is measured.

Possible errors due to these causes would be very much diminished by the use of fine fibres of quartz, etc., in place of the needle-shaped crystals. Further experiments along these lines are likely to yield very interesting results, and will show to what extent the conductivity

term may be applied to the two cases under review, and indeed, to problems of wider scope.

17. *Conclusion.*

The experiments described in this paper provide evidence that

(1) Every substance shows a definite cataphoretic velocity in water, which varies according to the conductivity of the water, and which may in some cases have either sign, according to the nature of the substance and the conductivity of the water.

(2) Conducting substances are in no way an exception to this rule, and although every precaution was taken to ensure that the conducting particles did not form adhering layers of insulators, no conductor was found to have zero mobility.

(3) This is explained by reference to the Debye-Hückel theory.

(4) The velocity of cataphoresis varies in the manner predicted by Helmholtz in so far as changes in viscosity and electric field are concerned.

(5) The velocity is not, as Helmholtz suggested, constant for all shapes and sizes of the same substance. It varies slightly with the diameter of the particle, and considerably with shape. The variation with shape seems to be according to the equations given by Henry in the paper already quoted, though further work is needed to verify the exact relationship.

(6) The phenomena are explained most satisfactorily by the theory of Debye and Hückel as modified by Paine to include the relaxation effect. This theory accounts for the behaviour of conductors, the variation of mobility with size and with the conductivity of the liquid phase, and the variation with shape as applied to the long crystals which have been investigated in this work (and also the spheres and broken particles investigated by Miss Newton[5]).

According to the Debye-Hückel theory the ratio of the velocities for the two positions of the long crystals should be 1 : 2, whereas experiment showed a ratio 1 : 1·8. As detailed in section 16 there are several considerations, in addition to experimental error, which could have

produced such a discrepancy, and the experimental figures thus lend considerable support to the theory.

Further research may demand the introduction of a conductivity term as given by Henry, though this evidently breaks down in the case of good conductors, and could, therefore, only apply to insulators and partial conductors.

The modified Debye-Hückel theory seems capable of explaining all the known phenomena.

I wish to express my sincere thanks to Prof. J. A. Crowther and to Dr. W. N. Bond for their continual help and interest in this work, to Mr. J. S. Burgess for innumerable hints with regard to the apparatus, and also to the Research Board of Reading University for grants which enabled the work to be carried out.

18. *References.*

(1) Helmholtz, *Ann. der Phys.* vii. p. 337 (1879).
(2) Mooney, Phys. Rev. xxiii. p. 396 (1924).
(3) McTaggart, Phil. Mag. xxvii. p. 297, and xxviii. p. 367 (1914).
(4) Freundlich, ' Colloid and Capillary Chemistry,' p. 248.
(5) Miss D. A. Newton, Phil. Mag. ix. p. 729 (1930).
(6) Alty, Proc. Roy. Soc. A, cvi. (1924).
(7) Mooney, *loc. cit.*
(8) Debye and Hückel, *Phys. Zeits.* xxv. p. 49 (1924).
(9) Hückel, *Phys. Zeits.* xxv. p. 204 (1924).
(10) Henry, Proc. Roy. Soc. A, cxxxiii. p. 821 (1931).
(11) Bourdillon, J. Chem. Soc. ciii. p. 791 (1913).
(12) H. H. Paine, Proc. Camb. Phil. Soc. xxviii. p. 83 (1932).
(13) See Freundlich, ' Colloid and Capillary Chemistry.'
(14) Burton, ' The Physical Properties of Colloidal Solutions.'
(15) Lachs and Gestel, *Kolloid Zeits.* lix. p. 170 (1932).

LXXII. *The Radioactivity of the Rare Earths.* *By* H. J. Walke, *M.Sc., A.Inst.P., Demonstrator in Physics, Washington Singer Laboratories, University College, Exeter* *.

I. *Introduction.*

THE radioactivity of samarium was first observed by Hevesy and Pahl †, who noted the emission of α-rays of range 1·13 cm. from samarium oxide, the substance having for equal surface area an activity equal to 1/3

* Communicated by Prof. F. H. Newman, D.Sc.
† Hevesy and Pahl, ' Nature,' cxxx. p. 846 (1932).

that of a thick layer of potassium chloride. This activity is not due to radioactive impurities, for repeated chemical and radioactive purification did not cause the least variation in activity. Libby and Latimer * independently discovered the α-ray emission of samarium by means of a Geiger-Müller counter.

Curie and Takvorian † have measured the radioactivity of various fractions of neodymium and samarium by a very sensitive method. They found that neodymium was not active, and that pure samarium had an activity at least eight times as great as the probable error of the measurements, the activity being reduced by more than half by $0{\cdot}6\,\mu$ Al, and being completelystopped by $6{\cdot}3\,\mu$ Ag.

The intermediate fractions were more active, the activity being greatest in the fraction which contained element 61 in excess. In these samples an activity 53 times as great as the probable error of the measurements was observed, this being reduced to 47 times by $0{\cdot}6\,\mu$ Al and to about 12 times by $6{\cdot}3\,\mu$ Ag.

These results confirm the radioactivity of samarium, and also establish the existence of the radioactivity of illinium (atomic number 61). The radiation observed from this element is stated by Curie and Takvorian to be too penetrating to be due solely to α-rays. It is, therefore, probable that illinium emits β-radiation. It will be shown that this is in line with the process of nuclear evolution suggested in previous papers ‡.

II. *The Isotopes of Neodymium, Illinium, and Samarium.*

In previous papers § it has been shown that the synthesis of the stable isotopes can be explained in terms of a process of neutron capture and β-radioactivity of certain missing isotopes. Using the results obtained by Aston with his mass spectrograph, it has been indicated that most of the main isotopic species may be built up in this way. In view of Aston's more detailed results for the rare earths ‖ recently announced, it is proposed to consider the observed isotopic configuration of some of these elements, as they show certain interesting

* Libby and Latimer, J. Amer. Chem. Soc. lv. p. 433 (1933).
† Curie and Takvorian, *Comptes Rendus*, excvi. p. 923 (1933).
‡ Walke, Phil. Mag. xviii. p. 795 (1934), and xix. p. 33 (1935).
§ Walke, *loc. cit.*
‖ Aston, Proc. Roy. Soc. A, cxlvi. p. 46 (1934).

features which shed additional light on the problem of radioactivity and nuclear synthesis.

Praseodymium is a single element of mass number 141, being formed as a result of the β-radioactivity of the missing Ce_{58}^{141}. The missing isotope Pr_{59}^{142}, formed when Pr_{59}^{141} captures a neutron, is, as has already been suggested, a β-radioactive synthesis link which is spontaneously transformed into Nd_{60}^{142}. The other neodymium isotopes are formed by neutron capture, though Nd_{60}^{143} is synthesized by the double β-ray transformation following the formation of the missing Ce_{58}^{143}, thus :—

$$Ce_{58}^{143} \rightarrow Pr_{59}^{143} \rightarrow Nd_{60}^{143}.$$

Aston's results show that neodymium has isotopes from mass number 142 to 146. The missing isotope Nd_{60}^{147}, formed by the addition of a neutron to Nd_{60}^{146}, is the synthesis β-radioactive link which results in the formation of the missing element illinium. Hence if this element were stable we should have

$$Nd_{60}^{147} \rightarrow \beta \rightarrow Il_{61}^{147}.$$

On the hypothesis suggested, therefore, the synthesis of the lightest samarium isotope produced in the direct evolution would result from β-ray emission from the missing Il_{61}^{148} when the supposed stable isotope captured a neutron. The other stable samarium isotopes of greater mass number would then be produced by the nuclear synthesis process of neutron capture as already suggested.

There exist, however, samarium isotopes of mass number 144 and 147 which are not produced in the direct synthesis, if it is assumed that Il_{61}^{147} is a stable nuclear configuration. The isotope of mass 144 is probably synthesized by a secondary process of the type which has been discussed previously *. It is to be noted that β-ray emission from an element of odd atomic number results in the formation of a new nuclear α-particle, so that, following the β-ray emission of Il_{61}^{148}, it is probable that Sm_{62}^{148} is formed in a state of excess energy which may be demonstrated by the symbol $\overset{*}{Sm}_{62}^{148}$. In the

* Walke, *loc. cit.*

majority of such nuclei formed in this way the newly formed α-particle is bound within the nuclear structure to produce the normal Sm_{62}^{148}, the excess energy being emitted in the form of γ-radiation. It is suggested, however, that in a small number of such nuclei the newly formed α-particle is ejected on formation, leaving a neodymium nucleus $\overset{*}{N}d_{60}^{144}$, also in a state of excess energy. This nucleus may also return to the normal state by emitting γ-radiation, though in some cases β-radiation is emitted as follows :—

$$\overset{*}{N}d_{60}^{144} \rightarrow Il_{61}^{144} \rightarrow \beta \rightarrow Sm_{62}^{144}.$$

The presence of Sm_{62}^{144} is thus to be attributed to the radioactive formation of Sm_{62}^{148} from the missing parent isotope Il_{61}^{148}, and the origin of this lighter isotope is directly connected with the synthesis of Sm_{62}^{148}. It is to be noted that the suggested α-ray emission from Sm_{62}^{148} does not involve the spontaneous radioactivity of this isotope. The nuclei formed in a state of excess energy sometimes emit the excess energy by ejecting, at the moment of formation, an α-particle, the excess nuclear energy being thus emitted in the form of kinetic energy of the α-particle.

Such an action does not, however, account for the presence in relatively high abundance of Sm_{62}^{147}. This isotope could be formed if Sm_{62}^{146} captured a neutron, but as Sm_{62}^{145} and Sm_{62}^{146}, if they do exist, would be formed from Sm_{62}^{144} by neutron capture, its abundance would be very small. As, however, Aston has not detected isotopes of samarium with mass numbers 145 and 146, it appears unlikely that Sm_{62}^{147} could have been produced in this way other than in vanishingly small amount. This isotope may, therefore, be evolved by the emission of β-radiation from Il_{62}^{147}, so that we have the action

$$Nd_{60}^{147} \rightarrow \beta \rightarrow Il_{61}^{147} \rightarrow \beta \rightarrow Sm_{62}^{147}.$$

It is thus apparent that the isotopic constitution of neodymium and the high relative abundance of the samarium isotope of mass number 147 indicate that illinium (element 61) consists of a single isotope Il_{61}^{147},

this isotope being spontaneously β-radioactive. This is in good accord with the results of Curie and Takvorian *.

It is to be noted, in addition, that Sm_{62}^{147} is the lightest abundant samarium isotope, and since, therefore, in this nucleus the ratio of protons to neutrons is greater than in any other isotope (except the small abundance isotope of mass number 144), it is probable that the spontaneous α-ray emission of samarium originates in this isotope. It is therefore possible (if this isotope is α-radioactive) that some α-rays will be observed from the fractions tested by Curie and Takvorian containing element 61 in excess, according to the reaction

$$Il_{61}^{147} \rightarrow \beta \rightarrow Sm_{62}^{147} \rightarrow \alpha \rightarrow Nd_{60}^{143}.$$

As, however, the Sm_{62}^{147} resulting from the β-radioactivity would be formed only in minute quantities, it is possible that the α-radiation would not be detected.

Curie and Takvorian have suggested, however, that Sm_{62}^{148} may be the radioactive isotope. It appears possible to test this suggestion, as will be shown in the next section.

III. *The Synthesis of Europium and Gadolinium.*

According to the evolutionary process by neutron capture and β-radioactivity, the synthesis of europium from samarium results from the emission of β-radiation from the missing samarium isotopes with mass numbers 151, 153, and 155, formed when the stable isotopes Sm_{62}^{150}, Sm_{62}^{152}, and Sm_{62}^{154} capture a neutron. Europium has, however, only two stable isotopes, namely, Eu_{63}^{151} and Eu_{63}^{153}, so that Eu_{63}^{155} is itself β-radioactive, and the gadolinium isotope of mass number 155 is synthesized directly from samarium by the double β-ray transformation

$$Sm_{62}^{155} \rightarrow \beta \rightarrow Eu_{63}^{155} \rightarrow \beta \rightarrow Gd_{64}^{155}.$$

Synthesis from europium to gadolinium should result from the β-radioactivity of the missing isotopes Eu_{63}^{152} and Eu_{63}^{154}. Aston has, however, shown quite definitely that the corresponding gadolinium isotopes are missing, and as by the synthesis process discussed these should

* Curie and Takvorian, *loc. cit.*

be the lightest isotopes (and, therefore, the isotopes in which the proton neutron ratio is highest), it appears most likely that these isotopes were spontaneously radioactive by α-ray emission, and have, therefore, disappeared. Thus we have the following short radioactive series :—

$$Eu_{63}^{152} \rightarrow \beta \rightarrow Gd_{64}^{152} \rightarrow \alpha \rightarrow Sm_{62}^{148},$$
$$Eu_{63}^{154} \rightarrow \beta \rightarrow Gd_{64}^{154} \rightarrow \alpha \rightarrow Sm_{62}^{150}.$$

These reactions suggest that it may be possible to test the samarium isotope of mass number 148 for α-radioactivity by reproducing it artificially. This could be done by subjecting europium to bombardment by neutrons from a powerful source for a long period. As neutron capture appears to be the most probable reaction with the heavier elements, it is almost certain that Eu_{63}^{152} and Eu_{63}^{154} will be produced. These β-radioactive products (probably of short life) would decay to give the α-ray unstable gadolinium isotope discussed above, and these could be separated chemically from the europium and tested for α-radioactivity. The detection of α-rays of the same range as those from samarium would be evidence in favour of the suggestion that Sm_{22}^{148} is the radioactive isotope.

In view, however, of the fact that the isotope of mass number 147 has a higher proton-neutron ratio, it seems more probable that this isotope is the source of the samarium α-particles. A search for α-particles of the same range as those emitted by samarium in samples (such as those used by Curie and Takvorian) of neodymium containing excess of illinium would confirm this suggestion.

IV. *α-radioactive Isotopes of Dysprosium and Ytterbium.*

Aston's latest results also indicate that other rare-earth elements have probably lost unstable isotopes which have been spontaneously transformed into stable isotopes of lower atomic number by α-ray emission.

For example, the synthesis process on the theory for the evolution of terbium from gadolinium is by the reaction

$$Gd_{64}^{158} + n \rightarrow Gd_{64}^{159} \text{ (missing)} \rightarrow \beta \rightarrow Tb_{65}^{159},$$

and the lightest dysprosium isotope on the theory adopted would then be Dy_{66}^{160}, due to the β-radioactivity of the missing Tb_{65}^{160}. The missing Gd_{64}^{161} results in the synthesis of Dy_{66}^{161}, since Tb_{65}^{161} is itself missing, and, according to the theory, β-radioactive, so has, therefore, disappeared by the action

$$Gd_{64}^{161} \rightarrow \beta \rightarrow Tb_{65}^{161} \rightarrow \beta \rightarrow Dy_{66}^{161}.$$

The lightest isotope of dysprosium of mass number 160 is, however, missing, and it therefore appears probable that this isotope has disappeared because it was α-radioactive. Hence we have

$$Tb_{65}^{160} \rightarrow \beta \rightarrow Dy_{66}^{160} \rightarrow \alpha \rightarrow Gd_{64}^{156}.$$

Similarly synthesis from erbium to thulium is due to the radioactivity of the missing isotopes Er_{68}^{169} and Er_{68}^{171}, the former producing the stable thulium isotope of mass number 169, the latter giving rise to a missing β-radioactive thulium isotope which is spontaneously transformed to ytterbium by the action

$$Er_{68}^{171} \rightarrow \beta \rightarrow Tm_{69}^{171} \rightarrow \beta \rightarrow Yt_{70}^{171}.$$

The lightest ytterbium isotope by the direct synthesis process should be Yt_{70}^{170}, formed as a result of the β-radioactivity of the missing Tm_{69}^{170}. This isotope, Yt_{70}^{170}, should again be the lightest of the group (and, therefore, has the highest proton-neutron ratio), so it was probably α-radioactive, and has disappeared according to the reaction

$$Tm_{69}^{170} \rightarrow \beta \rightarrow Yt_{70}^{170} \rightarrow \alpha \rightarrow Er_{68}^{166}.$$

V. *The β-radioactivity of Masurium.*

As has been shown, the relationship between the isotopes of neodymium and samarium suggest that illinium is spontaneously β-radioactive. It is interesting to note that the isotopic configuration of the analogous group of elements molybdenum and ruthenium suggest also that masurium is spontaneously β-radioactive.

The missing isotopes of molybdenum are Mo_{42}^{99} and Mo_{42}^{101}, which, according to the theory adopted, should emit β-radiation to produce Ma_{43}^{99} and Ma_{43}^{101} if masurium were

a stable element, and these are both possible isotopes of this element. The negative evidence of Noddack and Tacke * on the atomic weight of masurium, which they state lies between 98 and 99·5, suggests that the isotope of mass number 99 is the main, if not the only, existing isotope. It is, therefore, possible that Ma_{43}^{101} is itself a short-lived and missing β-radioactive isotope, the missing Mo_{42}^{101} on formation (when Mo_{42}^{100} captures a neutron) transforming into Ru_{44}^{101} by the double β-ray synthesis

$$Mo_{42}^{101} \rightarrow \beta \rightarrow Ma_{43}^{101} \rightarrow \beta \rightarrow Ru_{44}^{101}.$$

Synthesis of ruthenium would accordingly be due to the β-radioactivity of the missing isotopes Ma_{43}^{100} and Ma_{43}^{102} giving rise to Ru_{44}^{100} and Ru_{44}^{102} by the reactions

$$Ma_{43}^{100} \rightarrow \beta \rightarrow Ru_{44}^{100}; \quad Ma_{43}^{102} \rightarrow \beta \quad Ru_{44}^{102},$$

so that, according to the theory, Ru_{44}^{100} should be the lightest ruthenium isotope produced by the direct synthesis process.

As, however, Ru_{44}^{96} and Ru_{44}^{98} exist in small abundance, it has been suggested that these isotopes are produced as a result of the secondary reactions, which are similar to that discussed for corresponding isotopes of samarium. The actions are :—

$$Ma_{43}^{100} \rightarrow \beta \rightarrow \overset{*}{R}u_{44}^{100} \rightarrow \alpha \rightarrow \overset{*}{M}o_{42}^{96} \rightarrow \beta \rightarrow Ma_{43}^{96} \rightarrow \beta \rightarrow Ru_{44}^{96},$$

$$Ma_{43}^{102} \rightarrow \beta \rightarrow \overset{*}{R}u_{44}^{102} \rightarrow \alpha \rightarrow \overset{*}{M}o_{44}^{98} \rightarrow \beta \rightarrow Ma_{43}^{98} \rightarrow \beta \rightarrow Ru_{44}^{98}.$$

In addition, it is noteworthy that Ru_{44}^{99} (analogous to Sm_{62}^{147}) exists in relative abundance which is much greater than is to be expected if it is formed by the action

$$Ru_{44}^{98} + n \rightarrow Ru_{44}^{99},$$

since, if Ru_{44}^{98} does exist, it does so in such small abundance that it is only just detectable with the mass spectrograph. Hence by analogy with illinium (whose isotope of mass number 147 is probably spontaneously β-radioactive), the lighter isotope (and this is probably the only existing isotope) of masurium, with mass number 99, is

* Noddack and Tacke, *Naturwiss.* xiii. p. 567 (1925)

also spontaneously radioactive by emitting β-radiation, and this has resulted in the unexpectedly high abundance of Ru_{44}^{99}, which is, therefore, synthesized by two succeeding β-ray transformations, viz.,

$$Mo_{42}^{99} \rightarrow \beta \rightarrow Ma_{43}^{99} \rightarrow \beta \rightarrow Ru_{44}^{99}.$$

The Artificial Production of Elements 85 *and* 87.

The synthesis of uranium from thorium may occur * as a result of the β-radioactivity of the missing thorium isotope Th_{90}^{233}, the isotope of element 91 thus produced being itself β-radioactive, transforming spontaneously to U_{92}^{233}. These isotopes, it was shown, could be considered links in a missing radioactive series which had died out, of which U_{92}^{237} was the head, and in which the missing elements eka-cæsium and eka-iodine were produced as follows :—

$$U_{92}^{237} \rightarrow \alpha \rightarrow Th_{90}^{233} \rightarrow \beta \rightarrow Eka.Ta_{91}^{233} \rightarrow \beta \rightarrow U_{92}^{233} \rightarrow \alpha \rightarrow Th_{90}^{229}$$
$$\rightarrow \beta \rightarrow Eka.Ta_{91}^{229} \rightarrow \alpha \rightarrow Ac_{89}^{225} \rightarrow \alpha \rightarrow Eka.Cs_{87}^{221} \rightarrow \alpha \rightarrow Eka.I_{85}^{217}.$$

Th_{90}^{233} could be reproduced artificially by bombarding Th_{90}^{232} with neutrons. It is significant that Fermi † and his co-workers have observed induced β-radioactivity with two periods of 1 m. and 15 m. respectively when thorium was bombarded with neutrons. It is probable that by the observed reaction the initial process suggested for the evolution of the lightest uranium isotope was reproduced thus :—

$$Th_{90}^{232} + n \rightarrow Th_{90}^{233} \rightarrow \beta \rightarrow Eka.Ta_{91}^{233} \rightarrow \beta \rightarrow U_{92}^{233}.$$

It is therefore suggested that by subjecting thorium to prolonged bombardment by strong sources of neutrons, the missing elements may be artificially produced following the decay of the newly formed uranium isotope of mass number 233.

* Walke, Phil. Mag. xix. p. 54 (1935).
† E. Fermi, Proc. Roy. Soc. A, cxlvi. p. 483 (1934).

LXXIII. *The Structure of Methyl Ammonium Alum*, $NH_3(CH_3)Al(SO_4)_2 . 12H_2O$.

By H. Lipson, *M.Sc.*, *Oliver Lodge Fellow in Physics, University of Liverpool* *.

Introduction.

AN interesting question which was raised by Wyckoff† and discussed by Cork ‡ arises from the existence of ammonium alum. The structure of the alums, of which the formula $KAl(SO_4)_2.12H_2O$ may be taken as typical, has been shown § to be based on the space group $Pa3(T_h^6)$ with K and Al on centres of symmetry on the triad axes. In ammonium alum the potassium is replaced by NH_4, although the hydrogens cannot conform in any reasonable manner with the requirements of symmetry; this must thus be considered as a case in which either the symmetry of the crystal is not influenced by the light hydrogen atoms, or the NH_4 group is spherically symmetrical.

The latter explanation would be the more probable were it not for the fact that there exist organic alums in which one or more of the hydrogens of the NH_4 group is replaced by an organic radical. There seems to be evidence || that these organic alums have not the symmetry of the pyritohedral class, to which the inorganic alums belong. For example, Le Bel ¶ has stated that the alum formed from active amylamine is itself optically active, and thus cannot have a centre of symmetry. This conclusion was supported by a study of etch-figures, and these also seemed to indicate that coniin-alum has no centre of symmetry. Traube **, however, could find no optical activity in this latter crystal.

The investigation into the structure of methyl ammonium alum, $NH_3(CH_3)Al(SO_4)_2.12H_2O$, was undertaken in order to obtain additional evidence regarding the symmetry by means of X-rays. The difference between

* Communicated by Prof. L. R. Wilberforce.

† Amer. J. of Science, v. p. 209 (1923).

‡ Phil. Mag. iv. p. 688 (1927).

§ Beevers and Lipson, 'Nature,' cxxxiv. p. 327 (1934).

|| Groth, 'Chemische Krystallographie,' ii. p. 555.

¶ *Ber. d. d. chem. Ges.* v. p. 391 (1872).

** *N. Jahrb. f. Min. usw.* Beil.-Bd. 9, p. 625 (1895); and *Zeits. f. Krist.* xxvii. p. 531.

the pyritohedral and the tetartohedral classes is that the latter has neither the centre nor the planes of symmetry of the former. The planes of symmetry manifest themselves in the alum structure as glide planes, the presence or absence of which can be detected by X-rays.

Crystal Class.

Crystals of methyl ammonium alum were prepared by evaporation at ordinary temperatures of a solution obtained by dissolving in water equivalent parts of methylamine hydrochloride, sulphuric acid, and aluminium sulphate. Though obviously cubic the crystals bore

Fig. 1.

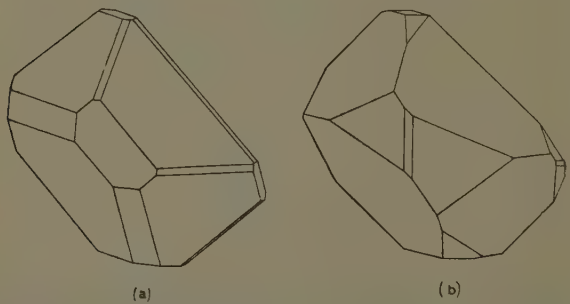

Typical crystals of (*a*) potash alum and (*b*) methyl ammonium alum.

little resemblance to those of potash alum; in this the forms usually developed are {111}, {100}, and {110}, while in methyl ammonium alum the usual forms are {111}, {210}, and {100}. These are illustrated in fig. 1.

The observed habit will not distinguish between the pyritohedral and tetartohedral classes.

A test for pyroelectricity gave no result, indicating centro-symmetry.

Four 30° oscillation photographs were taken with the crystal rotating about a crystallographic axis. On none of these could be detected any reflexions *hko* with *h* odd. This indicates the presence of glide planes, and thus that the crystals must be assigned to the pyritohedral class of the cubic system.

Determination of the Structure.

The size of the unit cell was estimated by the powder method* as $12{\cdot}479 \pm {\cdot}002$ Å. This is larger than any of the inorganic alums measured by Cork †.

Analysis of the oscillation photographs showed that intensities were in most cases completely different from those of potash alum, indicating at least that there are large changes of parameters.

An estimate of the sulphur parameter was made as follows. From Cork's observations empirical relations had been established for potash alum between photographic and absolute intensity. By comparison of the exposures of the potash and methylammonium alum photographs similar relations were established for the latter. It is realized that this method is liable to large absolute errors, but it was thought that relative errors would be much smaller. This view was fully justified by results. The F values calculated for the *hko* reflexions with k even were assumed to be positive, as they have a large positive contribution from the aluminium at the origin. The contribution of these F's to the electron density projected on to the (100) plane at the points (·31, ·31), (·32, ·32), (·33, ·33) was calculated. This showed a peak between ·32 and ·33, and ·32 was taken as the sulphur parameter. The accuracy is uncertain on account of the possibility of wrong signs of the F's and of displacement by oxygen peaks.

Nevertheless, the parameter seemed definitely greater than the value ·31 in potash alum. The changes in the other parameters attendant on this displacement of the SO_4 group were deduced, and it was thought that the structure should thus be defined approximately. The element of doubt lay in the distance of the water molecules from the centre of symmetry at $(\frac{1}{2}\ \frac{1}{2}\ \frac{1}{2})$, but it was thought that this would not affect the low orders of reflexion seriously.

The agreement between calculated and observed intensities was, however, definitely wrong, indicating that the proposed structure was incorrect.

It was observed, however, that the calculations for the *hko* reflexions with k even agreed rather better with

* Bradley and Jay, Phys. Soc. Proc. xlv. p. 507 (1933).
† *Loc. cit.*

the observed intensities *kho*. This is illustrated in Table I. The parameters used were :—

Al	(0	0	0)				
S	(·32	·32	·32)				
O's	(·25	·25	·25)	and	(·27	·43	·33)
H_2O's	(·16	·00	·00)	and	(·30	·05	·16)

(CH_3 and NH_3 were omitted, in the absence of any indication of their positions.)

TABLE I.

hko.	Calc. F.	Obs. *hko*.	Obs. *kho*.
420.....	18	m.	s.
620.....	7	s.	o.
820.....	21	m.	m.–s.
240.....	$\overline{14}$	s.	m.
640.....	24	o.	m.
840.....	17	w., v.	m.
260.....	45	o.	s.
460.....	3	m.	o.
280.....	20	m.–s.	m.
480.....	13	m.	w., v.

(Intensities were divided into the classes, v.s. (very strong), s. (strong), m.–s. (medium-strong), m. (medium), w.-m. (weak-medium), w. (weak), v. (very weak), and o. (absent). The recorded intensities are averages of several observations.)

The explanation of this seemed to be that the parameters x, y, z should be changed to z, y, x, but it was found that this could not be done without radically affecting interatomic distances. These, however, could be brought right by the change of sign of the sixth water parameter, and this alteration will not affect the intensities in Table I. It was found that these

parameters gave approximate agreement with the other low order *hko* reflexions.

It was assumed, therefore, that this structure was approximately correct, and from it were deduced the signs of the F's of the *hko* reflexions. Several of the signs were doubtful, as the parameters were still appreciably wrong, and these F's were omitted in the computation of electron density by the method of Fourier series *. The signs were obtained from the more accurate values of the parameters given by the approximate Fourier synthesis, which was then corrected for the omissions.

The F's finally used are shown in Table II.

TABLE II.

Values of F_{hko}.

$F_{hko}=F_{\bar{h}ko}$ when k is even ; $F_{hko}=-F_{\bar{h}ko}$ when k is odd.

k.	h.													
	$\bar{1}\bar{4}$	$\bar{1}\bar{2}$	$\bar{1}\bar{0}$	$\bar{8}$	$\bar{6}$	$\bar{4}$	$\bar{2}$	0	2	4	6	8	10	12	14
0	0	17	$\bar{8}$	0	30	27	0	124	0	27	30	0	$\bar{8}$	17	0
1	$\bar{6}$	0	9	0	0	23	$\bar{1}\bar{6}$	0	16	$\bar{2}\bar{3}$	0	0	$\bar{9}$	0	6
2	9	0	8	12	24	$\bar{1}\bar{1}$	23	0	23	$\bar{1}\bar{1}$	24	12	8	0	9
3	0	0	0	$\bar{1}\bar{2}$	0	12	$\bar{1}\bar{5}$	0	15	$\bar{1}\bar{2}$	0	12	0	0	0
4	7	0	0	5	0	6	22	27	22	6	0	5	0	0	7
5	0	0	0	0	0	0	0	0	0	0	0	0	0	0	0
6	0	10	0	9	27	12	0	30	0	12	27	9	0	10	0
7	0	0	8	$\bar{9}$	0	10	$\bar{1}\bar{7}$	0	17	$\bar{1}\bar{0}$	0	9	$\bar{8}$	0	0
8		0	6	8	0	12	19	0	19	12	0	8	6	0	
9		0	0	0	0	0	0	0	0	0	0	0	0	0	
10		0	0	0	0	0	9	$\bar{8}$	9	0	0	0	0	0	
11			$\bar{5}$	5	0	$\bar{8}$	8	0	$\bar{8}$	8	0	$\bar{5}$	5		
12			0	0	10	0	0	17	0	0	10	0	0		
13				0	0	0	0	0	0	0	0	0			
14					0	0	6	0	6	0	0				
15					0	0	0	0	0	0	0				

The resulting contour map of electron density projected on the 100 plane is shown in fig. 2, together with (fig. 3) the atomic positions deduced from it.

* W. L. Bragg, Proc. Roy. Soc. A, cxxiii. p. 537 (1929) ; Beevers and Lipson, Phil. Mag. (7) xvii. p. 855 (1934).

The structure is expressed by the parameters :—

4 Al	on	0	0	0	
8 S	on	·33	·33	·33	etc.
8 O's	on	·26	·26	·26	etc.
24 O's	on	·27	·34	·44	etc.
24 H_2O's	on	·15	·00	·00	etc.
24 H_2O's	on	·05	·27	$\cdot\bar{1}\bar{6}$	etc.

Fig. 2.

Contour map of electron density projected on to (100). Contours are drawn at intervals of 140, with the level 200 (dotted lines) inserted to emphasize the smaller peaks.

(The positions of CH_3 and NH_3 will be considered later.)

These parameters agreed satisfactorily with all the calculations of the higher order reflexions (above $\sin\theta/\lambda = \cdot 25$), and it was not considered that any of the observed intensities justified any modification *.

* *Cf.* Lipson and Beevers, " The Structure of the Alums " (in press).

Positions of NH_3 *and* CH_3.

The Fourier synthesis (fig. 2) shows no departure from spherical symmetry of the complex NH_3CH_3. In view, however, of the approximate nature of the data from which this synthesis was derived, a more thorough investigation of the question was attempted.

There are three possible ways of explaining the glide-planes (or pseudo-glide planes) which exist in the structure.

Fig. 3.

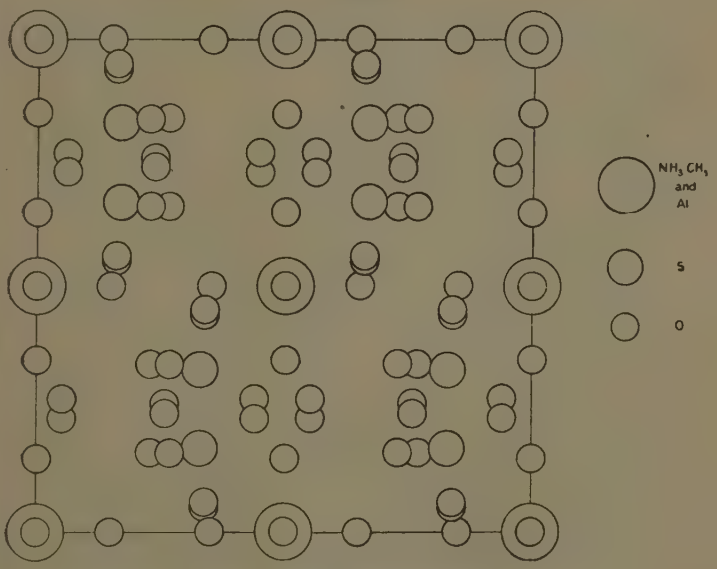

Atomic positions deduced from fig. 2.

Firstly, NH_3CH_3 may have spherical symmetry. It is not easy to see how this can be so, but considerations of space suggest it. The immediate environment consists of six waters at a distance of 3·55 Å. and six oxygens at a distance of 3·58 Å.

Secondly, the NH_3 and CH_3 groups may be symmetrically disposed about the centre of symmetry. Owing to their practical equivalent as scattering units the space-group Pa3 would be simulated. In monomethyl

ammonium iodide * the distance between C and N is 1·3 Å., and the radii of CH_3 and NH_3 are 1·75 Å. and 1·4 Å. respectively. A group of this size can just fit into the available space along the triad axis, but the large distance (3·6 Å.) from NH_3 to H_2O is not readily accounted for.

Thirdly, N may be on the centre of symmetry and C may occupy at random the two possible positions on

Fig. 4.

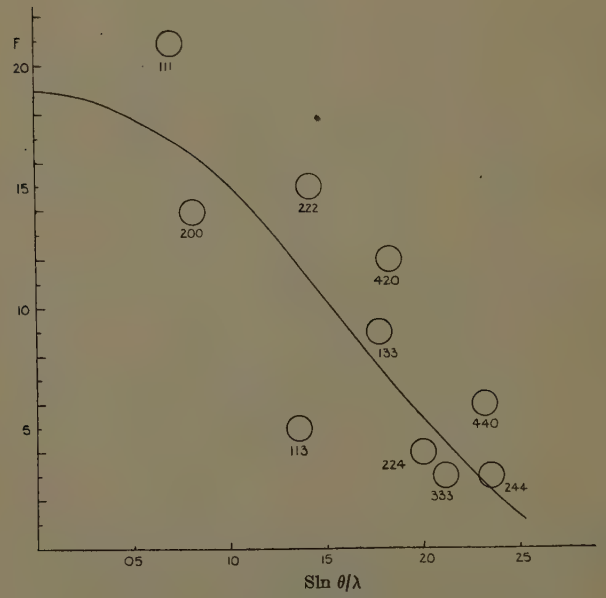

F-curve for NH_3CH_3.

either side of it. There is, however, no room for this arrangement, assuming the radii given above.

Unfortunately, it is not possible to distinguish between these possibilities by X-ray intensities. NH_3 and CH_3 are light groups, of which the scattering factor falls off rapidly with θ, so that they do not affect the higher

* S. B. Hendricks, *Zeits. f. Krist.* lxvii. p. 106 (1928).

orders of reflexion; and the lower orders cannot distinguish such fine detail in the structure. The reflexions above $\sin\theta/\lambda = \cdot 25$ agreed well with the calculations neglecting NH_3 and CH_3, and the reflexions *hko* with *k* odd agreed well at all angles, as would be expected if NH_3CH_3 were on the centre of symmetry. Some general reflexions were examined, and they also agreed with this. From those reflexions with *h*, *k*, and *l* even, and *h*, *k*, and *l* odd, an F curve was deduced. This, together with those reflexions from which it was derived, is shown in fig. 4.

Comparison of observed intensities and those calculated using this F curve are shown in Table III.

TABLE III.

Comparison of Calculated and Observed Intensities.

h.	*k.*	*l.*	F.	Obs.	*h.*	*k.*	*l.*	F.	Obs.
1	1	1	2600	m.	6	1	0	30	o.
2	0	0	30	o.	6	2	0	4700	s.
2	1	0	8600	s.	2	6	0	50	o.
2	1	1	610	m.	3	4	4	160	v.
2	2	0	6500	v.s., s.	4	5	0	0	o.
1	2	2	2500	m.–s.	6	3	0	70	w., v.
1	1	3	920	m.–s.	6	4	0	30	o.
2	2	2	600	m.	4	6	0	550	m.
2	3	0	1100	m.–s.	2	7	0	820	m.–s.
2	1	3	10	o.	6	5	0	10	v.
2	3	1	2400	s.	8	0	0	200	v.
4	0	0	8400	v.s.	8	1	0	140	v.
3	2	2	860	m.–s.	4	7	0	680	m.,w.–m.
4	1	0	2400	s.	8	2	0	680	m.
4	1	1	10	v., o.	2	8	0	680	m.–s.
1	3	3	3300	s.	6	6	0	1500	s.
4	2	0	1100	m.	8	3	0	300	m.
2	4	0	4300	s.	8	4	0	60	w., v.
1	2	4	930	m.–s.	4	8	0	430	m.
1	4	2	0	o.	2	9	0	0	v.
2	3	3	0	o.	6	7	0	0	o.
2	2	4	270	w.	8	5	0	10	v.
4	3	0	330	m.	4	9	0	0	o.
4	1	3	0	v.	6	8	0	50	o.
4	3	1	570	w.–m..	8	6	0	440	w.–m.
3	3	3	1100	m.–s., m.	10	0	0	490	w.–m.
2	5	0	60	o.	10	1	0	250	w.–m.
3	2	4	260	v.	10	2	0	290	w.–m., w.
3	4	2	470	w.–m.	2	10	0	580	w.–m.
4	4	0	240	w.–m.,w.	10	3	0	40	o.
1	4	4	0	o.	8	7	0	440	w.–m.
4	3	3	10	v.	10	4	0	50	o.
2	4	4	1700	m.–s.	4	10	0	0	o.
6	0	0	4500	v.s.	6	9	0	0	o.

TABLE III. (*cont.*).

h.	*k.*	*l.*	F.	Obs.	*h.*	*k.*	*l.*	F.	Obs.
2	11	0	200	w.–m., w.	10	9	0	10	o.
10	5	0	40	v.	8	11	0	100	w.
8	8	0	480	w.–m.	4	13	0	50	v.
10	6	0	170	v.	12	7	0	20	o.
6	10	0	50	o.	14	0	0	100	v.
4	11	0	170	w.–m.	14	1	0	270	w.–m.
8	9	0	20	o.	10	10	0	270	v., o.
12	0	0	1200	m.–s.	14	2	0	520	w.–m.
12	1	0	10	o.	2	14	0	430	w.–m.
12	2	0	80	v.	14	3	0	10	o.
2	12	0	30	v.	6	13	0	30	o.
10	7	0	260	w.–m.	12	8	0	10	o.
12	3	0	0	o.	8	12	0	150	v.
6	11	0	0	o.	4	14	0	210	v.
12	4	0	0	o.	14	4	0	200	w.–m.
4	12	0	160	o.	10	11	0	200	w.
10	8	0	90	w.–m., w.	14	5	0	30	o.
8	10	0	50	o.	12	9	0	20	o.
12	5	0	110	o.	2	15	0	200	o.
2	13	0	20	o.	6	14	0	140	w., v.
12	6	0	750	m.	14	6	0	180	v.
6	12	0	300	m.					

It will be seen that the agreement is quite good, but emphasis must be laid on the fact that this does not prove that the group NH_3CH_3 is spherically symmetrical.

Consideration of the Structure.

In many features the structure, as is to be expected, resembles that of potash alum. The waters are of two kinds, one forming octahedral coordination groups around the aluminiums, and the other linking together the SO_4 groups, $Al6H_2O$ groups, and NH_3CH_3 groups.

The SO_4 group is tetrahedral with an average O–O distance of 2·5 Å. and S–O distance of 1·5 Å. (Actually the parameters adopted do not give a perfect tetrahedron, but it was found that changes of less than ·005 in the three parameters which define the general oxygen would give exact regularity. It was not, however, thought worth while to make these small changes which could not be justified by intensities.)

The $Al6H_2O$ group is a perfect octahedron with $Al–H_2O=1·87$ Å., and $H_2O-H_2O=2·65$ Å. Each of the waters in this group has external contacts to an oxygen

at a distance of 2·61 Å. and a water molecule at a distance of 2·57 Å. The arrangement of the three bonds to each water is shown in fig. 5 (*a*), and it will be seen that they are exactly coplanar.

The other water has four contacts, arranged tetrahedrally, to NH_3CH_3 at 3·55 Å., to H_2O at 2·57 Å., and to two O's at 2·83 Å. and 2·68 Å. The angles between these four bonds are shown in fig. 5 (*b*).

In addition to these linkages, there also appear to be bonds direct from the NH_3CH_3 group to the general

Fig. 5.

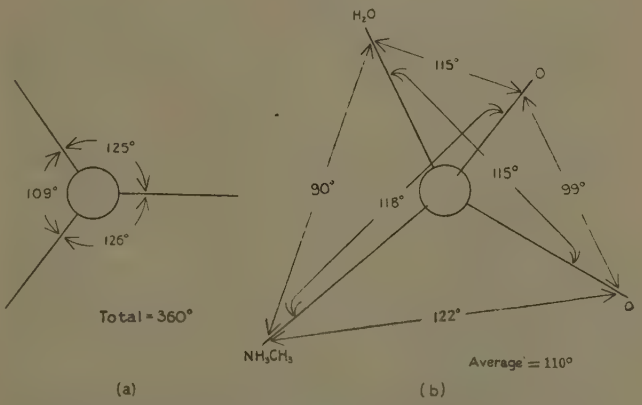

Disposition of bonds around the two kinds of water molecules.

oxygens. It has already been stated (p. 893) that these oxygens are as close to the centre of symmetry as are the waters, and thus if the NH_3CH_3 group is not spherical, the oxygens are actually closer. NH_3CH_3 thus has twelve bonds, which must thus of necessity be weak, and this may be the explanation of the large distance to H_2O.

It is in the direct contacts between the methylammonium groups and the sulphate groups that the structure differs from that of potash alum, but there are also some geometrical differences. These are illustrated in fig. 6 (*a*) and (*b*).

Fig. 6.

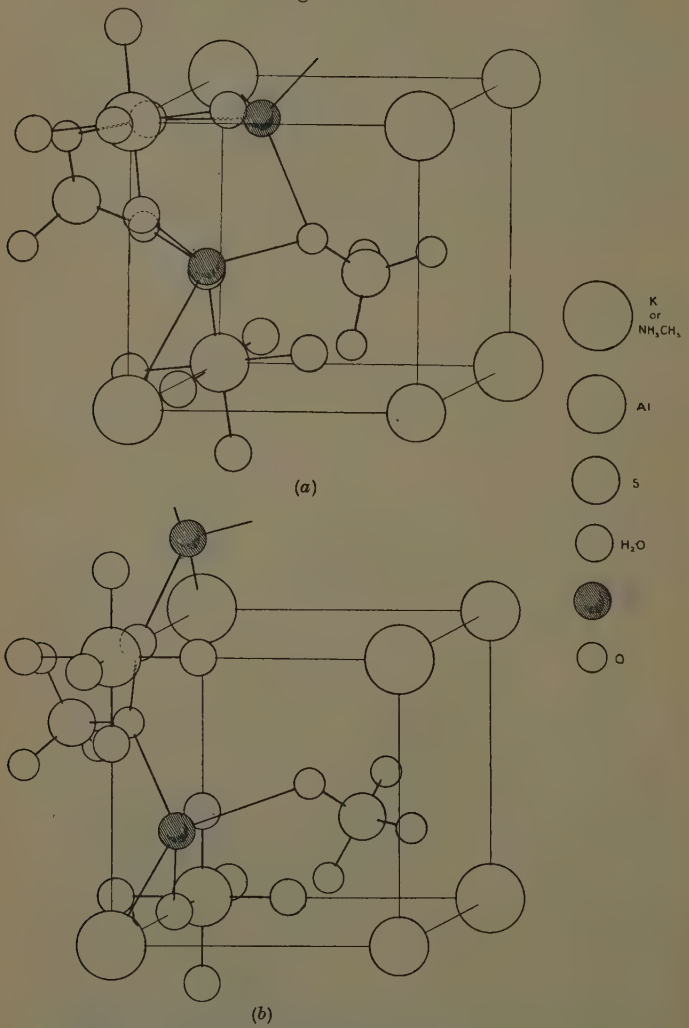

Comparison of the arrangement of groups in the structures of (*a*) potash alum and (*b*) methyl ammonium alum. The cube shown has its bottom left-hand corner at the point ($\frac{1}{2}$ 00).

These show corresponding parts of the unit cells of (*a*) potash alum, and (*b*) methyl ammonium alum. The tetrahedral natures of the shaded molecules are apparent; they have contacts to two oxygens which are similarly situated in the two structures, but the fourth contact, to water, is quite different. The contacts of the other water are still more dissimilar in the two structures. They form octahedral groups which are only slightly different in orientation, but it will be seen that the planes of the external contacts in two corresponding cases are almost at right angles to each other.

Some general Inferences concerning the Alums.

The fact that two salts which undoubtedly belong to the same type have essentially different structures seems so remarkable that further investigation is desirable.

Since the structures belong to the same crystal class, any differences in external development cannot decisively distinguish between them; but the forms of potash alum* and methyl ammonium alum grown under ordinary conditions are so definite that it was thought that they may, nevertheless, provide such a distinction. This idea is supported by an examination of the details given by Groth †, for practically all the alums appear to possess one or the other of the two sets of forms ‡. $KAl(SO_4)_2.12H_2O$, $KCr(SO_4)_2.12H_2O$, and $KAl(SeO_4)_2.12H_2O$ have been shown to possess § similar structures, and they have, under ordinary conditions, the same forms.

Many of the alums have the other forms, and it would be interesting to see whether these crystals have the "methyl-ammonium" alum structure.

A few intensities were estimated from a crystal of cæsium alum, which showed only the forms {111} and {210}. While the evidence cannot be regarded as definite until more exact estimations of the parameters are made, the low orders of reflexion did indicate that

* *Cf.* Buckley, *Zeits. f. Krist.* lxxiii. 5/6, p. 443 (1930).

† 'Chemische Krystallographie,' ii. pp. 565–574.

‡ Chrome alum is recorded as being able to show both the forms {210} and {110}, but an examination, by the author, of many crystals grown under ordinary conditions failed to reveal any {210} faces.

§ Beevers and Lipson, 'Nature,' cxxxiv. p. 327 (1934). The work of Cork (*loc. cit.*) cannot distinguish between the two structures.

the structure belongs to the same type as methyl ammonium alum. Some of the more decisive reflexions are shown in Table IV.

TABLE IV.

h. k. l.	Calculated F. (*a*)	Calculated F. (*b*)	Observed intensity.
2 1 0.....	22	35	s.
2 3 0.....	11	16	m.
4 2 0.....	54	15	m.
6 1 0.....	34	3	o.
6 2 0.....	46	81	s.

This table gives the F calculated from the parameters of (*a*) potash alum and (*b*) NH_3CH_3 alum.

A still more interesting question lies in the possibility of inducing the "methyl-ammonium" alum structure in potash alum and *vice versa*. An attempt was made to deposit methyl ammonium alum of a crystal of chrome alum, but this was unsuccessful, the edges of the crystal merely acting as centres of growth for individual crystals. On the other hand, it has been observed * that if a solution of potash alum be acidified with hydrochloric acid the crystals deposited have the {110} form eliminated and the {210} form present. It should be interesting to see whether this change implies also a change in structure.

Summary.

The question of the symmetry of the organic alums is discussed, and the crystal methyl ammonium alum, $NH_3CH_3Al(SO_4)_2.12H_2O$, is considered in detail.

Intensities of reflexion of X-rays, estimated from oscillation photographs, show that the structure is not similar to that of potash alum, and the correct structure is deduced. The positions of the light carbon and nitrogen atoms are not, however, definitely indicated, though considerations of space suggest that the group NH_3CH_3 is spherical.

* Buckley, *loc. cit.*

The structure differs essentially from that of potash alum in having direct bonds from the SO_4 groups to NH_3CH_3. There are also geometrical differences. It is suggested that the two alum structures may be distinguished by their external forms. This is supported by the X-ray data from $KCr(SO_4)_2.12H_2O$, $KAl(SeO_4)_2.12H_2O$, and $CsAl(SO_4)_2.12H_2O$. Further tests are suggested.

The author wishes to thank Prof. W. L. Bragg for the interest he has shown in this work and for the loan of a crystal of cæsium alum; also Mr. C. A. Beevers, of Manchester, whose discussion with the author of the problems involved proved very helpful, and who made the spacing measurement and carried out the test for pyroelectricity which the author later verified.

LXXIV. *The Thermal Conductivity and the Accommodation Coefficient of Carbon Dioxide.* *By* C. T. Archer, *M.Sc., A.R.C.S., F.Inst.P., Lecturer in Physics* *.

Introduction.

In a paper on the "Field of Force and the Form of the Carbon Dioxide Molecule," the authors, Ibbs and Wakeman [1], arrive at the conclusion that a definite change in the molecular field of force of the gas occurs at a temperature of about 145° C. This conclusion is reached from the results of their experiments on the thermal diffusion of the gas, which apparently shows a discontinuity at this temperature. Further evidence in support of their conclusion is based on their work on the viscosity of the gas, the variation of which with temperature is, according to their deductions, not continuous in the neighbourhood of the same temperature.

They further discussed other properties of carbon dioxide, amongst them the thermal conductivity in the neighbourhood of this temperature, but the data available were not sufficient to enable definite conclusions to be drawn.

* Communicated by Prof. G. P. Thomson, M.A., F.R.S.

Since the relation

$$K = f\eta C_v,$$

in which K is the thermal conductivity, C_v is the specific heat at constant volume, and f is a numerical constant depending on the forces operating on the molecules during collisions, involves the viscosity η, there seems to be some expectation that the discontinuity above mentioned would be reflected in the variation of the thermal conductivity of the gas with temperature.

The present work has been carried out for the purpose of testing this, and with this object in view the value of the thermal conductivity of carbon dioxide at various temperatures between 0° C. and 320° C., together with the values of the accommodation coefficient of the gas at different temperatures over the same range, have been determined.

A summary of the work which has been carried out and of the various methods which have been employed in the determination of the thermal conductivity of carbon dioxide is contained in a paper by Trautz and Zundel [2], references being quoted to cover the period from 1840 to 1931.

In the case of almost all the observers the value at one temperature only, 0° C., has been determined. In the case of Stafford [3], however, using the hot-wire method introduced by Schleiermacher [4], values were obtained at different temperatures between 23° C. and 546° C. It would appear that these values are too small in comparison with those of other observers, the extrapolated value at 0° C. being some 10 per cent. smaller than the average value given in the International Critical Tables, viz., 0·0000327 cal. cm.$^{-1}$ sec.$^{-1}$ deg.$^{-1}$, and some 15 per cent. smaller than the latest published value of 0·0000343 obtained by Weber (1927) [5] and by Kannuluik and Martin (1934) [6].

The chief difficulty associated with the measurement of the thermal conductivity of a gas is due to convection in the gas, a point which has been discussed fully in previous papers. Such convective losses of heat can be obviated in the plate method as used by Hercus and Laby [7]. In recent years, however, the hot-wire method has been used almost exclusively in work on thermal conduction in gases, and the results obtained by the various

observers are consistent, although a satisfactory method of dealing with convection from a theoretical aspect is not yet forthcoming. At the same time, the temperature-drop effect between the wire and the gas is inherent in the hot-wire method. Experiment has shown that the two effects overlap, so that by reducing the pressure of the gas with the object of minimizing or destroying the convection the temperature-drop effect is enhanced. It has been found possible to eliminate both these effects in one operation, and the importance of the method adopted in the present paper lies in this elimination, whereby the thermal conductivity of the gas and the accommodation coefficient are obtained from the observations.

Theory of Method.

The method used in the present series of measurements is the modification of the hot-wire method, described fully in a recent paper by Gregory [8], and used by him in the case of hydrogen.

It is not considered necessary to give a detailed account of the method here, but the following *résumé* indicates the essential points.

The temperature-drop at the surface of separation of a heated solid and a gas was defined by Kundt and Warburg [9] by the relation

$$\delta\theta = -\gamma \frac{d\theta}{dn},$$

where γ is a quantity proportional to the mean free path of the gas-molecules and $\frac{d\theta}{dn}$ the normal temperature gradient at a point in the gas near the solid.

Smoluchowski [10], by using Maxwell's hypothesis regarding molecular repulsion, found that the temperature-drop was represented by the relation

$$\delta\theta = -\frac{15}{2\pi} \cdot \frac{2-\alpha}{2\alpha} \cdot \lambda \frac{d\theta}{dn},$$

where α is the accommodation coefficient as defined by Knudsen [11], and λ the mean free path of the gas-molecules.

In the case of a heated wire maintained at a temperature T_1 in contact with a gas, and coaxial with a tube whose internal wall is maintained at a temperature T_2, the temperature discontinuity between the gas and the surface of the wire is

$$\delta\theta_1 = T_1 - T',$$

and the accommodation coefficient is given by

$$\alpha = \frac{T - T'}{T_1 - T'},$$

where T' and T denote the average temperatures of the molecules approaching and leaving the wire.

Hence

$$\delta\theta_1 = \frac{\lambda_0 P_0}{P} \cdot \frac{15}{2\pi} \cdot \frac{2-\alpha}{2\alpha} \cdot \frac{Q_0}{2\pi K_1 l r_1}.$$

Similarly, at the internal wall of the tube, the temperature-drop between the gas and the surface

$$\delta\theta_2 = \frac{\lambda_0' P_0}{P} \cdot \frac{15}{2\pi} \cdot \frac{2-\alpha'}{2\alpha'} \cdot \frac{Q_0}{2\pi K_2 l r_2}.$$

In the above expressions λ_0 and λ_0' are the mean free paths of the gas-molecules at the temperatures of the wire and the tube-wall respectively, and at a pressure of one atmosphere P_0, P the pressure of the gas, l the length of the heated wire assumed to be uniform in temperature throughout its length, K_1 and K_2 the thermal conductivities of the gas at the wire and wall temperatures, r_1 and r_2 the radii of the wire and the tube, and Q_0 the heat transferred in the absence of temperature-drop and convection.

By Fourier's law, for a cylindrical temperature distribution, we have, then,

$$Q \log_e \frac{r_2 - \lambda'}{r_1 + \lambda} = 2\pi K l (T' - T''),$$

T'' referring to the molecules near the wall of the tube and K the absolute thermal conductivity of the gas at a mean temperature of $(T_1+T_2)/2$,

i. e.,
$$Q \log_e \frac{r_2 - \lambda'}{r_1 + \lambda} = 2\pi K l (T_1 - \delta\theta_1 - \overline{T_2 + \delta\theta_2})$$
$$= 2\pi K l \theta - 2\pi K l (\delta\theta_1 + \delta\theta_2),$$

where $\theta = T_1 - T_2$.

Hence $$Q \log_e \frac{r_2-\lambda'}{r_1+\lambda} = 2\pi K l\theta - \frac{15}{2\pi} \cdot \frac{2\pi K l P_0}{P} \cdot \frac{Q_0}{2\pi l} \left\{ \frac{2-\alpha}{2\alpha} \cdot \frac{\lambda_0}{K_1 r_1} + \frac{2-\alpha'}{2\alpha'} \cdot \frac{\lambda_0'}{K_2 r_2} \right\}.$$

Since r_2 is about $100 r_1$, the second term, $\frac{2-\alpha'}{2\alpha'} \cdot \frac{\lambda_0'}{K_2 r_2}$, is small compared with the first, and it is, accordingly, justifiable to substitute α for α'. Thus

$$\frac{Q}{\theta} \log_e \frac{r_2-\lambda'}{r_1+\lambda} = 2\pi K l - \frac{15}{2\pi} \cdot \frac{2-\alpha}{2\alpha} \cdot \frac{P_0}{P\theta} \cdot \frac{2\pi K l Q_0}{2\pi l} \left\{ \frac{\lambda_0}{K_1 r_1} + \frac{\lambda_0'}{K_2 r_2} \right\}.$$

But

$$Q_0 = \frac{2\pi K l\theta}{\log_e \frac{r_2}{r_1}}.$$

Therefore

$$\frac{Q}{\theta} \log_e \frac{r_2-\lambda'}{r_1+\lambda} = 2\pi K l - \frac{15}{2\pi} \cdot \frac{2-\alpha}{2\alpha} \cdot \frac{P_0}{2\pi P l} \cdot \frac{(2\pi K l)^2}{\log_e \frac{r_2}{r_1}} \left\{ \frac{\lambda_0}{K_1 r_1} + \frac{\lambda_0'}{K_2 r_2} \right\}. \quad (1)$$

Plotting values of $\frac{Q}{\theta} \log_e \frac{r_2-\lambda'}{r_1+\lambda}$ against values of $\frac{1}{P}$, a linear relation holds. The intercept of the line is a measure of the quantity $(2\pi K l)$, from which the value of K is determined. The slope of the line is a measure of the quantity

$$\frac{15}{2\pi} \cdot \frac{2-\alpha}{2\alpha} \cdot \frac{P_0}{2\pi l} \cdot \frac{(2\pi K l)^2}{\log_e \frac{r_2}{r_1}} \left\{ \frac{\lambda_0}{K_1 r_1} + \frac{\lambda_0'}{K_2 r_2} \right\},$$

from which the value of α is determined.

By writing $K_1 = K_2$, which is justified, since the value of the term $\frac{\lambda_0}{K_1 r_1}$ is small compared with $\frac{\lambda_0'}{K_2 r_2}$, the

above expression for the slope of the line is modified, and becomes

$$\frac{15}{2\pi}\cdot\frac{2-\alpha}{2\alpha}\cdot P_0\cdot\frac{2\pi Kl}{\log_e\frac{r_2}{r_1}}\cdot\frac{K}{K_1}\left\{\frac{\lambda_0}{r_1}+\frac{\lambda_0'}{r_2}\right\}, \quad . \quad . \quad (2)$$

which is the working expression used in the present instance.

Experimental Details.

(a) *Thermostat.*

The thermostat employed in the present work was the same as that used by Gregory [8] in his work on hydrogen. A special thermostat oil supplied by Messrs. C. C. Wakefield & Co., Ltd., was used, the oil being heated electrically by means of a number of resistance coils immersed in it, rheostats providing the control of current required for the different temperatures. Circulation of the oil in the bath was maintained by a motor-driven propeller so arranged that a constant stream of oil flowed past the gas-tube system.

(b) *Gas-tube System.*

The apparatus consisted of a single pair of compensated glass tubes and platinum wires, as usually employed in the hot-wire method, with the addition of an external platinum wire to measure the wall temperature.

The glass tubes were cut from a selected piece of Pyrex tubing, the tubing having been examined carefully for uniformity of bore, and the internal and external radii of the chosen length were determined. The internal radius was found by the method of weighing the quantity of mercury required to fill a measured length of the tubing and the external radius by the use of accurate slide calipers. It was considered necessary to use a tube of fairly small internal radius in order to minimize the effects of convection.

The internal platinum wires were cut from a length of pure platinum resistance thermometer wire, the radius of the whole length being determined from its mass. Here again it was considered necessary to use wire of small diameter in order to enhance the temperature-drop effect. At the same time, by using thin wires the

radiation correction is reduced and the accuracy of the temperature measurements is increased. These thin wires were attached to thick platinum leading wires and springs and sealed carefully in the tubes so as to secure accurate compensation of end-effects etc., and also a uniform radial distribution of temperature.

The external platinum wires were also of pure platinum, but of larger diameter. In order to ensure accuracy in the measurement of the external wall temperatures, this wire was first given a thin coating of Pyrex glass and then fused to the outer wall of the tube in the form of a spiral along the whole length of each tube. The walls of the tubes being fairly thick, it was found possible to do this without deforming the tubes in any way, and to secure the wire to the walls with little difficulty.

The dimensions of the tubes and the internal wires were :—

Radius of wire (r_1)	= 0·003823 cm.
Effective length (l)	=20·32 cm.
Internal radius of tube (r_2)	= 0·3263 cm.
External „ „ (r_3)	= 0·4592 cm.

(c) *Other Apparatus.*

The necessary temperature measurements were made by using Callendar-Griffiths bridges for both the internal and the external wires. Each system of compensated wires was calibrated in the usual manner at the temperatures of melting ice and of steam from boiling water, the calibrations obtained being :—

Resistance of internal wire at	0° C.	=4·354 ohm.
„ „ „	100·07° C.	=6·049 „
	Fundamental interval	=1·695 „
Resistance of external wire at	0° C.	=1·731 „
„ „ „	100·14° C.	=2·406 „
	Fundamental interval	=0·675 „

From these figures the temperatures of the wires corresponding to any bridge-setting can be calculated.

The current required to maintain the internal wire at any specified temperature during the observations was obtained by means of a Crompton potentiometer, using

a standard 1-ohm resistance coil in the circuit. Adjustment of the current for balance in the bridge-circuit of the internal wires was effected by variable resistances, fine adjustment being obtained by using a sensitive mercury rheostat.

Variations of the pressure of the gas were made by using a Hyvac pump, and measurements of the pressure obtained from readings on a mercury manometer mounted with an accurate mirror-scale.

(d) *Preparation of Gas.*

The carbon dioxide used in the observations was prepared from pure air-free calcite and pure hydrochloric acid, using a Kipp's apparatus. The gas was thoroughly dried by being passed through a series of wash-bottles containing pure concentrated sulphuric acid before being admitted to the tube system.

Experimental Procedure.

The experimental procedure followed in taking the observations was substantially the same as that followed in previous work on thermal conduction in gases, using a compensated hot-wire system in which the author has taken part and which is described fully elsewhere [12], except that an oil thermostat heated electrically was used instead of an ice-bath.

The oil in the thermostat was heated to some predetermined temperature, and the current in the heating coils adjusted until a slight cooling of the bath commenced. By this means the heating up of the tube-walls during the course of the experiment was obviated. The platinum wire in the tube system containing the gas having been calibrated previously by means of the Callendar-Griffiths bridge, the bridge was then set to correspond to a temperature of the wire some 20° C. above that of the bath, and the current through the wire was adjusted until balance of the bridge was obtained, the strength of current being observed by means of the Crompton potentiometer, the pressure of the gas also being observed. At the same time the temperature of the external walls of the tube system was observed by means of the platinum wire in contact with the walls in conjunction with the second Callendar-Griffiths bridge, this platinum wire

also having been calibrated previously. A new set of observations was then made after reducing the pressure by a suitable amount and adjusting, if necessary, the current passing through the internal platinum wire to effect balance of the bridge-circuit and assure constancy of temperature of this heated wire. This procedure was repeated, reducing the pressure of the gas in stages until observations were obtained over a range of pressure sufficient to meet the conditions imposed by the theoretical treatment with regard to convection and temperature-drop.

Similar sets of observations were made with the oil-bath at various temperatures up to about 300° C., the highest temperature being safely below the flash-point of the oil used in the thermostat, eleven series of readings in all being taken.

Corrections and Calculations.

(a) *Temperatures.*

The temperatures of the internal and external wires, calculated from the observations on the Callendar-Griffiths bridges, must be reduced from the platinum scale to the centigrade scale. For this purpose the tables of corrections compiled by Hoare [13] were used, and the temperatures quoted below are those obtained after such corrections had been applied.

From the temperatures given by the external platinum wires the temperatures of the internal surface of the tube-walls must be determined. For this purpose a knowledge of the thermal conductivity of Pyrex glass and its variation with temperature is required. The desired temperatures can then be found from the relation

$$\theta_g = \theta_w + \frac{Q \log_e \frac{r_3}{r_2}}{2\pi K_g l},$$

where θ_w is the observed temperature of the external walls, K_g the thermal conductivity of the glass, and Q the total quantity of heat transmitted through the walls. The thermal conductivity of Pyrex glass over a range of temperature from $-182°$ C. to 250° C. has been determined by Stephens [14], his results being expressed in the form

$$K_g = -0{\cdot}00352 + 0{\cdot}00245 \log_{10} T,$$

where T is temperature on the absolute scale. This relation was employed to calculate the values of θ_g required.

(b) *Heat Transmission.*

The total quantity of heat in calories transmitted from the hot wire through the gas is given by the relation

$$Q = \frac{C^2R}{J},$$

where C is the observed value of the current in amperes, R the resistance of the hot wire in ohms obtained from the bridge-settings for the internal wire, and J the mechanical equivalent of heat (4·184 joules per calorie).

(c) *Radiation.*

The total quantity of heat transmitted from the wire includes a small percentage due to radiation from the surface of the platinum wire, and a correction is necessary, therefore, to allow for this. In the present instance it was found sufficiently accurate to calculate the correction, for each set of temperature conditions employed in the work, by using the relation obtained by Milverton [15]. The heat lost by radiation per unit length of platinum wire is given by

$$\phi = 1{\cdot}87\ (T_1^{3{\cdot}82} - T_2^{3{\cdot}82}) \times 10^{-14}\ \text{cal.},$$

where T_1 is the absolute temperature of the platinum wire and T_2 that of the tube-wall.

(d) *Mean Free Path.*

The working expression above (2) used in the determinations requires a knowledge of the mean free path of the gas-molecules at the temperature of the hot wire, and also of the walls of the tube, for each set of observations. The necessary values can be calculated by using the relation

$$\lambda = \frac{2{\cdot}02\,\eta}{\sqrt{P\rho}},$$

where η is the viscosity of the gas at the required temperature, P is a pressure of one atmosphere in dynes per cm.^{2}, and ρ the density of the gas at N.T.P. in gm.

per c.c. The values used for the viscosity were those obtained by Trautz and Kurz [16], and from these the values of λ_0 and λ_0' at one atmosphere pressure were found for each set of observations.

Since

$$\lambda = \frac{\lambda_0 P_0}{P} \quad \text{and} \quad \lambda' = \frac{\lambda_0' P_0}{P},$$

and since the pressure P is varied through a set of observations, it was found convenient to put the left-hand side of the working equation above (1) in the form

$$\frac{Q}{\theta} \log_e \frac{r_2}{r_1} \left\{ \frac{P - \frac{\lambda_0' P_0}{r_2}}{P + \frac{\lambda_0 P_0}{r_1}} \right\},$$

which simplified the calculations considerably and was used throughout the work.

Observations and Results.

Typical examples of the observations made in the course of the work are tabulated below, each table representing a different set of temperature conditions. In the tables the following symbols are used :—

P = Pressure of gas in cm. of mercury.

θ_P = Temperature of hot wire in ° C.

θ_w = Temperature of external wall of tube in ° C.

θ_g = Temperature-difference between external and internal wall of tube in ° C.

θ = Temperature-difference between hot wire and internal wall of tube in ° C. given by the relation

$$\theta = \theta_P - (\theta_w + \theta_g).$$

Q = Total heat-loss in calories, corrected for radiation.

C = Current in amperes passing through hot wire.

R = Resistance in ohms of hot wire at temperature θ_P° C.

ϕ = Radiation correction in calories.

TABLE I.

R = 9·231 ohms.

ϕ = 0·00176 cal.

θ_P = 296·61° C.

$\frac{1}{P}$.	C.	θ_w.	θ_g.	$\frac{Q}{\theta}\log_e\frac{r_2-\lambda'}{r_1+\lambda}$.
0·0372	0·1740	268·86	0·07	0·010436
0·0596	0·1730	268·88	0·07	0·010310
0·0880	0·1718	268·93	0·07	0·010157
0·1078	0·1711	268·99	0·07	0·010085
0·1271	0·1707	268·96	0·07	0·010020
0·1477	0·1703	268·91	0·07	0·009946
0·1862	0·1696	268·83	0·07	0·009814
0·2288	0·1683	268·72	0·06	0·009602
0·3155	0·1662	268·68	0·06	0·009299
0·4032	0·1644	268·59	0·06	0·009025
0·7092	0·1622	268·55	0·06	0·007821

Intercept = 0·01050.
Slope = 0·003772.
Mean temperature of gas = 282·75° C.

TABLE II.

R = 7·794 ohms.

ϕ = 0·00102 cal.

θ_P = 206·36° C.

$\frac{1}{P}$.	C.	θ_w.	θ_g.	$\frac{Q}{\theta}\log_e\frac{r_2-\lambda'}{r_1+\lambda}$.
0·0220	0·1668	179·53	0·06	0·008438
0·0339	0·1666	179·53	0·06	0·008412
0·0463	0·1659	179·61	0·06	0·008357
0·0618	0·1654	179·64	0·06	0·008311
0·0775	0·1650	179·67	0·06	0·008274
0·0944	0·1645	179·65	0·06	0·008211
0·1192	0·1638	179·69	0·06	0·008143
0·1669	0·1627	179·77	0·05	0·008039
0·2045	0·1618	179·77	0·05	0·007935
0·2639	0·1605	179·79	0·05	0·007790
0·3460	0·1590	179·82	0·05	0·007625
0·5025	0·1563	179·83	0·05	0·007310

Intercept = 0·008424.
Slope = 0·002272.
Mean temperature of gas = 193·05° C.

TABLE III.

R=4·769 ohms.
ϕ =0·00022 cal.
θ_P=24·224° C.

$\frac{1}{P}$.	C.	θ_w.	θ_g.	$\frac{Q}{\theta}\log_e\frac{r_2-\lambda'}{r_1+\lambda}$.
0·0265	0·1505	0	0·034	0·004701
0·0371	0·1504	—	0·034	0·004694
0·0469	0·1503	—	0·034	0·004686
0·0627	0·1501	—	0·034	0·004673
0·0978	0·1499	—	0·034	0·004655
0·1277	0·1497	—	0·034	0·004638
0·1742	0·1495	—	0·034	0·004619
0·2825	0·1490	—	0·034	0·004570
0·4274	0·1483	—	0·033	0·004510
0·7463	0·1468	—	0·033	0·004378

Intercept=0·004716.
Slope=0·000474
Mean temperature of gas=12·129° C.

The tables above constitute part of the data obtained in the course of the experiments, the whole being represented by the eleven graphs reproduced in fig. 1. As already explained, these graphs are obtained by plotting the values of $\frac{1}{P}$ against the values of $\frac{Q}{\theta}\log_e\frac{r_2-\lambda'}{r_1+\lambda}$. Each line refers to a particular average temperature of the gas, the values of which, in order reading from the top of the figure, are given in Table IV. (p. 914). From the value of the intercept in each case the thermal conductivity of the gas at the average temperature shown is calculated, and from the value of the slope of the line in each case the accommodation coefficient for the gas at the temperature of the heated wire. The temperatures given are quoted on the absolute scale and the values of the thermal conductivity in the usual units, *i. e.*, cal. cm.$^{-1}$ sec.$^{-1}$ deg.$^{-1}$ C.

The values of the thermal conductivity thus obtained are shown in column 2 of Table IV. (p. 914).

Fig. 1.

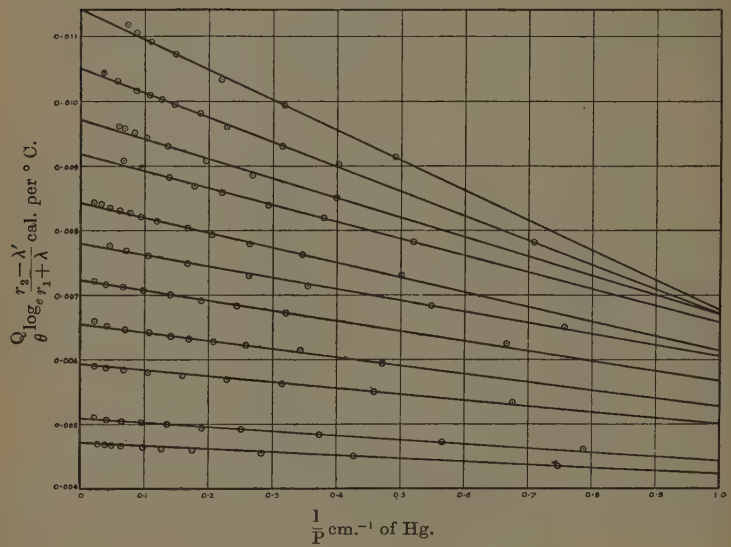

TABLE IV.

Mean temperature of gas.	$K_{obs.}$	$K_{calc.}$	Percentage difference.
591·8	0·0000894	0·0000888	+0·7
555·8	822	822	0
527·7	761	772	−1·4
501·1	719	725	−0·8
466·0	660	664	−0·6
431·6	611	605	+1·0
406·5	566	562	+0·7
373·6	512	507	+1·0
347·7	465	465	0
309·7	399	404	−1·2
285·1	369	365	+1·1

With reference to the variation of the thermal conductivity with temperature, the logarithms of the observed values of K were plotted against the logarithms of the ratio T/T_0 ($T_0=273°$ Å.), and the result is shown graphically in fig. 2.

The graph is evidently nearly rectilinear, implying the relation

$$\log K=\log K_0+n \log (T/T_0)$$

or

$$K=K_0\left(\frac{T}{T_0}\right)^n,$$

Fig. 2.

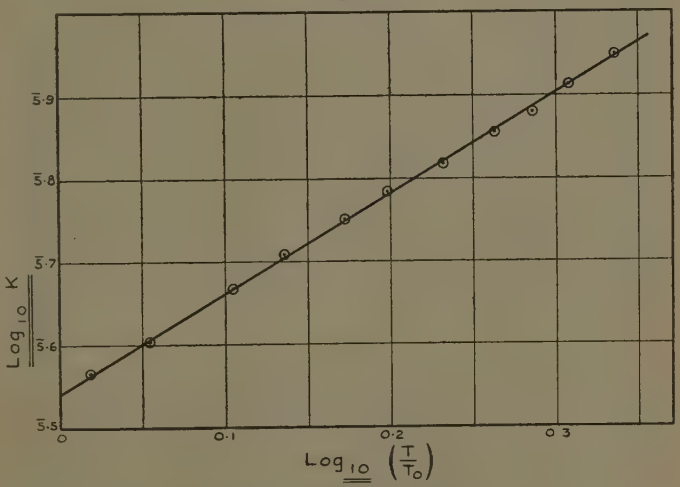

where $\log K_0$ is represented by the intercept on the log K axis and n by the slope of the line.

To obtain these constants the best straight line (shown in the diagram) was drawn through the experimental points.

The results thus found are

$$n=1\cdot216$$

$$K_0=0\cdot0000347 \text{ cal. cm.}^{-1} \text{ sec.}^{-1} \text{ deg.}^{-1} \text{ C.}$$

The value of K_0 is in good agreement with that obtained by other recent observers, namely, 0·0000343 cal. cm.$^{-1}$ sec.$^{-1}$ deg.$^{-1}$ C. found by Weber [5] and by Kannuluik and Martin [6].

The percentage-differences between the observed and calculated values of K (found by using the values of n and K_0 above) are shown in column 4 of Table IV. These are of the same order as the errors to which the experiments are liable.

The change in the relation between the viscosity and temperature for carbon dioxide, which Ibbs and Wakeman[1] claim to have found at about 145° C., appears in their paper as a discontinuity at 145° C. of the log (viscosity)–log (temperature) curve. This is represented by two straight lines of different slopes above and below this temperature.

An inspection of the relation between log K and log (T/T_0), having regard to the accuracy of the measurements, does not indicate any discontinuity, either at 145° C. or elsewhere. Accordingly these results do not give support to the findings of Ibbs and Wakeman[1] that there is an abrupt change of the molecular field of force of carbon dioxide at this temperature.

With regard to the accommodation coefficient of the gas, the values calculated as explained above are shown in the following table, together with the corresponding absolute temperature of the heated platinum wire in each case.

TABLE V.

Temperature of wire.	Accommodation coefficient.
604·8	0·28
569·6	0·29
541·7	0·32
514·3	0·33
479·4	0·33
445·2	0·37
418·9	0·36
385·7	0·39
359·9	0·42
321·3	0·45
297·2	0·51

These results are shown graphically in fig. 3, the graph representing the variation of the accommodation coefficient with the absolute temperature of the wire.

These values represent entirely new data. It should be pointed out that they are obtained from observations over a range of pressure where the accommodation coefficient is independent of pressure.

Although a considerable amount of work has been carried out on the accommodation effect in various gases, few values of the coefficient for carbon dioxide are available for comparison with the present results. Knudsen [17], who obtained values for several gases from observations on the conduction of heat through the gases in a rarefied state, quotes the value for carbon dioxide as 0·86, and

Fig. 3.

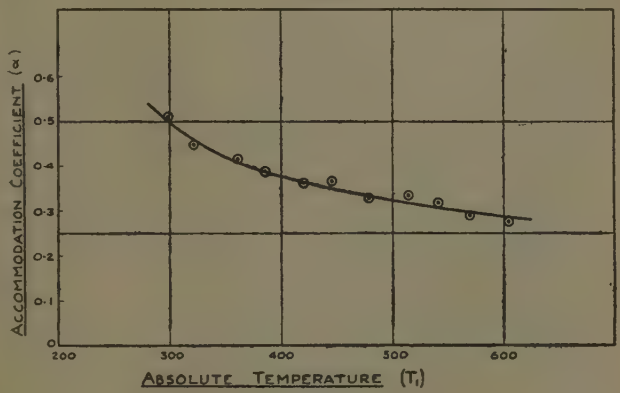

Dickins [18] gives an average value of 0·91 at a temperature of about 12° C. obtained from observations on the thermal conductivity of the gas. It has been shown, however, that the latter value is reduced considerably when the more rigorous theory of the effect of accommodation used in the present instance is applied to the observations.

Summary.

The thermal conductivity of carbon dioxide has been determined, using the hot-wire method, at different temperatures over a range of about 300° C., the values found varying from 0·0000347 at 0° C. to 0·0000894 cal. cm.$^{-1}$ sec.$^{-1}$ deg.$^{-1}$ at 318·8° C. A constant temperature oil-bath heated electrically was used, the temperatures

being measured by means of platinum wire fixed on the glass walls of the tube system.

The variation of the thermal conductivity of the gas with temperature has been found to obey a law of the type $K_T = C.T^n$, in which $n = 1{\cdot}216$ for the range of temperature dealt with. The results do not indicate any change in accordance with the conclusions of Ibbs and Wakeman.

The accommodation coefficient of the gas in contact with a platinum surface at different temperatures over the same range of temperature has been obtained also from the observations, the values ranging from 0·51 at 24·2° C. to 0·28 at 331·8° C.

References.

(1) Ibbs and Wakeman, Proc. Roy. Soc. A, cxxxiv. p. 613 (1932).
(2) Trautz and Zundel, *Zeits. tech. Phys.* xii. p. 273 (1931).
(3) Stafford, *Zeits. Phys. Chem.* lxxvii. p. 66 (1911).
(4) Schleiermacher, Wied. *Ann.* xxxiv. p. 623 (1888).
(5) Weber, *Ann. d. Phys.* (4) lxxxii. p. 479 (1927).
(6) Kannuluik and Martin, Proc. Roy. Soc. A, cxliv. p. 496 (1934).
(7) Hercus and Laby, Proc. Roy. Soc. A, xcv. p. 190 (1919).
(8) Gregory, Proc. Roy. Soc. A, cxlviii. p. 866 (1935).
(9) Kundt and Warburg, Pogg. *Ann.* clvi. p. 177 (1875).
(10) Smoluchowski, *Ann. d. Phys.* xxxv. p. 983 (1911).
(11) Knudsen, *Ann. d. Phys.* xxxiv. p. 593 (1911).
(12) Gregory and Archer, Proc. Roy. Soc. A, cx. p. 91 (1926).
(13) Hoare, Jour. Sci. Inst. vi. p. 3 (1929).
(14) Stephens, Phil. Mag. (7) xiv. p. 897 (1932).
(15) Milverton, Phil. Mag. (7) xvii. p. 397 (1934).
(16) Trautz and Kurz, *Ann. d. Phys.* ix. p. 983 (1931).
(17) Knudsen, *Ann. d. Phys.* xl. p. 492 (1913).
(18) Dickins, Proc. Roy. Soc. A, cxliii. p. 517 (1934).

Royal College of Science,
London S.W. 7.

LXXV. *The Intensity Ratios of the Fluorescent X-ray Emission Lines in the L-region and their Dependency on the Voltage.* *By* H. Hirst, *Nat.Phil.D., B.Sc.(Eng.),* *and* Dr. Ing. E. Alexander *.

THE interest in the X-ray fluorescence radiation which played such an important part in the pioneer work of Barkla has much increased in later years. The work on quantitative chemical analysis by X-rays may be quoted, where fluorescent radiation is applied to mixtures

* Communicated by Prof. W. L. Bragg, M.A., F.R.S.

which undergo changes on the application of cathode rays. The work with fluorescent radiation was much facilitated by the construction of an effective X-ray tube, giving a strong secondary radiation, and its several successors *.

The aim of the present research was the determination of the ratios of the intensities of the L-lines when excited by X-radiation and their dependency on the applied voltage. The knowledge of these ratios is important in connexion with the above-mentioned work and also from a theoretical point of view. When comparing L-lines originating from the same level, the intensity ratio must be independent of the applied voltage. When, however, lines belonging to different electron groups are compared, which is often the case in X-ray analysis, a dependency on the voltage is to be expected. This dependency originates from two causes. Firstly, wave-lengths between the two absorption edges of the compared lines will only excite the line belonging to the softer edge. Therefore the amount of these wave-lengths in the exciting radiation in comparison with that of shorter wave-lengths, which are able to excite the other line also, must have an influence on the intensity ratio of the two lines, this ratio being zero for all voltages up to the exciting voltage of the harder absorption edge. With further increase of the voltage the amount of line-intensity due to the wave-lengths between the edges will be comparatively less, the intensity ratio, therefore, increasing with the voltage.

Secondly, when two fluorescent X-ray lines originating from different electron levels are excited by monochromatic primary rays of different wave-lengths, the intensity ratio of the lines is dependent on the exciting wave-length. This dependency is due to the fact that the absorption ratio of different levels—for instance L_I : L^{III}—is dependent on the absorbed wave-length, and, therefore, the same dependency must arise for the intensity ratio of the corresponding emission lines †.

* Coster and Druyvesteyn, *Z. Phys.* xl. p. 756 (1927); Alexander and Faessler, *Z. Phys.* lxviii. p. 260 (1931).

† H. W. Skinner, Proc. Cambridge Phil. Soc. xxii. p. 39 (1925); G. v. Hevesy and E. Alexander, 'Nature,' cxxix. p. 315 (1932). E. Alexander, *Z. Phys.* lxxv. p. 391 (1932); G. Schur, *A. d. Phys.* (5) iv. p. 433 (1930); H. R. Robinson, Proc. Roy. Soc. civ. p. 445 (1923).

When, therefore, the fluorescent radiation is excited by continuous X-radiation, as was done in the present research, it was to be expected that the intensity ratio of emission lines not belonging to the same electron level would be dependent on the voltage, due to the two above-mentioned causes. Both effects increase the intensity ratio with increasing voltage in favour of the line belonging to the harder absorption edge.

One of the aims of the present research was to investigate this dependency of the intensity ratio of fluorescent X-ray lines on the voltage of the exciting continuous radiation, and to ascertain whether there is a minimum voltage above which the intensity ratio of two lines originating from different levels remains constant. In spite of the two above-mentioned effects there can be practically a voltage at which the harder wave-lengths of the exciting radiation are absorbed in so small an amount and at so great a depth that their contribution to the resulting intensities of the fluorescent lines is practically negligible, thus giving rise to a constant maximum intensity ratio at the higher voltages.

The L-lines of tungsten, thallium, and uranium were investigated, the lines being excited by the continuous radiation of tungsten.

A summary of the work which has been done on intensity ratios, using primary radiation, is to be found in Siegbahn's 'Spektroskopie der Röntgenstrahlen.' Up to the present time, however, no work other than that described in this paper and that of Woo * on the K emission lines, has yet been carried out in this field with fluorescent radiation.

Apparatus employed.

The vacuum spectrograph † and the X-ray tube used in these experiments were ones which had been developed in the laboratory at Freiburg specially for this kind of work. High tension direct current was supplied to the tube after rectification by valves.

Agfa Laue films coated on both sides were used, special care being taken over the development and measurement

* Y. H. Woo, Phys. Rev. ii. xxviii. p. 427 (1926).
† E. Alexander, *Z. Phys.* lxxxiii. p. 512 (1933).

of the films, so as to obtain uniform results. The measurements of the intensities of the emission lines were carried out on a Koch and Goos photometer.

Experimental Results.

In order to be able to compare the intensity of the very strong α_1 line with that of other lines, the following method was adopted. At each voltage three or four films were exposed for different lengths of time. After measuring the intensities on the photometer, the time of exposure was plotted as a function of the electrometer deflexion. Where the curve deviated from a straight line—and this was generally the case for the α_1 line—the tangent to the

Fig. 1.

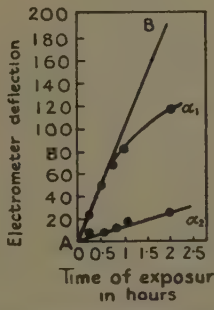

Dependency of the photometric reading on the time of exposure. The straight line AB shows the value of the electrometer deflexion, which is to be considered when comparing line-intensities.

curve through the origin was drawn. Fig. 1 shows this process applied to the lines $L\alpha_1$ and $L\alpha_2$ of thallium at a voltage of 33 kv. and tube-current of 40 milliamperes. As seen from Table I., the above method gives uniform results for each time of exposure excepting very short exposures.

At certain voltages above the exciting voltage the intensity ratios of the following five lines of tungsten were measured:—

Level.	Line.
L_I	β_3.
L_{II}	β_1.
L_{III}	α_1, α_2, β_2.

Table II. gives the intensities of these lines for various times of exposure after corrections had been made for the absorption of the rays in (1) the aluminium foil over the slit, and (2) the cellophane window, and for the dependency of the amount of absorption of the rays by the film on the wave-length of the rays concerned. Another correction taken into account is that due to the smaller amount of absorption of the harder rays in the secondary radiator as compared with the softer rays. For the above-mentioned lines of tungsten the maximum correction due to this effect amounts to only 12 per cent. For the same lines of uranium, however, the correction is 60 per cent. This correction is very important when

TABLE I.

Time of exposure (hours).	Intensity. Experimental value.		Intensity. After graphical interpolation.		Intensity ratio.
	α_1.	α_2.	α_1.	α_2.	α_1/α_2.
0·25 ..	23·0	4·7	23·0	4·7	5·10
0·5 ...	49·2	6·2	49·2	6·2	7·94
0·75 ..	67·0	8·9	72·0	8·9	8·08
1	81·3	13·3	96·0	13·3	7·22
2	114	23·5	182	23·5	7·74

comparing lines excited by cathode and by X-rays. In the former case the lines are emitted from a very thin surface-layer of the radiator, so that a correction for the above-mentioned effect is unnecessary. When this correction is omitted for the excitation by X-rays, however, the intensity of the harder rays is too great as compared with that of the softer rays.

The intensity ratios at the different voltages are shown in Table III., whilst fig. 2 gives the results in graphical form.

The intensity ratios of the lines originating from the same level, namely, α_1, α_2, and β_2, are independent of the voltage. The other ratios, however, show a strongly marked dependency on the applied voltage, and reach

TAB

Intensities of the Tungsten L-line

Voltage (k.v.).	Time of exposure (hours).	α_2.			α_1.		
		Experimental values.	After graphical interpolation.	With corrections.	Experimental values.	After graphical interpolation.	With corrections.
18...	2·0	3·20	3·20	9·55	23·8	23·8	72·7
	3·5	5·00	5·00	14·9	41·5	41·5	127
	5·0	7·00	7·00	20·9	56·8	58·8	180
23...	1·0	4·50	4·50	13·4	37·2	37·2	114
	1·5	7·00	7·00	20·9	55·5	55·5	170
	2·0	9·00	9·00	26·8	69·3	74·5	228
	2·5	11·3	11·3	33·7	81·2	93·0	284
28...	0·85	5·70	5·70	17·0	47·0	47·0	144
	1·0	7·50	7·50	22·3	56·3	56·3	173
	1·25	9·30	9·30	27·6	70·7	70·7	216
	1·65	11·7	11·7	34·8	83·6	92·4	282
32...	0·5	5·20	5·20	15·5	42·8	42·8	131
	1·0	11·0	11·0	32·9	81·0	85·0	260
	1·15	13·0	13·0	38·6	88·7	98·3	301
	1·25	13·7	13·7	40·8	93·9	107	327
36·5 .	0·5	5·70	5·70	17·0	42·8	42·8	131
	0·75	7·60	7·60	22·7	64·5	64·5	197
	1·0	10·9	10·9	32·5	78·1	85·8	263
	1·25	13·7	13·7	40·8	88·4	108	329
40...	0·25	—	—	—	38·9	38·9	119
	0·5	9·30	9·30	27·7	71·7	75·6	232
	0·7	12·9	12·9	38·4	92·9	103·6	317
	0·85	16·2	16·2	48·1	103·4	128·5	392
45...	0·5	7·30	7·30	21·8	58·3	58·3	178
	1·0	14·7	14·7	43·8	95·3	116	355

[*To face* p. 922.

LE II.

s. (Tube-current 20 ma.)

Intensity.

β_1.			β_3.			β_2.		
Experimental values.	After graphical interpolation.	With corrections.	Experimental values.	After graphical interpolation.	With corrections.	Experimental values.	After graphical interpolation.	With corrections.
6·90	6·90	26·8	—	—	—	3·80	3·80	15·5
1·9	11·9	45·9	—	—	—	6·70	6·70	27.4
6·8	16·8	64·9	1·80	1·80	7·16	9·80	9·80	40·1
3·6	13·6	52·3	—	—	—	6·10	6·10	24·9
1·0	21·0	81·0	2·40	2·40	9·55	9·60	9·60	39·3
8·7	28·7	111	3·00	3·00	11·9	12·1	12·1	49·4
5·1	35·1	136	3·70	3·70	14·7	15·2	15·2	62·3
9.8	19·8	76·6	—	—	—	7·8	7·8	31·9
4·0	24·0	92·8	2·40	2·40	9·56	9·5	9·5	38·8
1·3	31·3	121	3·30	3·30	13·2	12·7	12·7	51·7
0·1	40·1	155	4·70	4·70	18·7	15·6	15·6	63·8
9·6	19·6	75·8	2·20	2·20	8·76	7·50	7·50	30·7
8.6	38·6	149	4·50	4·50	17·9	14·0	14·0	57·2
3·5	43·5	168	4·70	4·70	18·7	16·4	16·4	67·0
9·3	49·3	191	4·90	4·90	19·5	17·1	17·1	69·7
0·3	20·3	74·8	—	—	—	7·90	7·90	32·3
0·2	30·2	117	3·30	3·30	13·0	10·8	10·8	44·0
9·1	39·1	151	4·30	4·30	17·1	14·8	14·8	60·3
9·5	49·5	191	5·40	5·40	21·5	17·5	17·5	71·6
—	—	—	—	—	—	—	—	—
4·8	34·8	135	3·90	3·90	15·5	12·2	12·2	49·8
7·5	47·5	183	5·30	5·30	21·0	17·0	17·0	69·3
7·5	57·5	222	6·30	6·30	25·0	20·6	20·6	84·1
7·1	27·1	105	3·00	3·00	11·9	9·60	9·60	39·3
3·1	53·1	205	5·90	5·90	23·4	19·0	19·0	77·5

their maximum value at three to four times the excitation voltage.

TABLE III.

Intensity Ratios of the Tungsten L-lines.

(Excited by X-rays.)

Voltage. kv.	$\frac{\alpha_1}{\alpha_2}\cdot\frac{L_{III}}{L_{III}}$	$\frac{\beta_1}{\beta_2}\cdot\frac{L_{II}}{L_{III}}$	$\frac{\beta_3}{\beta_2}\cdot\frac{L_I}{L_{III}}$	$\frac{\beta_1}{\alpha_2}\cdot\frac{L_{II}}{L_{III}}$	$\frac{\beta_2}{\alpha_2}\cdot\frac{L_{III}}{L_{III}}$	$\frac{\beta_3}{\alpha_2}\cdot\frac{L_I}{L_{III}}$	$\frac{\beta_1}{\alpha_1}\cdot\frac{L_{II}}{L_{III}}$	$\frac{\beta_2}{\alpha_1}\cdot\frac{L_{III}}{L_{III}}$	$\frac{\beta_3}{\alpha_1}\cdot\frac{L_I}{L_{III}}$
18 ..	8·24	1·67	0·178	3·00	1·79	0·343	0·363	0·217	0·098
23 ..	8·39	2·13	0·240	3·99	1·86	0·445	0·474	0·221	0·0533
28 ..	8·03	2·39	0·265	4·37	1·83	0·481	0·544	0·231	0·0608
32 ..	8·04	2·58	0·289	4·61	1·79	0·518	0·573	0·222	0·0643
36·5.	8·12	2·55	0·294	4·69	1·86	0·542	0·579	0·229	0·0654
40 ..	8·25	2·66	0·304	4·74	1·78	0·541	0·575	0·216	0·0655
45 ..	8·14	2·66	0·303	4·74	1·79	0·541	0·583	0·220	0·0663

Fig. 2.

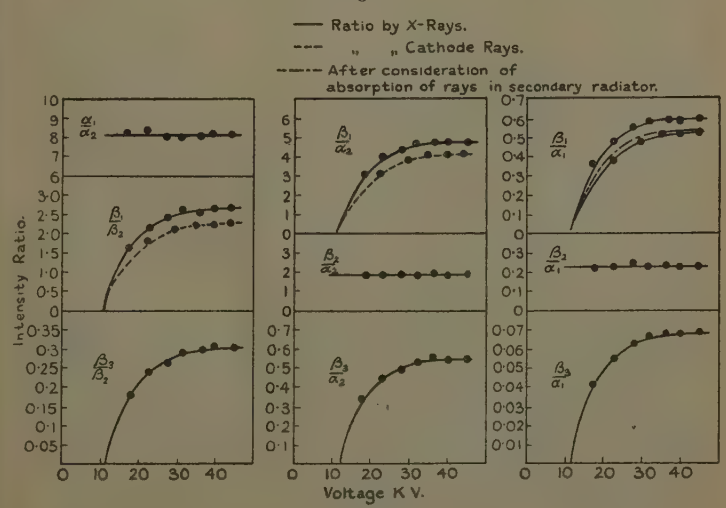
Ratio by X-Rays.
" " Cathode Rays.
After consideration of absorption of rays in secondary radiator.
Intensity Ratio.
Voltage K V.

To determine whether the intensity ratios when using cathode-ray excitation show a dependency on the voltage, a few intensity measurements were carried out using this kind of excitation. Table IV. gives the results, the curve being shown in fig. 2. It is seen that the shape of the curves is the same, whether cathode or X-ray excitation is used.

Table V. shows the result of considering the dependency of the intensity of reflexion of the crystal on the reflexion-angle for each line when using Allison's values * and

TABLE IV.

Intensity Ratios of the Tungsten L-lines.
(Excited by Cathode Rays.)

Voltage kv.	$\frac{\alpha_1}{\alpha_2}$.	$\frac{\beta_1}{\beta_2}$.	$\frac{\beta_1}{\alpha_2}$.	$\frac{\beta_2}{\alpha_2}$.	$\frac{\beta_1}{\alpha_1}$.	$\frac{\beta_2}{\alpha_1}$.
22·5	8·52	1·77	3·19	1·82	0·374	0·211
30·0	8·37	2·12	3·90	1·85	0·465	0·220
35·0	8·22	2·20	4·15	1·88	0·505	0·228
40·0	8·11	2·26	4·19	1·85	0·517	0·228
44·0	7·81	2·29	4·05	1·78	0·519	0·226
Mean.....	8·21			1·84		0·223

when the intensities of the lines are divided by the fourth power of the frequency. As seen from Table VI., the intensity ratio of the lines α_1, α_2, and β_1, show a good agreement with the theoretical values given by Burger and Ornstein when the former correction is considered, but a poor one when the ν^4 correction is taken into account. This latter result was also observed by Hicks † for the tantalum lines using cathode-ray excitation.

The curves obtained for the intensity ratios of the thallium and uranium lines show the same shape as those for the tungsten lines, the ratios reaching their maximum values at a tube-voltage of approximately 45 kv. Tables VII. and VIII. give these values after taking into account the several corrections.

* S. K. Allison, Phys. Rev. xli. p. 1 (1932).
† V. Hicks, Phys. Rev. xxxvi. p. 1273 (1930); xxxviii. p. 572 (1931).

The theoretical aspect of the results obtained in this work will be discussed fully in another paper.

TABLE V.

Relative Intensities of Tungsten L-lines.

	(Excited by Cathode Rays.)			(Excited by X-rays.)		
Line.	After consideration of the absorption of the rays in their path.	After further consideration of the dependency of intensity of reflexion on reflexion-angle.	After further consideration of the ν^4 correction.	After consideration of the absorption of the rays in their path.	After further consideration of the dependency of intensity of reflexion on reflexion-angle.	After further consideration of the ν^4 correction.
l	—	—	—	1·4	1·3	2·2
α_2	12·2	12·1	12·4	12·2	12·1	12·4
α_1	100	100	100	100	100	100
n	—	—	—	0·8	0·8	0·7
β_4	—	—	—	4·1	4·5	2·7
β_6	—	—	—	2·0	2·2	1·3
β_1	51·6	57·0	32·3	58·2	64·2	36·4
β_3	—	—	—	6·6	7·4	4·0
β_2	22·3	25·0	12·6	22·2	24·9	12·5
γ_1	—	—	—	7·1	8·6	2·6
γ_2	—	—	—	0·8	1·0	0·27
γ_3	—	—	—	1·0	1·2	0·32
γ_4	—	—	—	0·6	0·75	0·18

TABLE VI.

Intensity Ratios of the Tungsten L-lines.

(Excited by Cathode Rays.)

Line.	According to the Burger-Ornstein Law.	After consideration of the absorption of the rays in their path.	After further consideration of the dependency of intensity of reflexion on reflexion-angle.	After further consideration of the ν^4 correction.
$\alpha_1 : \alpha_2 : \beta_1$ ..	9 : 1 : 5	9 : 1·1 : 4·7	9 : 1·1 : 5·1	9 : 1·1 : 2·9

TABLE VII.

Relative Intensities of the Thallium L-lines.

Line.	After consideration of the absorption of the rays in their path.	After further consideration of the dependency of intensity of reflexion on reflexion-angle.	After further consideration of the ν^4 correction.
α_2	13	13	13·5
α_1	100	100	100
β_1	71	79	39·4
β_2	28·8	32	15·5
β_3	7·6	8·5	4·0

TABLE VIII.

Relative Intensities of the Uranium L-lines.

Line.	Allison's values.	After consideration of the absorption of the rays in their path.	After further consideration of dependency of intensity of reflexion on reflexion-angle.	After further consideration of the absorption of the rays in uranium.	After further consideration of the ν^4 correction.
α_2	11	11·1	11·0	11·5	12·1
α_1	100	100	100	100	100
β_2	28	26·8	29·3	18	8·5
β_4	—	4·3	4·8	2·9	1·2
β_1	49·4	33·3	36·8	21·4	8·4
γ_1	10·9	10·5	12·0	9·6	2·0

Summary.

The dependency on the tube-voltage of the intensity ratios of the L-emission lines of tungsten, thallium and uranium when excited by X-rays has been investigated. It was found that the value of the ratios of lines originating from the same electron level are independent of the tube-voltage. The other intensity ratios depend critically on the voltage ; they reach their maximum values at a voltage from three to four times the

excitation voltage. The intensity ratios of the L-lines are the same, whether the lines are excited by cathode or by X-rays.

The authors gratefully acknowledge the advice given and interest shown by Professor Dr. G. v. Hevesy, under whose direction this work was carried out in the Institut für physikalische Chemie, Freiburg-im-Breisgau. Thanks are also due to Mr. A. P. M. Fleming, C.B.E., Director-Manager, Research and Education Departments, Metropolitan-Vickers Electrical Co., Ltd., for permission to publish this paper.

LXXVI. *The Scattering of Light by Drops in a Wilson Chamber.* *By* C. G. Webb, *B.Sc.**

THE following experiments were carried out with the double purpose of making possible the calculation of exposure in Wilson chamber photography and of providing preliminary information for more accurate experiments on the scattering of light by fairly large drops.

The light scattered in a given direction by an isolated spherical drop illuminated with parallel unpolarized light will depend on the size and refractive index of the drop and on the wave-length of the incident light. The theory of such scattering has been developed in detail by Rayleigh for drops which are small in comparison with the wave-length of light[1], for drops whose circumference is comparable with the wave-length[2], and for drops of low relative refractive index[3]; and in outline by Mie for drops of any size[4]. Experimental work has been carried out by Rayleigh and Mie and described in the above papers, and by Ryde[5] on certain special cases, but no data appear to exist on the scattering of light by drops whose diameter is a fairly large number of wave-lengths.

In the experiments to be described a Wilson chamber was used to produce large isolated drops, which were illuminated with a parallel unpolarized beam of white light from a carbon arc. The drops were photographed at a number of different angles to the incident beam.

* Communicated by Prof. P. M. S. Blackett, F.R.S.

the exposure and lens aperture being so varied that images of similar density were obtained in each position. The variation in the intensity of the scattered light with the angle of scattering can then be calculated. This method was adopted in the first study of the problem in order to conform fairly closely to current practice of cloud photography, with the hope of yielding results directly applicable to the calculation of exposures when photographing at different angles to the illuminating beam. A more accurate photometric method will be developed shortly.

If the intensity of the scattered light at an angle θ to the incident beam is I, then an image of the drop, formed by a lens of area S, has intensity proportional to IS/σ, where σ is the area of the image. The actual size of the photographic images obtained is a result of several factors, the more important being probably lens imperfections and the limited resolving power of the photographic emulsion used, and to a lesser extent the normal diffraction broadening.

However, over the range of apertures used in the experiments the observed size of the images on the photographic plates was found to be appreciably constant, so that σ could be taken as constant, and so the intensity of the image is proportional to IS.

The density of the photographic image I′ will depend on the intensity of the actual image, on the time t of exposure, and on the nature of the plate and of its development. If only the first two vary, the density of photographic image is given by $I'=r\log(IS t^p)-i$, where r, p, and i are constants. For plates of equal density we have

$$\frac{I_1}{I_2}=\left(\frac{t_2}{t_1}\right)^p\frac{S_2}{S_1},$$

or, in other words, the intensity of the scattered ray in arbitrary units is $\frac{1}{S.t^p}$.

The chamber was of an oil-sealed metal piston type operated by a hand trigger and arranged so that when an expansion occurred the motion of the piston released the camera shutter through a delay mechanism consisting of a spring controlled pendulum.

Two jellies were used to saturate the chamber, one (glycerine 6 parts, water 4, gelatine 1 by weight) giving

water vapour, and the other (water 3 parts, alcohol 3, gelatine 1 by weight) giving a mixed vapour of alcohol and water. The ratio of expansion was adjusted in each case until about twelve drops were observed per square cm. of the chamber.

No ionizing source was used. The drops were therefore what may be called background drops, formed on uncharged nuclei. The ratio of expansion was 1·31 for water vapour and 1·14 for alcohol-water vapour[6].

The camera, which could be placed so as to photograph the drop from differing angles, was of simple design, with an Aldis anastigmat lens ($f/2{\cdot}9$, F = 5 cm.), and of Ilford Hypersensitive Panchromatic plates were used, nominal sensitivity 8000 H. & D. for artificial light.

As a check on the constancy of the arc and of sensitivity of the plates in many, but not all experiments, a second camera was placed so as to receive the whole of the transmitted beams through a very dark filter. No large systematic change occurred.

The final size of the drops was calculated from the rate of fall using Stokes's Law. The shutters used were calibrated by photographing a line on a rotating disk, the variable stop in the camera lens was checked, and p, Schwarzschild's constant for the plates, was measured and found to be 0·70.

The results are shown in the following tables :—

TABLE I.

Measured Values. Water Drops.

Rate of fall 1·0 cm./sec. Radius $0{\cdot}96 \times 10^{-3}$ cm.

θ.	S.	t.	I.	log I.
20°	0·24 cm.^{2}	0·012 sec.	90	1·954
40	1·49	0·012	14·5	1·162
60	1·49	0·188	2·16	0·334
80	1·62	0·667	0·82	−0·086

TABLE II.

Measured Values. Alcohol-water Drops.

Rate of fall 1·15 cm./sec. Radius $1·15 \times 10^{-3}$ cm.

θ.	S.	t.	I.	log I.
20°	0·17 cm.^{2}	0·027 sec.	73	1·864
40	0·90	0·027	13·9	1·144
60	1·62	0·072	3·90	0·592
80	0·90	0·294	2·61	0·417
100	1·62	0·589	0·90	−0·045

Fig. 1.

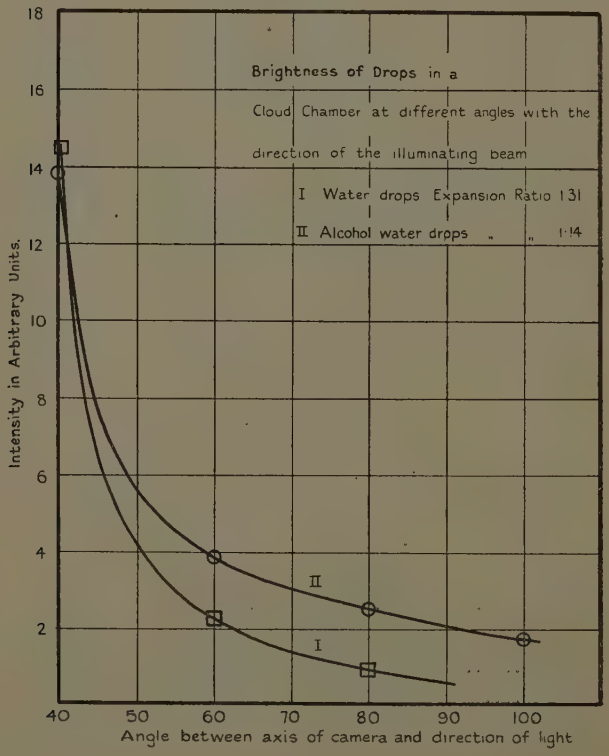

Fig. 1 shows the results down to $\theta = 40°$, plotted graphically, and fig. 2 shows all the results plotted on a logarithmic scale.

Table III. gives the intensities at different angles as obtained from the logarithmic curves.

Fig. 2.

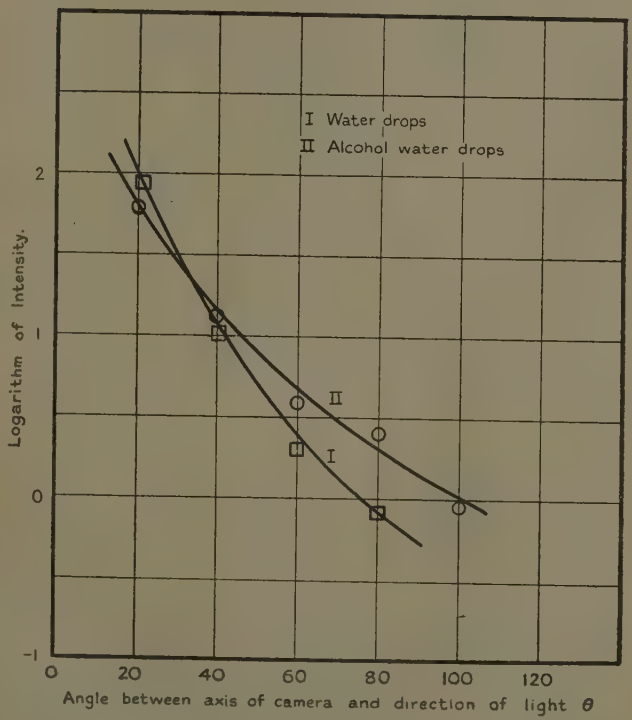

The accuracy of these figures is determined principally by the constancy of the arc intensity. Considerable fluctuations occurred in this, which were, however, reduced in importance by taking six exposures at each angle.

It appears from fig. 2 that log I is subject to errors of about 0·1, indicating that I has an accuracy of about 25 per cent.

The most noticeable features of these results are as follows :—

1. The intensity of the scattered light, that is, the brightness of the drops, increases very rapidly as the angle with the incident beam is diminished. For the water drops the intensity at 20° to the beam is about one hundred times that at 90°, while for the alcohol-water drops the ratio is about fifty to one.

2. The brightness of both types of drops is about the same at an angle of about 40°. For larger angles the

TABLE III.

Mean Values obtained from fig. 2.

θ.	I_1 (water).	I_2 $\left(\frac{\text{alcohol}}{\text{water}}\right)$.	Ratio $\frac{I_2}{I_1}$.
20....	100	63	0·63
30....	32	27	0·85
40....	12·0	12·9	1·1
50....	5·0	7·4	1·5
60....	2·5	4·7	1·9
70....	1·4	3·0	2·1
80....	·83	2·0	2·4
90....	·56	1·4	2·5
100....	....	1·0	

alcohol-water drops are brighter. At 90° they are about two and a half times as bright as water drops.

The greater intensity of the alcohol-water drops at large angles of scattering is in accordance with common experience that such drops are generally easier to photograph than water drops.

Since the refractive indices of alcohol and water are not very different, it seems probable that the difference in the distribution of scattered light in the two cases must be due mainly to the difference in size of the drops. Actually the diameter of the alcohol-water drops, as calculated from their rate of fall, a second or two after the expansion, was only 20 per cent. greater than the

diameter of the water drops. As it seems hardly likely that this small difference in size is sufficient to account for the difference in scattering, it appears possible that the two kinds of drops may grow at different rates, so that there may be a greater difference between their sizes when photographed one-fifth of a second after the expansion than when measured by their rate of fall one or two seconds later. Special experiments on the rate of growth of these drops will be required to verify this suggestion.

If it is true that the size of the drop is chiefly responsible for the scattering distribution, one would expect that the scattering distribution for drops of a given kind will vary with all the factors which govern their size, that is, with the expansion ratio used, and so with the available liquid and with the number of drops in unit volume. It is well known, in fact, that the brightness of the drops does vary very rapidly with the expansion ratio. The drops actually used in these experiments were probably larger than those used normally in cloud photography since their number was smaller. Thus when photographing tracks in an alcohol-water mixture one might expect to find an angular distribution more like that found here for water drops. This seems to be the case in some β-ray photographs taken recently in this laboratory.

If this general view is correct, one may expect to find a higher scattered intensity at 90° compared with that at 45°, the larger the drops, that is, the larger the expansion ratio the fewer the drops in the chamber.

The variation of scattering with the wave-length of the light used still awaits investigation.

References.

(1) Lord Rayleigh, Coll. Papers, i. p. 104.
(2) Lord Rayleigh, Coll. Papers, v. p. 547.
(3) Lord Rayleigh, Coll. Papers, vi. p. 518.
(4) G. Mie, *Ann. der Physik*, xxv. p. 377 (1908).
(5) J. W. Ryde, Proc. Roy. Soc. A, cxxxi. p. 449 (1931).
(6) Froemke, Bloomquist, and Andren, *Zeits. f. Phys. Chem.* clxvi. p. 305 (1933).

Birkbeck College, London.
September 1934.

LXXVII. *Rotating Electromagnetic Waves.* *By* Dr. N. S. Japolsky, *formerly Lecturer, Technological Institute. Leningrad* *.

Contents.

	Page
1. Introduction	934
2. Differential Equations of E.M. Field	935
3. The Integral of Differential Equations of E.M. Field	939
4. Polarization of Rotating Cylindrical Waves	940
5. Compound Rotating Cylindrical Waves	943
6. The Magnetic Vector	947
7. The Energy Flux and the Energy Density	948
8. The average Speed of Energy Propagation. Comparison between the Rotating Cylindrical e.m. Waves and the "material" Waves of de Broglie. Conclusion	952
Appendix	955
Summary	957

1. *Introduction.*

THE speed c_1 of propagation, in isotropic and homogeneous non-conducting medium, of ordinary plane electromagnetic waves, *i. e.*, of plane e.m. waves with constant amplitude, is determined by the formula

$$c_1 = \frac{c}{\sqrt{\epsilon\mu}}, \quad . \quad . \quad . \quad . \quad . \quad . \quad (1.1)$$

where ϵ is the dielectric constant, μ the permeability, and c the ratio between abs. electromagnetic and abs. electrostatic units of electric charge, which is usually called "the speed of light."

However, c_1 is not the maximum speed of propagation of any kind of e.m. waves in the given medium. For instance, D. R. Hartree † described a certain kind of e.m. waves propagating with the speed c_2 greater than c_1.

We shall call the e.m. waves with $c_2 > c_1$ "superfast" e.m. waves.

When superfast e.m. waves are axially symmetrical and propagate along their axis of symmetry without spreading, we shall call them "superfast cylindrical waves."

* Communicated by Sir W. H. Bragg, O.M., K.B.E., F.R.S.

† Phil. Mag. vol. xlvi. p. 454 (1923).

In the general case our waves will not only *propagate along* the axis, but also *rotate about* it. They will be then called " rotating superfast cylindrical waves."

The purpose of this paper is to investigate theoretically rotating superfast cylindrical waves propagating in homogenous and isotropic non-conducting medium. Of course, we shall abbreviate this long descriptive term as occasion may allow.

It might be possible to obtain the expression for the electromagnetic field of the waves in question as a particular case of certain known general solutions of Maxwell equations.

We prefer, however, to start from the Maxwell equations and conduct the mathematical reasoning as close as possible to its physical interpretation. This will hardly make our discussion appreciably longer, but it will certainly make it easier to follow.

2. *Differential Equations of E.M. Field.*

The Maxwell equations for a homogeneous and isotropic perfect insulator, in cylindrical coordinates x, r, and θ*, are

$$\left.\begin{aligned}
\frac{c}{{c_1}^2}\dot{E}_x &= \frac{\partial}{r\partial r}(rB_\theta) - \frac{\partial}{r\partial\theta}B_r, & -\frac{1}{c}\dot{B}_x &= \frac{\partial}{r\partial r}(rE_\theta) - \frac{\partial}{r\partial\theta}E_r,\\
\frac{c}{{c_1}^2}\dot{E}_r &= \frac{\partial}{r\partial\theta}B_x - \frac{\partial}{\partial x}B_\theta, & -\frac{1}{c}\dot{B}_r &= \frac{\partial}{r\partial\theta}E_x - \frac{\partial}{\partial x}E_\theta,\\
\frac{c}{{c_1}^2}\dot{E}_\theta &= \frac{\partial}{\partial x}B_r - \frac{\partial}{\partial r}B_x, & -\frac{1}{c}\dot{B}_\theta &= \frac{\partial}{\partial x}E_r - \frac{\partial}{\partial r}E_x,
\end{aligned}\right\} \quad \ldots \quad (2.1)$$

where E_x, E_r, and E_θ are the components of the force of electric field in abs. el. static units B_x, B_r, and B_θ the components of the magnetic flux density (or magnetic induction) in abs. el. magn. units. The dot above the letter indicates, in the usual way, the differentiation with respect to time t.

It is assumed here that in our cylindrical coordinate system the positive direction of θ is clockwise when looking in the direction of the axis x.

* In connexion with the work which is proposed to follow the present one, it has been found more convenient to denote the axial coordinate by x, instead of more usual z.

On differentiating, with respect to t, the first group of equations (2.1) and substituting for $\dot{B}$ their expressions in the second group, we shall obtain

$$\left.\begin{aligned}
\frac{1}{{c_1}^2}\ddot{E}_x &= -\frac{\partial}{r\partial r}\left(r\frac{\partial}{\partial x}E_r\right)+\frac{\partial}{r\partial r}\left(r\frac{\partial}{\partial r}E_x\right) \\
&\qquad +\frac{\partial^2}{r^2\partial\theta^2}E_x-\frac{\partial^2}{r\partial\theta\,\partial x}E_\theta, \\
\frac{1}{{c_1}^2}\ddot{E}_r &= -\frac{\partial^2}{r^2\partial\theta\,\partial r}(rE_\theta)+\frac{\partial^2}{r^2\partial\theta^2}E_r+\frac{\partial^2}{\partial x^2}E_r-\frac{\partial^2}{\partial x\partial r}E_x, \\
\frac{1}{{c_1}^2}\ddot{E}_\theta &= -\frac{\partial^2}{r\partial\theta\,\partial x}E_x+\frac{\partial^2}{\partial x^2}E_\theta+\frac{\partial}{\partial r}\left(\frac{\partial}{r\partial r}(rE_\theta)\right)-\frac{\partial}{\partial r}\left(\frac{\partial}{r\partial\theta}E_r\right).
\end{aligned}\right\} \quad . \quad . \quad . \quad (2.2)$$

From these equations the magnetic vector is eliminated. We shall only deal at first with the electric vector, as the magnetic vector will be found from the second group of equations (2.1) after the electric vector has been determined *. Of course, in the same way we could eliminate the electric vector and deal first with the magnetic one.

Consider now e.m. waves, simple harmonic with respect to time, and having at each given moment of time a simple harmonic distribution *along* the axis x, and *around* this axis. In other words, the components of e.m. field are simple harmonic functions of x, θ. and t. In order that these functions be single valued, their period with respect to θ must be $\frac{2\pi}{|n|}$, where n is a positive or negative integer, and $|n|$ is its absolute value.

E can thus be expressed in the form

$$\left.\begin{matrix} E_x \\ r \\ \theta \end{matrix}\right\} = \left.\begin{matrix} \mathrm{E}_x \\ r \\ \theta \end{matrix}\right\} e^{i(\Omega t+\kappa x+n\theta)}, \quad . \quad . \quad . \quad . \quad . \quad (2.3)$$

where E_x etc., are the amplitudes of the corresponding components, which depend only on r, $i=\sqrt{-1}$, $\Omega=-2\pi\nu$ (where ν is the frequency) can be called "angular time frequency," $\kappa=\frac{2\pi}{\lambda}$ (where λ is the wave-length) can

* See Section 6.

be called "angular distance frequency"*. We shall call $2|n|$ "the number of poles."

The amplitudes E_x, etc. comprise also the initial phases, and, therefore, generally speaking, they are complex quantities.

The linear velocity, with which we must move a point in a given direction to keep its phase constant, we shall call the velocity of *propagation* of the waves *along* this direction, while the corresponding angular velocity of a point *about* a given axis we shall call the angular velocity of *rotation* of the waves *about* this axis.

It follows from this definition and from (2.3) that, while the velocity c_2 of *propagation* of the waves *along* the axis is

$$c_2 = -\frac{\dfrac{\partial}{\partial t}}{\dfrac{\partial}{\partial x}}(\Omega t+\kappa x+n\theta) = -\frac{\Omega}{\kappa} = \nu\lambda, \quad . \quad . \quad (2.4)$$

the angular velocity Ω_x of *their rotation about the axis* is

$$\Omega_x = -\frac{\dfrac{\partial}{\partial t}}{\dfrac{\partial}{\partial \theta}}(\Omega t+\kappa x+n\theta) = -\frac{\Omega}{n}, \quad . \quad . \quad (2.5)$$

Ω_x is positive when the waves rotate in the direction of positive θ, *i. e.*, clockwise if one looks on the direction of the axis. Thus Ω_x is positive when n is negative and *vice versa*.

It is clear from the above that the loci of equal amplitudes are cylindrical surfaces.

On the other hand, at any given moment of time a locus of a given phase will be represented by helical surfaces symmetrically situated round the axis x (equiphasial surfaces). To keep the phase at these helical surfaces constant we must either communicate to them a translatory motion along the axis x with the speed c_2 or, otherwise, rotate them with the angular velocity Ω_x. We can look upon the whole e.m. field of the waves either

* In my previous papers (*Arch. für Elektrotechnik*, vol. xiv. fasc. 1 (1924); *Zeit. für Phys.* vol. liv. 1 and 2; Engineering, 1926, July 9th and 23rd, and others) I called this quantity "angular space frequency" and denoted it by ω. The name which is given here appears more adequate. I changed the notation to bring it in line with those used in the majority of contemporary papers.

as moving or as rotating together with its equiphasial helical surfaces without changing its shape relatively to these surfaces, or, in other words, we can say that our waves can be looked upon either as propagating or as rotating without change of shape.

The waves thus described we shall call *rotating cylindrical e.m. waves.*

In a particular case when $n=0$ the waves are not rotating any more but simply propagating along the axis. Such waves we may call simply "cylindrical" instead of "rotating cylindrical."

On introducing the expressions from (2.3) into (2.2) we shall get

$$\left.\begin{aligned}
-\frac{\Omega^2}{c_1^2}\mathrm{E}_x &= -i\kappa\frac{d}{r\,dr}(r\mathrm{E}_r)+\frac{d}{r\,dr}\left(r\frac{d}{dr}\mathrm{E}_x\right)-\frac{n^2}{r^2}\mathrm{E}_x+\frac{n\kappa}{r}\mathrm{E}_\theta,\\
-\frac{\Omega^2}{c_1^2}\mathrm{E}_r &= -\frac{in}{r^2}\frac{d}{dr}(r\mathrm{E}_\theta)-\frac{n^2}{r^2}\mathrm{E}_r-\kappa^2\mathrm{E}_r-i\kappa\frac{d}{dr}\mathrm{E}_z,\\
-\frac{\Omega^2}{c_1^2}\mathrm{E}_\theta &= \frac{n\kappa}{r}\mathrm{E}_z-\kappa^2\mathrm{E}_\theta+\frac{d}{dr}\left(\frac{d}{r\,dr}(r\mathrm{E}_\theta)\right)-in\frac{d}{dr}\left(\frac{\mathrm{E}_r}{r}\right).
\end{aligned}\right\} \quad . \quad . \quad . \quad (2.6)$$

Multiply the first equation (2.6) by κr, multiply by $-ir$ and then differentiate with respect to r the second equation, multiply the third equation by n, and, finally, add all three equations. This will give

$$\kappa r\mathrm{E}_z-i\frac{d}{dr}(r\mathrm{E}_r)+n\mathrm{E}_\theta=0. \quad . \quad . \quad . \quad (2.7)$$

On multiplying (2.7) by $\frac{\kappa}{r}$ and adding it to the first equation (2.6), we find the differential equation for E_z which we can write in the form

$$\frac{d}{r\,dr}\left(r\frac{d}{dr}\mathrm{E}_z\right)+\left(\zeta^2\kappa^2-\frac{n^2}{r^2}\right)\mathrm{E}_z=0, \quad . \quad . \quad (2.8)$$

where we have put

$$\zeta=+\sqrt{\frac{\Omega^2}{\kappa^2c_1^2}-1}=+\sqrt{\frac{\nu^2\lambda^2}{c_1^2}-1}=+\sqrt{\frac{c_2^2}{c_1^2}-1}, \quad (2.9)$$

by (2.4).

On dividing (2.7) by ir, differentiating it with respect to r and comparing it with the second equation (2.6), and then using (2.9), we get

$$\frac{d}{dr}\left(\frac{d}{r\,dr}(rE_r)\right)+\left(\zeta^2\kappa^2-\frac{n^2}{r^2}\right)E_r-i\frac{2n}{r^2}E_\theta=0. \quad (2.10)$$

Eliminating E_r from the third equation (2.6) and from (2.7) we obtain

$$\frac{d}{dr}\left(\frac{d}{r\,dr}(rE_\theta)\right)+\left(\zeta^2\kappa^2-\frac{n^2}{r^2}\right)E_\theta+i\frac{2n}{r^2}E_r=0. \quad (2.11)$$

3. *The Integral of Differential Equations of E.M. Field.*

Denote $$\zeta\kappa r=r_1. \quad . \quad . \quad . \quad . \quad . \quad . \quad . \quad (3.1)$$

Then, on performing the differentiation, we can write (2.8), (2.10), and (2.11) in the form

$$\left.\begin{aligned}&\left[\frac{d^2}{dr_1^2}+\frac{d}{r_1dr_1}+\left(1-\frac{n^2}{r_1^2}\right)\right]E_x=0,\\&\left[\frac{d^2}{dr_1^2}+\frac{d}{r_1dr_1}+\left(1-\frac{n^2+1}{r_1^2}\right)\right]E_r-i\frac{2n}{r_1^2}E_\theta=0,\\&\left[\frac{d^2}{dr_1^2}+\frac{d}{r_1dr_1}+\left(1-\frac{n^2+1}{r_1^2}\right)\right]E_\theta+\frac{i2n}{r_1^2}E_r=0.\end{aligned}\right\} \quad (3.2)$$

Denote $$\left.\begin{aligned}U_+&=E_\theta-iE_r,\\U_-&=E_\theta+iE_r.\end{aligned}\right\} \quad . \quad . \quad . \quad . \quad . \quad (3.3)$$

Multiply the second equation (3.2) by $\mp i$ and add it to the third. Then, by (3.3),

$$\left[\frac{d^2}{dr_1^2}+\frac{d}{r_1dr_1}+\left(1-\frac{(n\pm1)^2}{r_1^2}\right)\right]U_\pm=0, \quad . \quad (3.4)$$

where only upper or only lower signs are to be used simultaneously.

The first equation (3.2) and the equation (3.4) are Bessel equations. Their only solutions which are finite throughout the space, and hence the only solutions suitable for our problem, are

$$\left.\begin{aligned}&E_x=A_xJ_n(r_1),\\U_+&=2A_1J_{n+1}(r_1), \quad U_-=2A_2J_{n-1}(r_1),\end{aligned}\right\}, \quad . \quad (3.5)$$

where A_x, A_1, and A_2 are constants, while $J_n(r_1)$ is, according to the usual notation, a Bessel coefficient of the order n of the variable r_1.

As all the Bessel functions in further discussion will be of the same variable r_1, we shall write simply J_n instead of $J_n(r_1)$, keeping the independent variable in mind.

Eliminating successively E_θ and E_r from both equations (3.3), we obtain

$$\left.\begin{aligned} iE_r &= -\tfrac{1}{2}(U_+ - U_-) = -A_1 J_{n+1} + A_2 J_{n-1}, \\ E_\theta &= \tfrac{1}{2}(U_+ + U_-) = A_1 J_{n+1} + A_2 J_{n-1}, \end{aligned}\right\} \quad . \quad (3.6)$$

by (3.5).

Since, in the process of deriving the equations (3.2) from the Maxwell equations, we used differentiation with respect to r, we must not expect A to be really independent of A_1 and A_2, as they may appear if we take the equations (3.2) by themselves.

To find out the relationship between these constants, introduce into (2.7) the expressions from the first formula (3.5) and from (3.6).

Then, recalling from the Theory of Bessel functions the relationships

$$r_1 \frac{d}{dr_1} J_{n+1} = r_1 J_n - (n+1) J_{n+1} \quad . \quad . \quad . \quad (3.7)$$

and

$$r_1 \frac{d}{dr_1} J_{n-1} = -r_1 J_n + (n-1) J_{n-1},$$

we find

$$A_x = -\zeta(A_1 + A_2) \quad . \quad . \quad . \quad . \quad . \quad (3.8)$$

hence, by the first formula (3.5),

$$E_x = -\zeta(A_1 + A_2) J_n \quad . \quad . \quad . \quad . \quad (3.9)$$

Note that to satisfy (2.7) a conventional rule

$$J_{-n} = (-)^n J_n \quad . \quad . \quad . \quad . \quad . \quad (3.10)$$

must be observed in the expressions (3.6) and (3.9).

4. *Polarization of Rotating Cylindrical Waves.*

If in the ordinary plane e.m. waves the extremity of the electric (and magnetic) vector at any given point is

describing an ellipse, we say that the vector is elliptically polarized. In the particular case when the axes of this ellipse are equal, we say that the vector is circularly polarized. In the extreme case when one of the axes of the ellipse of polarization becomes infinitesimal we say that the vector is plane polarized. A non-polarized vector can be always considered as a combination of polarized ones.

The same definition of the state of polarization of the electromagnetic vector applies to the rotating cylindrical waves.

There will be, however, an essential difference. In the case of rotating cylindrical waves the problem of polarization is a three dimensional one, and, as we shall see later, an ellipsoid is more appropriate for its representation than an ellipse.

Apart from this, in rotating cylindrical waves, in addition to the polarization of the vector, the other kind of polarization, which we shall call "the polarization of the *field as a whole*," must be considered.

The field as a whole can rotate without change of shape (circularly polarized field); it can periodically oscillate without changing its angular position (plane polarized field). A combination of mutually perpendicular plane polarized fields of unequal amplitudes, and with the phases in quadrature, will form an elliptically polarized e.m. field, in the manner analogous to the similar case of the electric (and magnetic) vector, and, finally, a combination of polarized fields can form any state of "non polarization."

Thus in rotating waves we must distinguish :—

(1) Polarization of the e.m. field as a whole (polarization of the field).

(2) Polarization of the electric (and magnetic) vector at a given point (polarization of the vector).

Let us first consider the polarization of the field.

From the definition of "rotating cylindrical waves," and at a glance upon the formula (2.3), we can see that the waves hitherto considered have circularly polarized field : right hand when n is negative, and left hand when n is positive (see formula (2.5)).

Putting

$$E_+ \pm E_- = 2E_{p\pm}, \quad . \quad . \quad . \quad . \quad . \quad (4.1)$$

we find by (2.3) the expression for a vector component of rotating cylindrical waves with plane polarized field

$$E_{p_\pm} = \mathrm{E}\cos\left(n\theta + (1\mp 1)\frac{\pi}{4}\right) e^{i\left(\Omega t + \kappa x + (1\mp 1)\frac{\pi}{4}\right)}. \quad (4.2)$$

The suffixes x, r and θ are omitted in (4.1) and (4.2) as they have no influence on the construction of the formula. The suffix p is put to indicate that the field as a whole is plane polarized. The suffix $\pm$ at the bottom of E_p corresponds to the double sign in the exponent and in the cos term.

It may be observed that the term "rotating waves with plane polarized field" may be considered as self-contradictory, for when the field is plane polarized the waves do not rotate any more but only propagate *. We prefer, however, to keep this term, as plane polarized waves can be always looked upon as a simple combination of circularly polarized ones.

A convenient, although not quite accurate, model of the electric field in rotating cylindrical waves in different states of polarization can perhaps be given by a magnetic field in the ordinary polyphase induction motor with $2n$ poles. The angle $n\theta$ will correspond then to so-called "electric" angle in the motor. In the ideal polyphase motor the field would be circularly polarized. Motor fed by two oppositely rotating systems of polyphase currents of equal strength would produce the effect similar to "plane" polarization. To complete the similarity, the conductors should be directed not axially but helically with the pitch of helix equal to the wave-length. Then the field would not only rotate and pulsate in azimuthal plane but also "propagate" in axial direction.

Consider now the polarization of the vector. We can see by a glance at (3.6) that if A_1 and A_2 (which may be generally complex numbers) have the same argument, the projection of the electric vector on the plane $r\theta$, *i. e.*, the resultant of the components E_r and E_θ, is elliptically polarized with the axes of the ellipse of polarization directed along r and θ. Similarly, at a glance on (3.6) and (3.9), we observe that the projection of the electric vector on the plane xr, i. e., the resultant of E_x and E_r,

* For the distribution of phases round the axis is stationary.

is also elliptically polarized, with the axes of the ellipse directed along x and r. Hence the end of the electric vector describes a line on the surface of an ellipsoid with the axes directed along x, r, and θ. We can call this ellipsoid "an ellipsoid of polarization" and say that the electric vector in rotating cylindrical waves is, in a general case, ellipsoidally polarized.

When $A_1=0$ or $A_2=0$ this ellipsoid becomes a circular ellipsoid, and the resultant of E_r and E_θ becomes circularly polarized, right hand when $A_1=0$ and left hand when $A_2=0$ (see formula (3.6)).

When $A_1=-A_2$ (formulæ (3.9) and (3.6)),

$$\left.\begin{aligned} E_x&=0,\\ iE_r&=-A_1(J_{n+1}+J_{n-1})=-2A_1\frac{n}{r_1}J_n,\\ E_\theta&=\ A_1(J_{n+1}-J_{n-1})=-2A_1\frac{d}{dr_1}J_n. \end{aligned}\right\} \quad . \quad (4.3)$$

Thus in this case an ellipsoid of polarization degenerates into an ellipse of polarization, for the x component disappears.

At $r_1>>1$, $E_r<<E_\theta$, and the electric field becomes so much elongated in the θ direction that, on the average, the lines of force can be considered as circular. When $n=0$ this will be true, not only approximately but exactly, and for any r.

In the same way, when $A_2=A_1$,

$$\left.\begin{aligned} E_x&=-2\zeta A_1J_n,\\ iE_r&=\ 2A_1\frac{d}{dr_1}J_n,\\ E_\theta&=\ 2A_1\frac{n}{r_1}J_n. \end{aligned}\right\} \quad . \quad . \quad . \quad . \quad . \quad (4.4)$$

In this case at $r>>1$ the electric vector can be practically considered as elliptically polarized in the axial plane When $n=0$ this will be true, not only approximately but exactly, and for any r.

5. *Compound Rotating Cylindrical Waves.*

Under this term we mean a resultant of several co-axial rotating cylindrical wave trains of the same wave-length

λ and speed c_2, but different n. We shall mark the notation of the resultant field components of the compound rotating cylindrical waves with an additional suffix c below.

It follows from this definition, and from the formula (2.3), that these waves can be expressed by the formulæ

$$E_{xc}=\mathrm{E}_{xc}e^{i(\Omega t+\kappa x)} \quad . \quad . \quad . \quad . \quad . \quad (5.1)$$

$$\text{etc.,}$$

where E_{xc} etc. are the amplitudes of the corresponding field components of the compound rotating cylindrical waves, which in their turn, can be expressed

$$\mathrm{E}_{xc}=\sum_n \mathrm{E}_{xn}e^{in\theta} \quad . \quad . \quad . \quad . \quad . \quad (5.2)$$

In the compound cylindrical waves, contrary to the simple ones, it is more convenient to include the function of θ in the amplitude.

The right-hand member of (5.2) represents the development of the left-hand one in Fourier series with respect to θ.

We shall consider here a special form of the compound rotating cylindrical waves, where the energy concentrates at one axial plane (" Principal plane ").

We shall call these waves " planar waves."

Imagine two rotating cylindrical wave trains having

$$\left.\begin{aligned} &n=2n_1, \qquad \mathrm{A}_1=\mathrm{A}_2=\frac{\mathrm{A}}{2}e^{2n_1\alpha} \\ \text{and} \qquad & \\ &n=-2n_1, \quad \mathrm{A}_1=\mathrm{A}_2=\frac{\mathrm{A}}{2}e^{-2n_1\alpha}, \end{aligned}\right\} \quad . \quad . \quad (5.3)$$

where n_1 is an integer. Writing now, for simplicity, n instead of n_1, we shall have by (3.6), (3.9), and (3.10) the following expressions for the resultant electric field of these waves :—

$$\begin{aligned}\mathrm{E}_{xc2n}=&-\frac{\zeta}{2}\mathrm{A}(\mathrm{J}_{2n}e^{i2n\theta+2n\alpha}+\mathrm{J}_{-2n}e^{-i2n\theta-2n\alpha} \\ &+\mathrm{J}_{2n}e^{i2n\theta+2n\alpha}+\mathrm{J}_{-2n}e^{-i2n\theta-2n\alpha}) \\ =&-2\zeta\mathrm{A}\mathrm{J}_{2n}\cos 2n\xi. \quad . \quad . \quad . \quad . \quad . \quad . \quad . \quad . \quad (5.4)\end{aligned}$$

$$iE_{rc2n} = \frac{A}{2}(-J_{2n+1}e^{i2n\theta+2n\alpha} - J_{-2n+1}e^{-i2n\theta-2n\alpha} + J_{2n-1}e^{i2n\theta+2n\alpha} + J_{-2n-1}e^{-i2n\theta-2n\alpha})$$

$$= A(-J_{2n+1}+J_{2n-1})\cos 2n\xi,$$

$$E_{\theta c2n} = \frac{A}{2}(J_{2n+1}e^{i2n\theta+2n\alpha} + J_{-2n+1}e^{-i2n\theta-2n\alpha} + J_{2n-1}e^{i2n\theta+2n\alpha} + J_{-2n-1}e^{-i2n\theta-2n\alpha})$$

$$= Ai(J_{2n+1}+J_{2n-1})\sin 2n\xi, \quad . \quad . \quad . \quad . \quad . \quad . \quad . \quad (5.5)$$

where

$$\xi = -\theta + i\alpha.$$

Exactly in the same way it is not difficult to find, on substituting in (5.3) $2n_1+1$ for $2n_1$,

$$\left.\begin{aligned} E_{xc(2n+1)} &= -2i\zeta A J_{2n+1}\sin(2n+1)\xi, \\ E_{rc(2n+1)} &= A(-J_{2(n+1)}+J_{2n})\sin(2n+1)\xi, \\ E_{\theta c(2n+1)} &= A(J_{2(n+1)}+J_{2n})\cos(2n+1)\xi. \end{aligned}\right\} \quad (5.6)$$

Construct now two compound wave trains comprising the $\sum_{n=0}^{\infty}$, one of the combined waves expressed by (5.4) and the other of the waves expressed by (5.6). Comparing these formulæ with the expressions of Fourier Series deduced in the Appendix (formulæ (7 ap.) and (8 ap.)), we can write the following expressions for the components of the resultant electric field (which we shall mark by suffix *pl* and by an additional suffix 0 and 1 under the letter for the waves corresponding to formulæ (5.4) and (5.6) resp.).

$$\left.\begin{aligned} &E_{0\,xpl} = -2\zeta AX, \quad E_{0\,rpl} = -AX\sin\xi, \quad E_{0\,\theta pl} = -AX\cos\xi, \\ &E_{1\,xpl} = 2\zeta A\bar{X}, \quad\quad E_{1\,rpl} = AX\sin\xi, \quad\quad E_{1\,\theta pl} = -AX\cos\xi, \end{aligned}\right\}$$

$$. \quad . \quad . \quad (5.7)$$

where (see Appendix formulæ (3 ap.) and (5 ap.))

$$X = e^{-r_1\bar{\eta}+ir_1\bar{\tau}}, \quad . \quad . \quad . \quad . \quad . \quad . \quad (5.8)$$

where

$$\eta = \sinh\alpha\cos\theta, \quad \tau = \cosh\alpha\sin\theta, \quad . \quad . \quad (5.9)$$

while the dash on X and η and τ in the exponent of (5.8) designates that these quantities must be taken with opposite sign within the interval

$$\frac{\pi}{2} < \theta < \frac{3\pi}{2}.$$

The electric field according to (5.7) has a discontinuity at $\theta = \pm\frac{\pi}{2}$, as can be seen from (5.8) (since $\bar{\tau}$ is changing sign; change of sign of $\bar{\eta}$ does not create a discontinuity because at $\theta = \pm\frac{\pi}{2}$, $\eta = 0$).

To eliminate this discontinuity add to the equations of the first line (5.7) similar equation but with $-\theta$ substituted for θ, and subtract the latter from the former in the equations of the second line.

Then by (5.5), (5.8), and (5.9)

$$\left.\begin{aligned}
\underset{0}{E}_{x\,pl} &= -2\zeta A e^{-r_1\bar{\eta}} \cos r_1\tau, & \underset{1}{E}_{x\,pl} &= -i2\zeta A e^{-r_1\bar{\eta}} \sin r_1\tau,\\
\underset{0}{E}_{r\,pl} &= -iA e^{-r_1\bar{\eta}}(\eta \cos r_1\tau - \tau \sin r_1\tau), & \underset{1}{E}_{r\,pl} &= -A e^{-r_1\bar{\eta}}(\bar{\eta} \sin r_1\tau + \tau \cos r_1\tau),\\
\underset{0}{E}_{\theta\,pl} &= -A e^{-r_1\bar{\eta}}(\bar{\eta}_1 \cos r_1\tau - \tau_1 \sin r_1\tau), & \underset{1}{E}_{\theta\,pl} &= iA e^{-r_1\bar{\eta}}(\bar{\eta}_1 \sin r_1\tau + \tau_1 \cos r_1\tau),
\end{aligned}\right\} \quad . \quad . \quad . \quad (5.10)$$

where

$$\eta_1 = \cosh\alpha \cos\theta, \qquad \tau_1 = \sinh\alpha \sin\theta. \quad . \quad . \quad (5.11)$$

The dash on a letter denotes, as before, that the variable has an opposite sign in the interval

$$\frac{\pi}{2} < \theta < \frac{3\pi}{2}.$$

The waves expressed by the left-hand and the right-hand side equations (5.10) are composed of even and odd harmonics resp. and, correspondingly, they can be called "even" and "odd" planar waves.

They have no discontinuities since η and η_1 are equal zero at $\theta=\pm\frac{\pi}{2}$, and, therefore $\bar{\eta}$ and $\bar{\eta}_1$ are continuous.

It is not difficult to see that $r_1\eta$ and $r_1\tau$ can also be considered as Cartesian coordinates.

The field of the planar waves is highly concentrated at the principal ($\theta=0$) plane.

It may be interesting to observe that by varying α a transversal structure of planar waves may be altered without interfering with the longitudinal structure (which is determined by ζ and κ).

6. *The Magnetic Vector.*

We shall seek the expression for the magnetic vector (B_x, B_r, B_θ) in the same form as for the electric one *i. e.*, in the form

$$B_x=\mathrm{B}_x e^{i(\Omega t+\kappa x+n\theta)}, \quad . \quad . \quad . \quad . \quad . \quad (6.1)$$

and so like E_x, where B_x, B_r, and B_θ are the components of the amplitude.

Then, on substituting in the second group of the Maxwell equations (2.1) for B_x, B_r, and B_θ their expression (6·1), and for E_x, E_r, and E_θ their expressions drawn from (2.3), (3.6), and (3.9), we shall obtain, after integrating with respect to t, the expressions for the amplitudes of the magnetic vector, which, after simple transformation on the ground of the formulæ (3.1) and (2.4) and the well-known relationships (3.7) and $\frac{2n}{r_1}\mathrm{J}_n=\mathrm{J}_{n+1}+\mathrm{J}_{n-1}$, we can write in the form

$$\left.\begin{aligned}\mathrm{B}_x&=-i\zeta(\mathrm{A}_1'+\mathrm{A}_2')\mathrm{J}_n,\\ \mathrm{B}_r&=-\mathrm{A}_1'\mathrm{J}_{n+1}+\mathrm{A}_2'\mathrm{J}_{n-1},\\ \mathrm{B}_\theta&=\ i(\mathrm{A}_1'\mathrm{J}_{n+1}+\mathrm{A}_2'\mathrm{J}_{n-1}),\end{aligned}\right\} \quad . \quad . \quad . \quad (6.2)$$

where

$$\left.\begin{aligned}\mathrm{A}_1'&=\ \frac{c}{c_2}\left[\mathrm{A}_1+(\mathrm{A}_1+\mathrm{A}_2)\frac{\zeta^2}{2}\right],\\ \mathrm{A}_2'&=-\frac{c}{c_2}\left[\mathrm{A}_2+(\mathrm{A}_1+\mathrm{A}_2)\frac{\zeta^2}{2}\right].\end{aligned}\right\} \quad . \quad . \quad (6.3)$$

It can be observed that the expression (6.2) can be obtained from the similar expressions (3.6) and (3.9) of the electric vector by substituting iA_1' and iA_2' for A_1 and A_2 resp.

The relationships (6.3) become especially simple in the case of rotating cylindrical waves with elliptically polarized vector (section 4).

When the ellipse of polarization of the electric vector lies in an azimuthal plane, *i. e.*, $A_1=-A_2$ (see formulæ (4.3)), the relationships (6.3) are reduced to

$$A_1'=\frac{c}{c_2}A_1, \qquad A_2'=-\frac{c}{c_2}A_2=A_1'. \quad . \quad . \quad (6.4)$$

When the ellipse of polarization of the electric vector lies approximately in an axial plane at, *i. e.*, $A_1=A_2$ (see formulæ (4.4)), we find on the ground of (2.9) that (6.3) reduces to

$$A_1'=\frac{c_2}{c}A_1, \qquad A_2'=-\frac{c_2}{c}A_2=-A_1'. \quad . \quad . \quad (6.5)$$

We can see from this that rotating cylindrical waves with an elliptically polarized electric vector have also a nearly elliptically polarized magnetic vector at $r_1>>1$, but their planes of polarization are different: while the ellipse of polarization of the electric vector lies in an azimuthal plane, the ellipse of polarization of the magnetic vector lies approximately in an axial plane at $r_1>>1$, and *vice versa*.

The expression of the magnetic vector of planar waves can be easily found from (6.5), (5.3), and (5.4).

7. *The Energy Flux and the Energy Density.*

The total amount of energy transported by e.m. waves through certain surface per unit time is usually called the energy flux though this surface. The energy flux per unit area of a surface at a given point is measured by a scalar product of a unit vector coinciding with the normal to this surface at the given point, drawn in the direction conventionally taken as a positive one, and a so called Poynting vector, which we shall denote by **S**.

The Poynting vector is equal to $\frac{c}{4\pi\mu}$ times vector product of the electric and magnetic vectors as they were defined

above (see section 2). Therefore the expression for the components of **S** can be easily found from (2.3), (3.6), (3.9), (6.1), and (6.2), according to the usual rules of calculation of a vector product. It should, however, be borne in mind that in this operation only real part of the complex expressions for E_x, E_r, and E_ϑ and B_x, B_r, and B_θ must be taken.

The result can be written as follows :—

$$\left.\begin{aligned}
\frac{4\pi\mu}{c}\mathrm{S}_x &= \mathrm{A}_1\mathrm{A}_1'\mathrm{J}^2_{n+1} - \mathrm{A}_2\mathrm{A}_2'\mathrm{J}^2_{n-1} \\
&\quad -(\mathrm{A}_1\mathrm{A}_2' - \mathrm{A}_2\mathrm{A}_1')\mathrm{J}_{n+1}\mathrm{J}_{n-1}\cos 2\,(\Omega t+\kappa x+n\theta), \\
\frac{4\pi\mu}{c}\mathrm{S}_r &= \zeta(\mathrm{A}_1\mathrm{A}_2' - \mathrm{A}_2\mathrm{A}_1') \\
&\quad \times(\mathrm{J}_{n+1} - \mathrm{J}_{n-1})\mathrm{J}_n \sin 2(\Omega t+\kappa x+n\theta), \\
\frac{4\pi\mu}{c}\mathrm{S}_\vartheta &= \zeta[(\mathrm{A}_1\mathrm{A}_1'\mathrm{J}_{n+1} - \mathrm{A}_2\mathrm{A}_2'\mathrm{J}_{n-1}) \\
&\quad -(\mathrm{A}_1\mathrm{A}_2'\mathrm{J}_{n+1} - \mathrm{A}_1'\mathrm{A}_2\mathrm{J}_{n-1})\cos 2(\Omega t+\kappa x+n\theta)]\mathrm{J}_n.
\end{aligned}\right\} \quad . \quad . \quad . \quad (7.1)$$

According to these formulæ we can resolve the vector **S** into two components : the one is constant for a given radial coordinate, while the other alternates with the frequency twice as great as that of the electric and magnetic field.

We shall denote the *average* value of the vector **S** and its components by a dash on the corresponding letter ($\bar{\mathbf{S}}$, $\bar{\mathrm{S}}_x$, etc.). In calculation of this average value the alternating part will disappear. Hence

$$\left.\begin{aligned}
\frac{4n\mu}{c}\bar{\mathrm{S}}_x &= \mathrm{A}_1\mathrm{A}_1'\mathrm{J}^2_{n+1} - \mathrm{A}_2\mathrm{A}_2'\mathrm{J}^2_{n-1}, \\
\bar{\mathrm{S}}_r &= 0 \\
\frac{4\pi\mu}{c}\bar{\mathrm{S}}_\theta &= \zeta(\mathrm{A}_1\mathrm{A}_1'\mathrm{J}_{n+1} - \mathrm{A}_2\mathrm{A}_2'\mathrm{J}_{n-1})\mathrm{J}_n.
\end{aligned}\right\} \quad . \quad (7.2)$$

The magnitude of **S** will be

$$\bar{\mathrm{S}} = \sqrt{\bar{\mathrm{S}}_x^2 + \bar{\mathrm{S}}_\theta^2}, \quad . \quad . \quad . \quad . \quad . \quad . \quad (7.3)$$

and it will be situated in the plane θx at the angle

$$\phi = \tan^{-1}\frac{\bar{\mathrm{S}}_x}{\bar{\mathrm{S}}_r} \quad . \quad . \quad . \quad . \quad . \quad . \quad (7.4)$$

to the plane $r\theta$.

A surface orthogonal to **S** is usually called a wave front. It can be seen from (7.1) that the wave front of rotating cylindrical waves will be an undulating surface but on the average it will be a helical surface, and the lines of propagation of the energy will be helices (formulæ (7.3) and (7.4)). On the other hand in simple cylindrical waves, *i. e.*, when $n=0$, the lines of propagation will be straight and the wave front plane *.

This screw-like propagation of energy gives further justification for calling our waves "rotating cylindrical," as we did at first on the ground of the screw-like propagation of the phase.

The energy density

$$\mathbf{E}=\frac{1}{8\pi}\left[\frac{1}{\mu}(B_x^2+B_r^2+B_\theta^2)+\epsilon(E_x^2+E_r^2+E_\theta^2)\right] \quad (7.5)$$

(taking only the real part of the expression for B_x, B_r, and B_θ, and E_x, E_r, and E_θ).

In this energy density we can distinguish two parts: the one which will be contributed by the components of **E** and **B** perpendicular to **S** and, therefore, contributing to the steady energy flux, and the other which will be contributed by the components of **E** and **B** parallel to $\bar{\mathbf{S}}$, and, therefore, not contributing to the steady energy flux. The first part we shall denote by $\mathbf{E}_1$, the second by $\mathbf{E}_2$, and again we shall indicate by a dash on the letter that an average value is to be taken.

Thus by definition

$$\begin{aligned}\bar{\mathbf{E}}_1 &= \frac{1}{8\pi}\left[\frac{1}{\mu}(\bar{B}_x^2\cos^2\phi+\bar{B}_r^2+B_\theta^2\sin^2\phi)\right.\\ &\qquad\left.+\epsilon(\bar{E}_x^2\cos^2\phi+E_r^2+E_\theta^2\sin^2\phi)\right]\\ &= \frac{1}{16\pi}\left[\left(\frac{B_x^2}{\mu}+\epsilon E_x^2\right)\frac{\bar{S}_\theta^2}{\bar{S}^2}+\frac{B_r^2}{\mu}+\epsilon E_r^2\right.\\ &\qquad\left.+\left(\frac{B_\theta^2}{\mu}+\epsilon E_\theta^2\right)\frac{\bar{S}_x^2}{\bar{S}^2}\right]. \quad (7.6)\end{aligned}$$

by (2.3), (6.1), and (7.4).

We shall now apply these formulæ to the case of elliptically polarized electric and magnetic vectors.

* Compare Hartree, *loc. cit.*

We shall limit ourselves to the case when $\epsilon=1$ and $\mu=1$.

Consider first the case when the ellipse of polarization of the electric vector is situated in an azimuthal plane, *i. e.*, when $A_1=-A_2$. Then we have by (6.4) and (7.2)

$$\left.\begin{aligned} \frac{4\pi}{c}\dot{S}_r &= \frac{c}{c_2}A_1^2(J_{n+1}^2+J_{n-1}^2) \\ \bar{S}_r &= 0 \\ \frac{4\pi}{c}S_\theta &= \zeta\frac{c}{c_2}A_1^2(J_{n+1}+J_{n-1})J_n = \zeta\frac{c}{c_2}A_1^2\frac{2n}{r_1}J_n^2, \end{aligned}\right\} \quad . \quad (7.7)$$

whence by (7.6), (4.3), and (6.2)

$$\mathbf{E}_1=\frac{A_1^2}{16\pi}\left[\frac{\dfrac{c^2}{c_2^2}\zeta^4\dfrac{4n^2}{r_1^2}J_n^6+\left[(J_{n+1}-J_{n-1})^2+\dfrac{c^2}{c_2^2}(J_{n+1}+J_{n-1})^2\right](J_{n+1}^2+J_{n-1}^2)}{(J_{n+1}^2+J_{n-1}^2)^2+\zeta^4\dfrac{4n^2}{r_1^2}J_n^4}+\frac{c^2}{c_2^2}(J_{n+1}-J_{n-1})^2+(J_{n+1}+J_{n-1})^2\right]. \quad (7.8)$$

When $r_1<<1$, we can neglect the terms containing r_1^{-2}. Hence by (7.3) and (7.7)

$$\bar{S}\underset{r_1<<1}{\cong}\bar{S}_x=\frac{c}{c_2}A_1^2(J_{n+1}^2+J_{n-1}^2), \quad . \quad . \quad (7.9)$$

and by (7.8)

$$\bar{\mathbf{E}}_1=\frac{A_1^2}{8\pi}\left(\frac{c^2}{c_2^2}+1\right)(J_{n+1}^2+J_{n-1}^2). \quad . \quad . \quad (7.10)$$

These expressions are practically suitable for the whole space with the exception of the part lying near to the axis.

When $A_2=A_1$ (see formulæ (4.4) and (6.5)) the expressions of $\bar{S}$ and $\bar{\mathbf{E}}_1$ will be obtained exactly in the same way as when $A_2=-A_1$, and the result will only differ

by the factor $\frac{c_2}{c}$, which in the former case will replace the factor $\frac{c}{c_2}$ in the latter.

8. *The average Speed of Energy Propagation. Comparison between the Rotating Cylindrical e.m. Waves and the Material Waves of de Broglie. Conclusion.*

The speed of energy propagation can be defined as the ratio between the Poynting vector and the energy density.

By the average speed of energy propagation at a given point we shall mean the ratio between the average value of the Poynting vector and the average density of the energy associated with the steady energy flux at this point. Denoting this average speed of energy propagation by $\bar{w}$ we can express this definition (see previous section) in the form

$$\bar{w}=\frac{\bar{S}}{\bar{\mathbf{E}}_1} \quad . \quad . \quad . \quad . \quad . \quad . \quad . \quad (8.1)$$

The average speed of the energy propagation of the rotating cylindrical wave train we shall define as the ratio between the total average energy flux through an azimuthal plane and the total energy, associated with the steady energy flux, per 1 cm. of the length of the axis of symmetry. Denoting this speed by $\bar{w}$ we can express this definition in the form

$$\bar{w}=\frac{\int_0^{\infty} \bar{S}_x r_1 dr_1}{\int_0^{\infty} \bar{\mathbf{E}}_1 r_1 dr_1} \quad . \quad . \quad . \quad . \quad . \quad . \quad (8.2)$$

We shall now apply this definition to the rotating cyl. waves with elliptically polarized electric and magnetic vectors.

In the case $A_1=-A_2$ (see previous section) we can use the approximate formulæ (7.9) and (7.10) for the definition of $\bar{S}_x$ and $\bar{\mathbf{E}}_1$, since they are applicable to the whole space except the space in the neighbourhood of the axis x. On introducing these formulæ into (8.2) we easily find

$$\bar{w} \cong \frac{2c}{\frac{c_2}{c}+\frac{c}{c_2}} = w. \quad . \quad . \quad . \quad . \quad (8.3)$$
$$r_1 >> 1$$

To apply this result to the case when $A_1 = A_2$ we must replace $\frac{c}{c_2}$ by $\frac{c_2}{c}$ (see the end of previous section). This, of course, will not alter the formula (8.3) which is, therefore, applicable to any elliptically polarized rotating cylindrical waves.

It can be noted that this relationship between the speed of energy propagation $\bar{w}$ and that of the phase propagation c_2, is very similar to the relationship between these quantities in the material waves according to the well-known de Broglie formula, which in our notation would be written $c_2 \bar{w} = c^2$. The main common feature is that when $c_2 \to c$, $\bar{w} \to c$, and when $c_2 \to \infty$, $w \to 0$.

Let us now assume that an elementary particle is associated with a rotating cylindrical wave train or a combination of such trains satisfying the formula (8.3).

Since, according to the experimental results, the particles do not lose any appreciable amount of energy as a result of their movement, it is natural to assume that the energy of the waves associated with the particle propagates with the same average speed as the particle itself. Denoting the speed of the particle by v we can write that $v = \bar{w}$, or, by (8.3)

$$v = \frac{2c}{\frac{c_2}{c} + \frac{c}{c_2}} \quad . \quad . \quad . \quad . \quad . \quad . \quad . \quad . \quad (8.4)$$

On the other hand, there is no necessity to postulate that the intrinsic energy mc^2 of the particle should be *equal* to one quantum $h\nu$ of the waves associated with the particle, although it is reasonable to assume that a certain relationship exists between the former and the latter.

We can, therefore, modify the Einstein-de Broglie formula $mc^2 = h\nu$ into

$$qmc^2 = h\nu, \quad . \quad . \quad . \quad . \quad . \quad . \quad . \quad (8.5)$$

where q is a coefficient.

By (8.5) and (2.4)

$$qmc^2 = \frac{hc_2}{\lambda}, \quad . \quad . \quad . \quad . \quad . \quad . \quad (8.6)$$

whence by (8.4) $$v = \frac{2c}{\frac{qmc\lambda}{h} + \frac{h}{qmc\lambda}} \quad . \quad . \quad . \quad . \quad . \quad (8.7)$$

Hence $$\lambda=\frac{h}{qmv}\left(1+\sqrt{1-\frac{v^2}{c^2}}\right). \quad . \quad . \quad . \quad (8.8)$$

The equation (8.7) is a quadratic equation, and we should have, in its solution (8.8), $\pm$ before the $\sqrt{\ }$.

We have, however, omitted the lower sign as unsuitable for our case, for it would mean by (8.8) that $\lambda\to 0$ when $v\to 0$ which, in its turn, would mean, by (8.5), that $\nu\lambda=c_2\to 0$ when $v\to 0$, which is contrary to our condition that $c_2>c_1$ (since $c_1=c$).

The well-known de Broglie formula is $\lambda=\frac{h}{mv}$.

Inasmuch as the latter formula is confirmed by the measurement of the electronic diffraction at $v<<c$ we must accept that for the electron $q=2$, or, in other words, we must assume that the internal energy of the electron is equal to one half of the quantum of the associated rotating cylindrical waves *.

Apart from the possible connexion between the rotating cylindrical waves and the " material " waves of de Broglie, it appears not to be improbable that the ordinary optical waves may be, by their structure, nearer to the rotating cylindrical waves, with c_2 approaching to c, and their combinations like planar waves, than to the ordinary plane waves with constant amplitude, which are usually considered as a suitable form of approximation.

The chief reason is that the rotating cylindrical and plane waves, are, to a considerable extent, concentrated at the axis of symmetry in the former case and at the principal plane in the latter case, and, therefore, they appear to be a more suitable representation of optical wave trains which have practically the whole energy flux passing through a limited section. The total energy flux of ordinary plane e.m. waves within a section of a radius r is of the order r^2, while for the rotating cylindrical and planar waves it is for $z<<\lambda$ of the order r.

The other reason is that the rotating cylindrical waves allow greater variety of forms of polarization than the

* When this paper was already in print, another possible connexion between the rotating cylindrical waves and de Broglie's material waves was found by the author, in which the Einstein–de Broglie formula $\lambda=\frac{h}{mv}$ would hold exactly.

The author hopes to return to this question in a separate paper.

ordinary plane e.m. waves may give. For example, in elliptically polarized rotating cylindrical waves the direction of the rotation of the electric vector must appear to change after reflexion from a mirror if the ellipse of polarization lies approximately in an axial plane (*i. e.*, of $A_1=A_2$), but it must appear to remain unchanged if the ellipse of polarization lies in an azimuthal plane (*i. e.*, $A_1=-A_2$).

This, perhaps, may help to explain certain phenomena relating to the elliptically (or, in a particular case, circularly) polarized optical e.m. waves.

However, further discussion of possible connexion between the rotating e.m. waves and optical waves lies outside the scope of this paper.

Appendix.

We have $$2\pi J_n(z)=\oint e^{-in\gamma+ir\sin\gamma}d\gamma\ *, \quad . \ . \ (1\text{ ap.})$$

where $\oint$ represents an integral taken in a conventionally positive (anticlockwise) direction along a closed contour, constituting the locus of extremities of vectors representing complex quantities $e^{i\gamma}$, making one complete revolution round the pole of these vectors.

The variable γ is, generally speaking, a complex quantity. If we put $\gamma=\theta+i\phi$ where θ and ϕ are real, then $e^{i\gamma}=e^{i\phi+i\theta}$ will be represented by a point with radial and angular coordinates $e^{-\phi}$ and θ resp. The pole of this system of vectors will correspond to $\phi=\infty$.

Take a contour of integration consisting of two half circumferences, the one of radius $e^{-\alpha}$, passing from $\theta=-\frac{\pi}{2}$ to $\theta=\frac{\pi}{2}$, and the other of radius e^{α} passing from $\theta=\frac{\pi}{2}$ to $\theta=\frac{3\pi}{2}$, and of two sections of radii the one at $\theta=-\frac{\pi}{2}$, and the other at $\theta=\frac{\pi}{2}$, connecting the

* More usual form of this formula can be obtained by putting $z=e^{i\gamma}$ (see, for example, Whittaker and Watson, 'Modern Analysis,' section 17, 23 (3rd edition)).

extremities of these half circumferences. Then (1 ap.) can be written as follows :—

$$2\pi J_n(r)=\left(\int_{-\frac{\pi}{2}}^{\frac{\pi}{2}} e^{n\alpha-r\sinh\alpha\cos\theta}+\int_{\frac{\pi}{2}}^{\frac{3\pi}{2}} e^{-n\alpha+r\sinh\alpha\cos\theta}\right)$$

$$\times e^{ir\cosh\alpha\sin\theta-in\theta}\,d\theta+\left(\int_{\alpha}^{-\alpha} e^{n\phi}+\int_{-\alpha}^{\alpha} e^{-n\phi}\right)e^{ir\cosh\phi}\,d\phi.$$

. . . (2 ap.)

Substitute $-\phi$ for ϕ in the second integral of the second term; then its subintegral expression will become identical to that of the first integral, while the limits will be reversed. Hence the second term of the right-hand number is equal zero.

Substitute in (2 ap.), $-\theta+2\pi$ for θ in the second integral, of the first term (with corresponding changes of the integral limits).

Form two modifications of the formula thus altered : the first in which $2n$ and $2n+1$ are substituted for *even* and *odd* n resp., and the second, in which n is correspondingly replaced by $-2n$ and $-2n-1$.

Add both modifications in the case if n was originally *even* and subtract second modification from the first in the case if n was originally *odd*.

Then denoting

$$\eta=\sinh\alpha\cos\theta,\quad \tau=\cosh\alpha\sin\theta,\ .\ .\ .\ (3\text{ ap.})$$

and marking the letters with a dash on the top, if the functions represented by them must be taken with opposite sign within the interval $\frac{\pi}{2}<\theta<\frac{3\pi}{2}$, we can write the result in the form

$$2\pi J_{2n}(r)=\oint X\cos 2n\xi\,d\xi$$

$$2\pi J_{2n+1}(r)=i\oint X\sin(2n+1)\,\xi\,d\xi,\ .\ .\ (4\text{ ap.})$$

where

$$X=e^{-\tau\eta+i\tau\bar{\tau}}$$

$$\xi=-\theta+i\alpha\ .\ .\ .\ .\ .\ .\ (5\text{ ap.})$$

By (4 ap.)

$$\pi(J_{2(n+1)}(r)\pm J_{2n}(r))=\oint X\begin{matrix}\cos\\-\sin\end{matrix}\xi\begin{matrix}\cos\\\sin\end{matrix}(2n+1)\,\xi\,d\xi$$

$$\pi(J_{2n+1}(r) \mp J_{2n-1}(r)) = i \oint \overline{\underline{X}} \begin{matrix} \sin \\ \cos \end{matrix} \xi \begin{matrix} \cos \\ \sin \end{matrix} 2n\xi \, d\xi. \quad . \quad (6 \text{ ap.})$$

By the well-known properties of Fourier Series * we have, from (4 ap.) and (6 ap.),

$$\left.\begin{aligned} X &= \sum_{n=0}^{\infty} J_{2n}(r) \cos 2n\xi \\ i\overline{X} &= \sum_{n=0}^{\infty} J_{2n+1}(r) \sin (2n+1)\xi \end{aligned}\right\} \quad . \quad . \quad (7 \text{ ap.})$$

$$\left.\begin{aligned} 2X \begin{matrix} \cos \\ -\sin \end{matrix} \xi &= \sum_{n=0}^{\infty} \left(J_{2(n+1)}(r) \pm J_{2(n-1)}(r) \right) \begin{matrix} \cos \\ \sin \end{matrix} (2n+1)\xi, \\ 2i\overline{X} \begin{matrix} \sin \\ \cos \end{matrix} \xi &= \sum_{n=0}^{\infty} \left(J_{2n+1}(r) \mp J_{2n-1}(r) \right) \begin{matrix} \cos \\ \sin \end{matrix} 2n\xi. \end{aligned}\right\} (8 \text{ ap.})$$

Summary.

Electromagnetic waves are discussed, which are axially symmetrical and propagate along the axis of symmetry, with the velocity greater than that of ordinary plane e.m. waves with constant amplitude, and simultaneously rotate about this axis. These waves are called "super-fast rotating cylindrical waves." Different states of polarization of these waves are considered.

A combination of co-axial wave trains of this kind with the same wave-length and frequency but different angular velocities of rotation is called "compound" waves.

A particular case of compound waves leading to waves having the energy concentrated in the plane of symmetry (principal plane) is discussed.

* In the usual form of Fourier Series ξ supposed to be real. In the generalized form of Fourier Theorem

$$F(x) = \sum_{n=-\infty}^{\infty} \frac{\int_a^b F(y) \bar{f}_n(y) \, dy}{\int_a^b f_n(y) \bar{f}_n(y) \, dy} f_n(x)$$

where $f_n(\ )$ and $\bar{f}_r(\ )$ are orthogonal functions, *i. e.*,

$$\int_a^b f_n(y) \bar{f}_m(y) \, dy = 0 \qquad m \neq n.$$

It is not difficult to see that $\sin n\xi$ or $\cos n\xi$ are orthogonal if $\xi = \pm\theta + i\alpha$ where α is constant.

This kind of compound waves is called "planar" waves.

The rotating cylindrical waves are compared with the de Broglie's material waves, and an assumption is considered that the former waves or their combination may play the part of the latter.

It is hinted that the rotating cylindrical waves or their combination may be used for approximate representation of the structure of optical waves.

I wish to thank Sir William Bragg, O.M., for his kind and encouraging interest, Prof. D. R. Hartree for very valuable suggestions, and Miss A. C. Lewis, B.Sc., for checking the formulæ.

This paper was written in connexion with experimental work which I am doing in the Davy Faraday Laboratory, Royal Institution, and I take this opportunity of expressing my thanks to the Managers of the Royal Institution for giving me the facilities for this experimental work.

The Royal Institution.

LXXVIII. *Photoelectric Fatigue and Oxidation.* *By* J. S. Hunter, *B.Sc., Ph.D., A.Inst.P.**

Introduction.

THE nature of the change undergone by a clean metallic surface on exposure to the air is not fully understood. Experiments on the corrosion of iron by U. R. Evans † indicate that the surface becomes covered with a film of oxide if left in contact with the air. Such a film may be formed instantaneously on the surface, be invisible to the eye, and in some cases may be so thin that its presence cannot be detected by interference methods. Even so it may still exert important protective

* Communicated by Prof. H. S. Allen, M.A., D.Sc., F.R.S.

† U. R. Evans, Journ. Chem. Soc. p. 1029 (1927); *ibid.* pp. 92 & 2651 (1929).

and strong electrochemical effects. Hume Rothery* is of the opinion that these oxide films are formed immediately the clean surface of nearly all metals comes in contact with the air.

On the other hand, there is much experimental evidence† to support the view that the photoelectric fatigue of a clean metal surface is due to a process of gas adsorption by the surface from the air, and the suggestion may be made that when a metallic surface comes in contact with the air it begins immediately to adsorb gas rather than to form a film of oxide.

In a previous paper by the writer‡ the results of experiments on the photoelectric properties of some turned metallic surfaces in air were given. In this present work some of these turned metallic surfaces were covered with a film of their oxide by heating in air or oxygen, and then examined photoelectrically under the same conditions as were the turned surfaces themselves. By comparing the photoelectric properties of these oxide films with those of the turned metallic surface further light upon the phenomena connected with surface change of a clean metallic surface can be obtained.

Preparation of Oxide Surfaces.

The metals oxidized were copper, silver, bismuth, and nickel. In the case of copper the metal was heated in a temperature-controlled electric furnace until the characteristic colour of either the cuprous or the cupric oxide appeared. In the case of silver the temperature was kept at about 250° C. during the oxidation, carried out in a stream of damp oxygen. The bismuth was heated at a temperature just below its melting-point in a stream of air. It is probable that the film formed in this case is a mixture of bismuth and bismuth trioxide. The oxide film of nickel, prepared in a similar manner to the above, is dark brown in colour and consists for the main part of nickelic oxide, although some monoxide is probably also present.

* 'The Metallic State,' p. 149.

† Hallwachs, *Phys. Zeits.* v. p. 489 (1904). H. S. Allen, Proc. Roy. Soc. lxxxii. p. 164 (1909); Phil. Mag. xx. p. 565 (1910).

‡ J. S. Hunter, Proc. Roy. Soc. Edin. liv. p. 102 (1934).

Experimental.

The apparatus used in the following experiments is the same as that described in the previous paper, except that a Dolezalek electrometer replaces the electrometer valve and Paschen galvanometer for measuring the currents. The relative intensities of the spectral lines in the region employed were measured as before. The following table gives the energy distribution throughout the spectral region $\lambda\lambda$ 2060—2600 Å. The intensities are given relative to the 2537 Å. line, the intensity of which is taken arbitrarily as 100, but in absolute units corresponded to

TABLE I.

Relative Intensities of Spectral Lines.

Wave-length.	Intensity.	Wave-length.	Intensity.
Å.U.		Å.U.	
2060	0·45	2270	5·55
2110	1·10	2310	6·3
2140	1·79	2350	10·0
2190	2·47	2410	18·6
2200	3·3	2450	24·35
2230	4·3	2540	100·0
2250	4·75	2600	87·2

an energy of 1·46 microwatts per second. It is seen that the spectral region is well in the ultra-violet, below 2400 Å.; the individual lines were so difficult to distinguish as such that intensity measurements below this wave-length were recorded every 10 or 20 Å. units.

The photoelectric currents obtained from each oxide surface were reduced to currents per unit intensity by means of the above table, and thus spectral distribution curves were obtained, some of which are reproduced in fig 1. By extrapolation of these curves to zero-current the apparent thresholds of the oxidized metallic surfaces could be obtained. True thresholds could be found by applying Fowler's theory to these results, and, although true and apparent thresholds do not differ greatly at

Fig. 1.

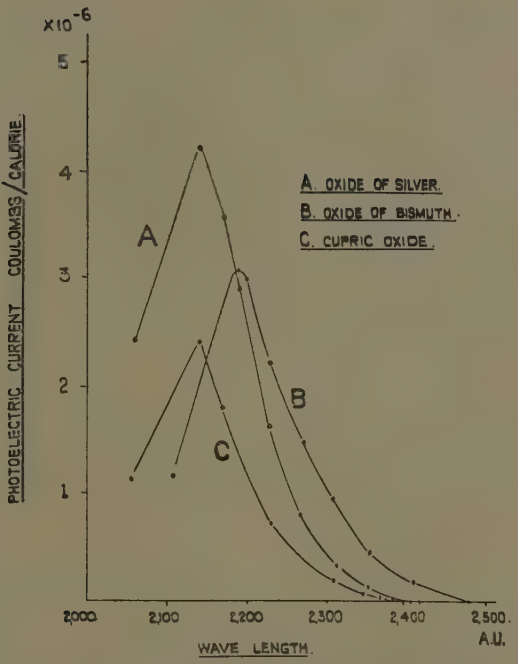

Spectral distribution curves of some oxide surfaces.

TABLE II.

Oxide.	Maximum current I_m.	Wave-length for λ_m.	Apparent threshold.	True threshold.
	coulombs/calorie.	Å.U.	Å.U.	Å.U.
Cuprous ..	9.6×10^{-6}	2150	2520	2500
Cupric	2·7	2110	2425	2402
Silver	4·23	2140	2410	2393
Bismuth ..	3·09	2190	2480	2460
Nickel	1·15	2190	2480	2451

ordinary temperatures, it was interesting to see that Fowler's theory was applicable with some success to these oxide surfaces. Table II. contains a list of the results.

Photoelectric thresholds have been determined previously only for the oxides of copper. Fleischmann gives for the apparent thresholds of cuprous and cupric oxides the values 2400 Å. and 2310 Å. respectively. An earlier determination by Millikan gives the threshold of oxidized copper as falling between 2530 and 2690 Å.U., but no spectral distribution curves were obtained by him. The experiments of Fleischmann were carried out in a high vacuum.

From Table II. it is seen that the value of the maximum yield lies between 10^{-5} and 10^{-6} coulombs

TABLE III.

Metal.	Turned surface.	Outgassed surface.	Oxide film surface.
	Å.U.	Å.U.	Å.U.
Copper	2985	2740	(cuprous) 2520 (cupric) 2425
Silver	3200	2610	2410
Bismuth	3075	2800	2480
Nickel	3125	2463	2480

per calorie and occurs at a wave-length below 2200 Å.U. for each oxide. The presence of this maximum is interesting, and it may be due to (1) a definite spectral selectivity of the surface, or (2) usual factors inducing maxima in normal spectral distribution curves. The former explanation would appear to be the most likely when the complex nature of these surfaces is borne in mind.

The writer has shown that the photoelectric thresholds of turned surfaces approximate to those of the partially outgassed state of the surface, so that now a comparison can be made between the oxide film surface, the turned surface, and the outgassed surface; Table III. contains

values of the photoelectric thresholds for these types of surface.

The values for the outgassed state are taken from the list of Hughes and Dubridge.

From Table III. it is seen that the thresholds for the turned metallic surfaces lie on the long-wave side of those for the outgassed clean metal surface. If, therefore, a clean metallic surface is exposed to the air its photoelectric threshold moves towards the longer wave-lengths. This is so whatever hypothesis is put forward to explain the actual process taking place at the surface. Now if it is true that a film of oxide does form instantaneously on the surface the above result suggests that the threshold of this oxide film, if present, should lie on the long-wave side of that for the outgassed clean metallic surface. From Table III., however, it is seen that the reverse is the case, and that thresholds for oxide films, except for the case of nickel, lie on the short wave-length side of those for the outgassed surface. Thus the thresholds for an oxidized metallic surface and for a turned metallic surface exposed to the air for a short time lie on opposite sides of the threshold for the clean outgassed metal surface.

This result shows that if a clean metal surface is exposed to the air the potential barrier at the surface is lowered, but that oxidation of the clean surfaces raises the potential barrier. The surface states therefore are not similar, and the results indicate that no oxide film is formed instantaneously on the clean surface or the turned surface when exposed to air.

It is well known that nearly all metals will tarnish or become oxidized to some extent if left in contact with the air for a sufficiently long time. This type of change does not come within the scope of the present problem, where the time factor is of the order of a few minutes.

It may be suggested that an oxide film had formed on these turned surfaces but was too thin to be detected by photoelectric means. This is rather improbable, for even films which are too thin to be detected by interference methods exert strong electrochemical effects. Also it would be expected that even the thinnest of films would exert such a profound effect on the surface potential barrier—this barrier being extremely sensitive to surface

changes—that its presence would be indicated by a change of photoelectric threshold.

It should be borne in mind that the oxidized surfaces produced in these experiments are definite oxides of the metal ; however, it would be erroneous to assume that any oxide film consisted entirely of one particular oxide. It is probable that one particular oxide is dominant and preponderates in the film.

It has been shown by Rideal and Wilkins* that the initial oxidation of copper at low pressures is governed by the rate of condensation of oxygen at the oxide/oxygen interface.

As the above investigation leads to the conclusion that, although the results cannot be taken to support a theory of gas adsorption, yet they do indicate that such a theory is preferable to one which postulates the instantaneous formation of a film of oxide, the writer would suggest that there is a prior stage to the one outlined by Rideal and Wilkins—a stage of gas adsorption.

Thus, when a clean metallic surface is exposed to the air there is an instantaneous adsorption of gas by the surface. The rate at which oxygen from the air is adsorbed by the surface would govern the subsequent time interval before true oxidation of the surface would commence. In the case of iron this time interval would appear to be very small, whereas in the case of the metals copper, silver, bismuth, and nickel the interval is apparently relatively large at ordinary temperatures. Once the oxidation has begun the subsequent rate of oxidation would then depend upon the rate of condensation of oxygen at the oxide/oxygen interface.

The writer wishes to express his thanks to Prof. H. S. Allen, F.R.S., for his interest and valuable help throughout the investigation, and to the Carnegie Trust for a Scholarship which enabled the work to be done.

Physics Laboratory, The University,
St. Andrews.
January 5th, 1935.

* Rideal and Wilkins, Proc. Roy. Soc. A, cxxviii. p. 394 (1930).

LXXIX. *The Theory of Electrocapillarity.*—III.

By S. R. Craxford, O. Gatty, *and* J. St. L. Philpot *.

Introduction.

In the first two papers of this series [1], [2] the relations between the surface tension and curvature of an interphase, and the pressure, temperature, and compositions of the phases on either side of it, were deduced thermodynamically by consideration of an idealized apparatus reproducing as nearly as possible the conditions under which surface tension is actually measured. In the present paper the same method will be used to deduce the relation between the surface tension and the applied electromotive force.

The aim of electrocapillary studies is to learn something of the distribution of particles at the interphase between two conducting phases. The experimental data consist of values of surface tension corresponding to various electrical potential differences across the interphase and to various compositions of the phases. In the systems which have been most frequently studied in the past one phase has been mercury and the other an aqueous solution of an electrolyte, and the potential difference across the interphase has been altered by polarization. The data obtained have been used in conjunction with two essentially different thermodynamic relationships, namely, the Lippmann equation and the electrical form of the Gibbs adsorption equation.

Lippmann [3] assumed that the interphase is "completely polarizable," *i. e.*, that its state may be altered reversibly by flowing a quantity of electricity on to it from an external circuit. This is equivalent to assuming that somewhere in the interphase there is a boundary that no charged particle can cross. On this basis he derived the equation

$$\left(\frac{\partial\gamma}{\partial\Delta\phi}\right)_s = -\left(\frac{\partial q}{\partial s}\right)_{\Delta\phi}, \quad \ldots\ldots \quad (1)$$

where

γ is the surface tension ;

$\Delta\phi$ is the electrical potential difference across the interphase ;

* Communicated by Sir Harold Hartley, F.R.S.

s is the area of the interphase ; and

q is the quantity of electricity that is flowed into the interphase by means of an external circuit, and is to be taken as positive when it flows externally against positive $\Delta\phi$.

There is direct experimental evidence for the validity of the Lippmann equation, because the two terms in it have been measured directly and found to be equal in a number of cases (see, for example, Frumkin [4], Philpot [5]*, and Craxford [6]); but, in spite of this, questions may arise on the following points :—(i.) The validity of the original assumption of complete polarizability in actual practical cases, and hence, of the reversibility of the various processes involved in the Lippmann proof ; (ii.) the definition of $\Delta\phi$, a matter discussed by Guggenheim [7] ; (iii.) the relation of q to the structure of the interphase, which is the problem of the structure of the double layer (see Stern [8]) ; and, finally, (iv.) the effect of the composition of the phases on the electrocapillary curve, a matter about which the Lippmann equation gives no information.

The Gibbs adsorption type of theory, evolved by Gibbs [9], Warburg [10], and Thomson [11], approaches the problem from a standpoint entirely different and unrelated to that of Lippmann. It is applied most readily to electrocapillary curves obtained by controlling the potential difference across the interphase, not by polarization, but by changing the chemical composition of the phases. This procedure is only possible if there is present some " potential determining " ion which can pass freely across the interphase. The complete electrocapillary equation is given for this case by combining the Gibbs adsorption equation with the Nernst equation for electrode potential:

$$d\gamma = -\Gamma' d\mu' - \Sigma \Gamma_i \, d\mu_i \quad . \quad . \quad . \quad . \quad . \quad . \quad . \quad (2\,a)$$

and

$$d\Delta\phi = +\frac{1}{z\mathrm{F}} \, . \, d\mu', \quad . \quad . \quad . \quad . \quad . \quad . \quad (2\,b)$$

* Dr. Brdička has pointed out (private communication) that equation (1 *b*) in this paper is incorrect. The results quoted were, however, calculated from the correct formula, and not from the misprinted one.

where

Γ_i is the amount of any ion i adsorbed ;

Γ' is the amount of the potential determining ion adsorbed ;

μ_i is the chemical potential of any ion i ;

μ' is the chemical potential of the potential determining ion, whose valency is z, and

F is the faraday.

One special case obtained by combining these equations is

$$\left(\frac{\partial\gamma}{\partial\Delta\phi}\right)_{s,\,\mu_i} = -z\mathrm{F}\Gamma', \qquad . \quad . \quad . \quad . \quad (2)$$

an equation formally analogous to the Lippmann equation. The use of the Gibbs electrocapillary equation is attended, however, by the following difficulties, namely, (i.) the placing of the arbitrary boundary required in the general definition of the Γ's ; (ii.) the relationship of the Γ's to the electrical properties of the double layer ; and (iii.) the integration of the equation when ions other than the potential determining ion are adsorbed. It is to be noted, however, that this method is capable of dealing with the problem of the change of electrocapillary curves with changing composition of the phases.

It has been the custom heretofore to apply the Gibbs treatment also to the case where the potential difference across the interphase is controlled by polarization, and so to the whole of electrocapillary data. This depends on the assumption that when the potential difference across the interphase is altered by flowing current across it, the primary effect of the current is to alter, by electrolysis, the concentration of the potential determining ion in the layer of solution next to the metal in such a way that its value is always related to the potential difference by the Nernst equation (2 *b*) for electrode potential. This being so, equations (2 *a*), (2 *b*), and (2) can be applied directly, μ' being equal to the chemical potential of the potential determining ion in the layer of solution next to the metal, which is maintained different to its value in the bulk of the solution, by electrolysis, in the way described. While this treatment allows the Gibbs method to be applied to the

problem of the effect of the composition of the phases on the electrocapillary curve, as has been done by Butler [12] and Frumkin [13], there is considerable doubt as to whether the underlying assumption described in this paragraph is correct. For the potential differences over the greater part of the electrocapillary curve the corresponding equilibrium concentrations of the potential determining ion are excessively small, going down to values of the order of 10^{-60}. In practice it is found that electrical potentials cannot be controlled by an ion whose concentration is much less than 10^{-10}, so that these very small concentrations of the potential determining ion cannot possibly control the properties of the interphase. This question has been discussed by Andauer and Lange [14], Craxford [15], and Koenig [16], and since then another argument against the assumption is provided by data in a recent paper by Samarcev [17], who showed that, even for very small polarizations, such as a few millivolts, the resulting adjustment of the concentration of the potential determining ion in the layer of solution next to the metal corresponds only to about half of the applied potential.

The electrocapillary equation derived in the present paper, while containing the two existing types of electrocapillary theory described in this section, as special cases, avoids their difficulties and overcomes their limitations. It may be described formally as an extension of the Lippmann treatment, in that electrical work done on the whole cell is considered, but from such considerations results are obtained that heretofore have only been accessible by the application of the Gibbs electrocapillary equation.

Reversible Electrolysis.

In the theory of capillarity it was found necessary to consider finite reversible alterations in the composition of a phase which were brought about by an unspecified process for the addition and removal of particles. In the case of electrocapillarity it is desirable to bring about these changes by electrolysis, but in this case it has first to be shown that such processes can be truly reversible. Let the particles of each of a complete set of the chemical components of a phase be added or subtracted from

reservoirs through an idealized boundary which is permeable only to the given component, is insoluble, and allows nothing to be deposited on it from the given phase. If the substance to be introduced is a liquid, the boundary may be thought of as an idealized semi-permeable membrane of the type used in measurements of osmotic pressure. If the substance to be introduced is an electrolyte, the boundary and its reservoir may be replaced by one idealized non-polarizable electrode for each of the constituent ions. Each of these electrodes, somewhere in its interphase with the solution, must have an idealized boundary that is permeable only to the ion concerned. Any number of boundaries defined in this way can be supposed to coexist in a solution, and they can be supposed to be used to bring about reversible osmosis and electrolysis. In thermodynamic reasoning expressions are used for the work done during these reversible changes; in practice measurements of this work depend upon the use of real semi-permeable membranes and real electrodes. These measurements give results that are not exactly equal to those expected for the case of the idealized boundaries, because the real membranes and electrodes are not completely impermeable to all the other components. In the case of real electrodes, however, there is another difficulty, since no electrolytic cell whose electromotive force is not zero is in true equilibrium. In every case the electromotive force depends on a difference in concentration of some component at the two electrodes, which must be maintained against diffusion. For instance, in the cell Zn | $ZnCl_2$ aq. | AgCl | Ag there is a saturated solution of silver chloride at the silver–silver-chloride electrode, which is the positive electrode. The resulting silver ions, in the absence of overvoltage, will deposit on any surface more negative than the silver–silver-chloride electrode with which they are in equilibrium. If, therefore, the silver chloride is given time to diffuse over to the zinc electrode, silver will be deposited on the zinc, and in contact with a saturated solution of silver chloride, it will eventually become another silver–silver-chloride electrode, so that the final electromotive force of the cell is zero. The substances whose concentrations are different at the two electrodes need not be electrolytes; in the cell Pt | H_2 | HCl aq. | Cl_2 | Pt, for example, they

are the gases hydrogen and chlorine. Fortunately the rate of diffusion of ions is so small, compared with the rate at which they can be moved by electricity, that it is possible to apply to experimental data thermodynamic equations obtained by neglecting the irreversible equalization of concentrations that slowly takes place. There are two types of cell which can thus be treated as thermodynamically reversible. They are, respectively, the cell with and without liquid junction. The former, being unsuited to the purpose of this paper, will not be considered here.

In the case of real electrodes, reversible alterations in the compositions of the bulk phases present the peculiar difficulty that they must involve diffusion from one electrode to the other, and this must occur at an infinitesimal rate if the process is to be truly reversible. During this diffusion process, however, the difference of concentration of the diffusing substance at the two electrodes, upon which the electromotive force depends, would have time to disappear, and the electromotive force would become zero. It is possible, however, to make infinitesimal additions of electrolyte to a cell in this state of pseudo-equilibrium, and not to wait for diffusion to equalize the concentration through the cell. Under these conditions the work of introducing an infinitesimal quantity, of the first order, of the electrolyte into the cell is a small quantity of the first order. The work required to equalize the concentration is required to equalize an infinitesimal concentration difference by transfer of an infinitesimal quantity of electrolyte, and it is, therefore, a small quantity of the second order. Therefore the work necessary to add a small quantity of electrolyte of the first order to the cell is the same, as far as small quantities of the first order, whether diffusion is subsequently supposed to take place or not. Therefore the ordinary thermodynamic theory of electromotive force is valid, and the work of reversible electrolysis can be calculated from a smooth curve drawn through a number of points obtained by plotting experimental determinations of electromotive force against concentration of electrolyte. Similarly it is possible to calculate the values of the electromotive force, if no suitable electrodes are available, from activity data obtained from other than electromotive measurements.

The above argument can be put on a quantitative basis, as follows :—Consider a cell containing an electrolyte AC of concentration c, and a diffusing electrolyte BC whose concentration is $c' << c$ at the positive electrode, and is vanishingly small at the negative. Let electricity be sent through the cell by applying an external electromotive force which at each instant is greater than E, the equilibrium electromotive force of the cell, by an amount δE. This causes c to change by electrolysis to $c+\Delta c$, so that E becomes $E+\Delta E$. The electrical work done, if the change is small, is equal to

$$(E+\delta E+\tfrac{1}{2}\Delta E)(\Delta q-\Delta q'), \quad . \quad . \quad . \quad . \quad (3)$$

where Δq and $\Delta q'$ are quantities of electricity corresponding respectively to the electrolysis of $V\Delta c$ of electrolyte into the solution of volume V and to the amount of ion B^+ which diffuses across the cell to take part in the reaction $B^+ + A \rightarrow B + A^+$. Of this work $(E+\frac{1}{2}\Delta E)\Delta q$ is reversible, and $\delta E(\Delta q-\Delta q')$ and $-(E+\frac{1}{2}\Delta E)\Delta q'$ are irreversible. The portion $\delta E(\Delta q-\Delta q')$ is due to the ohmic resistance of the solution, and to concentration polarization. It goes to set up a concentration gradient of AC and to warming the solution. The portion $-\Delta q'(E+\frac{1}{2}\Delta E)$ is due to diffusion of B^+. The ratio of irreversible to reversible work is small provided $\frac{\Delta q'}{\Delta q}$ and $\frac{\delta E}{E+\frac{1}{2}\Delta E}$ are both small.

It may be shown that $\frac{\Delta q'}{\Delta q}$ is of the order $\frac{c'}{200c\delta E}$.

The proof is as follows :—

$\frac{\Delta q'}{\Delta q} = \frac{\Delta m'}{\Delta m}$, where m and m' are the masses of AC and BC respectively equivalent to q and q', all the ions being univalent. These masses diffuse across the cell in the same time under concentration gradients that are proportional to δc and c' respectively, where δc corresponds to δE. Therefore $\frac{\Delta m'}{\Delta m} = \frac{D'c'}{D\delta c}$, where D and D' are the diffusion constants. But since

$$\delta E = \frac{2RT}{F}\delta \ln c = 0{\cdot}05\,\frac{\delta c}{c}$$

at 25° C., it follows that

$$\frac{\Delta q'}{\Delta q} = \frac{D'c'}{20c\delta E.D}.$$

The order of magnitude is obtained by putting $D=D'$, so that

$$\frac{\Delta q'}{\Delta q} \approx \frac{c'}{20c\delta E}. \quad . \quad . \quad . \quad . \quad . \quad . \quad . \quad (4)$$

In consequence the condition for practical reversibility in the theory of electromotive force is that

$$\frac{c'}{20c} << \delta E << E + \tfrac{1}{2}\Delta E. \quad . \quad . \quad . \quad . \quad (5)$$

If E is of the order of 1 volt, the irreversible work can be reduced to some 0·01 per cent. by making $c'/c = 2\times 10^{-7}$. This is a practical figure. For instance, with the normal calomel electrode $Hg \mid Hg_2Cl_2 \mid N.KCl$ aq. the ratio becomes $c_{Hg_2^{++}} \mid c_{KCl}$, and equals 10^{-13}. This shows that thermodynamics are directly applicable to the electromotive forces of cells without any idealization. It is curious, but understandable, that in this case the displacement from equilibrium represented by δE must be not only small enough, but also great enough.

In the theory of electrocapillarity the system has to be supposed to traverse a cycle where the reversible work term is the difference between $\Delta q(E+\frac{1}{2}\Delta E)$ and $E\Delta q$. The condition for reversibility then becomes

$$\frac{c'}{20c} << \delta E << \Delta E.$$

Thus ΔE can no longer be of the same order as δE, as in the usual theory of electromotive force; but, on the other hand, if ΔE is too great the differential calculus ceases to apply. If ΔE is 0·0001 volt, if $c'/c = 2\times 10^{-11}$, and if δE is of the order of 10^{-8} volt, the irreversible work is of the order of 0·01 per cent. Thus the theory of electrocapillarity is just applicable directly, but only just, to the sort of electrodes that are used in practice.

An Electrocapillary Apparatus.

A complete apparatus for the thermodynamic investigation of electrocapillarity is shown in the figure,

and is designed to allow the following processes to be performed and their associated work terms measured.

(i.) The reversible alteration of the area of the interphase is performed by means of pistons I. and II., as in the apparatus described in paper I. of this series [1]. These pistons also perform compressional work on the phases.

(ii.) Reversible additions of electrolytes to the phases are made by means of electrochemically reversible

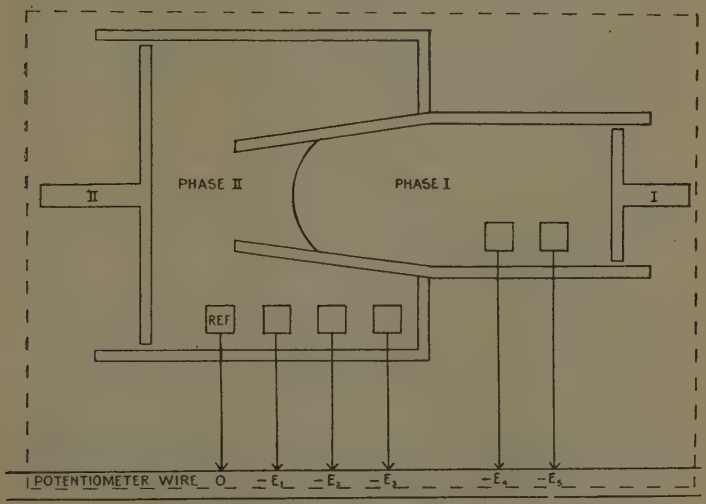

A generalized electrocapillary apparatus.

electrodes. Non-electrolytes are introduced by appropriate semi-permeable membranes, but the work of introducing them will always be handled in an electrochemical form, as will also the work of introducing metals into metallic phases even if this necessitates another aqueous phase. The system contains chemical components $1 \ldots r \ldots c$, and owing to the restriction of electrical neutrality it may therefore be said to contain $c+1$ component ions, for each of which there exists an idealized reversible electrode connected to a copper wire. Let the electrostatic potential of one of

these copper wires on some arbitrary scale be denoted by ϕ_0, and this electrode be called the reference electrode. Then for each of the remaining c electrodes whose copper wires are at potentials $\phi_1 \ldots \phi_r \ldots \phi_c$ on the same arbitrary scale let c electromotive forces E_r be defined by

$$E_r = \phi_0 - \phi_r (r = 1, \ldots c).$$

The reference electrode is shown in the figure along with other electrodes in each phase. The system contains copper wires with a fixed number of atoms of copper leading from each electrode, so that all the potential differences $E_1 \ldots E_r \ldots E_c$ are measured between phases of metallic copper, and so have a physical significance. In consequence all electrical work done externally on the system can be measured directly, at any rate in theory, and is given by

$$\sum_1^c E_r dq_r,$$

where quantities of electric charge $dq_1 \ldots dq_r \ldots dq_c$ flow externally from electrodes $1-\lambda-c$ into the reference electrode. Finally, no work other than external work can be done on this system. The use of electromotive forces with a definite physical significance falls into line with the work of Guggenheim [7], who pointed out that an electrical potential difference only has a physical significance when, as with E, but not with the interfacial potential difference $\Delta\phi$, the two points to which it refers are surrounded by material of the same composition. This is because the separation of electrochemical potential into chemical and electrical components is arbitrary.

(iii.) In Lippmann's treatment the interphase between phases I. and II. is completely polarizable, and so allows ${}^1\Delta^2\phi$ to change without changing the compositions of the phases. In that case $d\,{}^1\Delta^2\phi$ has a physical significance, although ${}^1\Delta^2\phi$ has not. In fact $d\,{}^1\Delta^2\phi$ is then equal to the appropriate dE, since the potentials of the other electrodes and the metal–metal-contact potentials remain constant. In any electrically conducting phase a difference of potential between two points fixed in space cannot exist on a time average, and any excess electric charge in the phase will proceed, owing to electrostatic repulsion, to the phase boundaries. Each of the E terms, therefore, represents the sum of all the interfacial potential differ-

ences in its circuit, since the circuits are supposed to consist of conducting media.

(iv.) In the most important case of all, where the interphase between phases I. and II. is completely polarizable, the interfacial potential difference can be controlled by these electrodes. Reversible additions of substance to either phase are made by flowing charge between the appropriate electrodes in that phase. If the substance does not contain the reference ion, this flow of electricity is formally to be regarded as flowing first into and then out of the reference electrode. Since no ions can cross the phase-boundary when the interphase is completely polarizable, this mathematical device must be used in that case to introduce substances into the phase that does not contain the reference electrode.

The Derivation of the General Electrocapillary Equation.

The condition for equilibrium of the capillarity apparatus described in paper I.[1], was

$$[dE = \mathrm{T}\,d\mathrm{S} - p_1\,d\mathrm{V}_1 - p_2\,d\mathrm{V}_2 + \gamma\,ds + \delta\mathrm{W}']_{s_k}, \quad . \quad (7)$$

where

E is the total energy of the whole system ;

T is the temperature ;

s is the area of an arbitrary boundary in the interphase ;

s_k is a restriction of surface expansions to normal expansions of the single interphase between phases I. and II ;

p_1 is the pressure of phase I., whose volume is V_1 ;

p_2 is the pressure of phase II., whose volume is V_2 ;

γ is the surface tension for the given arbitrary boundary s ;

W′ is any external work done on the system other than compressional work ; and

S is the entropy of the whole system.

In the electrocapillary apparatus shown in the figure the same equation applies except that (i.) $\delta\mathrm{W}'$ becomes

$$\sum_{\mathrm{I}}^{c} \mathrm{E}_r\,dq_r + \delta\mathrm{W}'',$$

where $\delta W''$ is zero because the apparatus permits of no work other than compressional or electrical ; and (ii.) dV_2 can conveniently be regarded as being split up into $dV_2'+dV_3'+dV_4' \ldots$, changes in the volumes of the auxiliary electrodes and their leads, as well as in V_2', the volume of phase II. itself. Expression (7), therefore, becomes

$$\left[dE = T\,dS - (p_1\,dV_1) - p_2 dV_2 + \gamma\,ds + \sum_1^c E_r\,dq_r\right]_{s_k,\,\delta W''=0.} \quad . \quad . \quad . \quad (8)$$

In the electrocapillary apparatus changes can be effected by no means other than (i.) the addition or subtraction of heat ; (ii.) work done on the two pistons ; and (iii.) electric work in the c circuits. The system, therefore, has $c+3$ degrees of freedom. The electrodes are idealized in the manner already described, so that they do not affect the degrees of freedom of the system any more than do the containing walls of the system which were discussed in paper I. [1]. Further, of the $c+3$ degrees of freedom, two must be extensive, in order to specify the extent of phases I. and II. If real electrodes are used, the same result is true, but is obscured by the fact that the system is then in a state of pseudo-equilibrium. A real electrode in the system is equivalent to P_e extra phases, C_e extra components, and R_e restrictions among the existing degrees of freedom. It can be shown that $P_e=C_e=R_e$, so that the replacement of an ideal electrode by a real one leaves the degrees of freedom of the system unaltered, because P_e of the additional degrees of freedom must be extensive, and R_e become anchylosed owing to the restrictions. For example, if a zinc and a silver–silver-bromide electrode are added to an aqueous solution of zinc bromide so as to form the cell Zn $ZnBr_2$ aq. | AgBr | Ag, it is legitimate to consider Zn, $ZnBr_2$, AgBr, and Ag as four separate chemical components, owing to the state of pseudo-equilibrium and the slow rate of diffusion of silver bromide. Thus, for these two electrodes the additional components are Zn, AgBr, and Ag, three in all, and each component corresponds to an extra phase. The restrictions are $(Zn)+(ZnBr_2)=$constant ; $(AgBr)+2(ZnBr_2)=$constant ; and $(AgBr)+(Ag)=$constant, where the number of particles of Zn, $ZnBr_2$, AgBr, and Ag

in the whole system are respectively (Zn), ($ZnBr_2$), (AgBr), and (Ag). This is so because no atomic nuclei are added to or subtracted from the system. For the zinc electrode $P_e=C_e=R_e=1$, and for the silver–silver-bromide electrode $P_e=C_e=R_e=2$.

If p_2, T, s, are taken as the independent degrees of freedom of the system, which is also subject to the conditions $\delta W''=0$, and s_k constant, there are still c degrees of freedom, of which two must be extensive. If each of these is to correspond to an electrical term, the remaining degrees of freedom are conveniently taken as αq's and βE's, where $\alpha+\beta=c$; $\beta \leqslant 0$; and, since the q's correspond to extensive degrees of freedom, $\alpha \leqslant 2$. Expression (8) can, therefore, be transformed to

$$\left[dZ=(V_1 dp_1)+V_2 dp_2+\gamma ds-S dT+\sum_1^{\alpha} E_L dq_L - \sum_1^{\beta} q_r dE_r\right]_{s_k,\,\delta W''=0}, \quad . \quad (9)$$

where dZ is a complete differential because electric charge dq_j, flowing in any circuit j, produces a definite change in the properties of the system, so that all the terms $dq_1 \ldots dq_r \ldots dq_c$ are complete differentials. Expression (9) has $c+3$ degrees of freedom, which have to be reduced to two in order to cross-differentiate, as in the derivation of the capillary equations. This may be done by keeping p_2 and T constant, and introducing α arbitrary relations about the q's and $\beta-1$ arbitrary relations about the E_r's, so that the properties of the system can be expressed as functions of s and of a single difference term E, which should be suitably chosen according to the nature of the problem concerned. Expression (9), therefore, becomes

$$\left[dZ=\left\{\gamma+V_1\left(\frac{\partial p_1}{\partial s}\right)_E+\sum_1^{\alpha} E_L\left(\frac{\partial q_L}{\partial s}\right)_E-\sum_1^{\beta} q_r\left(\frac{\partial E_r}{\partial s}\right)_E\right\}ds + \left\{V_1\left(\frac{\partial p_1}{\partial E}\right)_s+\sum_1^{\alpha} E_L\left(\frac{\partial q_L}{\partial E}\right)_s-\sum_1^{\beta} q_r\left(\frac{\partial E_r}{\partial E}\right)_s\right\}dE\right]_{X,\,\alpha,\,\beta-1}, \quad . \quad . \quad . \quad (10)$$

where the suffix X denotes constancy of p_2, T, and s_k, while $\delta W''=0$, and the suffix $\beta-1$ represents $\beta-1$

arbitrary relations about the βE's, and the suffix α refers to α arbitrary relations about the αq_r's. If equation (10) is cross-differentiated and rearranged it becomes

$$\left[\left(\frac{\partial\gamma}{\partial \mathrm{E}}\right)_s\left\{1-\left(\frac{\partial p_1}{\partial\gamma}\right)_s\left(\frac{\partial \mathrm{V}_1}{\partial s}\right)_{p_1}\right\}=-\sum_1^c\left(\frac{\partial q_r}{\delta s}\right)_{\mathrm{E}_r}\left(\frac{\partial \mathrm{E}_r}{\partial \mathrm{E}}\right)_s\right.$$
$$\left.=-\sum_1^c\left(\frac{\partial q_r}{\partial s}\right)_{\mathrm{E}}\left(\frac{\partial \mathrm{E}}{\partial \mathrm{E}}\right)_{q^r}\right]_{\mathrm{X},\,\alpha,\,\beta-1} \quad . \quad . \quad . \quad (11)$$

This is the general electrocapillary equation expressed in the Lippmann form.

Surface Adsorption.

If the $\left(\frac{\partial q_r}{\partial s}\right)_{\mathrm{E}_r}$ terms in the electrocapillary equation are expressed in terms of the superficial densities, Γ, of Gibbs, it is necessary to deal with the following difficulty. Although additional factors corresponding to electrostriction of the bulk phases have to be considered, they will be shown below to be small, and the volume correction term in the electrocapillary equations vanishes for the limit of small bulk phases and large radii of curvature of the interphase, as it does in the capillary equations. The left-hand side of the equation therefore becomes

$$\left(\frac{\partial\gamma}{\partial \mathrm{E}}\right)_{s,\,\mathrm{X},\,\alpha,\,\beta-1}$$

and γ is liable to a percentage variation of $100\,x/r$, according to the position of the phase boundary s, if the latter is to be wholly in an interphase, which is a spherical shell of thickness x and radius of curvature r on its outer boundary. The percentage error in $d\gamma$ is also $100\,x/r$. The quantities $d\mathrm{E}$ and the $d\mathrm{E}_r$'s are capable of unambiguous observation, and, therefore, the left-hand side of equation (11) is uniquely determined for an interphase where $x<<r$. Similarly $s \propto r^2$, and, therefore, $ds \propto r\,dr$; during an expansion of the interphase dr may be supposed to be an unambiguous quantity determined by observing some optical boundary, so that errors in ds due to the optical surface lying somewhere

in the interphase of finite thickness also amount to 100 x/r per cent. Since $d\mathrm{E}$ and all the $d\mathrm{E}_r$'s are capable of unambiguous observation, and so, too, is ds, provided that $x<<r$, it follows that all the $\left(\frac{\partial q_r}{\partial s}\right)_{\mathrm{E}_r}$ terms, and, therefore, the right-hand side of the electrocapillary equation, must be unambiguous under these conditions. Similar remarks apply to the $\left(\frac{\partial \mathrm{N}}{\partial s}\right)_{\bar{\mathrm{F}}}$ terms of Gibbs's adsorption equation as given in paper II.[2]. It is well known, however, that the values of the Γ's of Gibbs can be made positive or negative according to the position adopted for the phase boundary, even when $x<<r$, and, except for a numerical factor of proportionality, the terms

$$\left(\frac{\partial q_r}{\partial s}\right)_{\mathrm{E}_r, \mathrm{X}, \alpha, \beta-1} \text{ and } \left(\frac{\partial \mathrm{N}_r}{\partial s}\right)_{\bar{\mathrm{F}}_r, \mathrm{X}, \alpha, \beta-1}$$

should be the same as the Γ_r's, for they are the right-hand side of the same adsorption equation. Therefore Gibbs's statement that his adsorption equation is obeyed by Γ terms needs further investigation.

Let the

$$\left(\frac{\partial q_r}{\partial s}\right)_{\mathrm{E}_r, \mathrm{X}, \alpha, \beta-1} \text{ and } \left(\frac{\partial \mathrm{N}_r}{\partial s}\right)_{\bar{\mathrm{F}}_r, \mathrm{X}, \alpha, \beta-1}$$

terms be called $\mathcal{T}$ terms, such that

$$\mathcal{T}_r = \mathrm{M}_r\left(\frac{\partial \mathrm{N}_r}{\partial s}\right)_{\bar{\mathrm{F}}_r, \mathrm{X}, \alpha, \beta-1} = \frac{-1}{\zeta_r}\left(\frac{\partial q_r}{\partial s}\right)_{\mathrm{E}_r, \mathrm{X}, \alpha, \beta-1},$$

where M_r is the conventional molecular weight of component r, and ζ_r is the electrochemical equivalent of this component ion, taking account of its sign; and, if q_r is expressed in coulombs, it is given in coulombs per gram. Thus $\zeta_r = \mathrm{F} \cdot \mathrm{M}_r \times$ (the number of faradays necessary to electrolyze one gram molecule of r into the solution). The $\mathcal{T}$ terms behave differently to the Γ's, for they refer to the number of particles that have to be added to phases I. and II. during a reversible expansion at constancy of certain variables. The Γ's of Gibbs refer to a property of the static interphase itself, while the $\mathcal{T}$'s have values that depend, in general, upon which

variables are kept constant during the process of expansion considered.

There exists only one expansion for which the $\mathcal{T}$'s are simply related to a property of the static interphase. This is the expansion during which all the intensive variables are kept constant. Since the pressures are intensive variables, such an expansion implies constancy both of p_1 and of p_2. For an interphase where r is great and $x<<r$, this expansion is possible, since p_1-p_2 varies as $1/r$, so that constancy of p_1 implies constancy of p_2 in the limit as $1/r\rightarrow 0$. This shows that properties of the static interphase can only be related to expansions, and to $\mathcal{T}$ terms, that refer to a flat interphase. It is possible, at any rate in theory, to expand an interphase where $1/r\rightarrow 0$, and to observe the corresponding $\mathcal{T}$ adsorption terms ; for such expansions with all the intensive variables constant, the $\mathcal{T}$ adsorption terms will be denoted by $\mathcal{T}^*$. For an expansion of this sort the number of independent extensive variables must be reduced to their minimum, which is two, in order to specify the extent of phases I. and II. If the independent variables of the system are the group X, and c other electrical terms that consist of αq_r's and $\beta \mathrm{E}_r$'s, α must be equal to two and β equal to $c-2$. Let the two extensive variables considered be q_{L} and q_{M}, and let the two arbitrary relations about them be denoted by $\psi_1=$constant and $\psi_2=$ constant, so that the electrocapillary equation may be written, for constant intensive variables,

$$\left[\left(\frac{\partial\gamma}{\partial \mathrm{E}}\right)_s=-\sum_{\mathrm{I}}^{s}\left(\frac{\partial q_r}{\partial s}\right)_{\mathrm{E}r}\left(\frac{\partial \mathrm{E}_r}{\partial \mathrm{E}}\right)_s\right]_{\mathrm{X},\,\beta-1,\,\psi_1,\,\psi_2} \quad . \quad . \quad (12)$$

But since

$$\left[\left(\frac{\partial\gamma}{\partial \mathrm{E}}\right)_{\psi_2}=\left(\frac{\partial\gamma}{\partial \mathrm{E}}\right)_{\psi}+\left(\frac{\partial\gamma}{\partial\psi}\right)_{\mathrm{E}}\left(\frac{\partial\psi}{\partial \mathrm{E}}\right)_{\psi_2}\right]_{\mathrm{X},\,\beta-1,\,\psi_1,\,s},$$

where ψ is any variable, it is necessary that

$$\left[\left(\frac{\partial\gamma}{\partial \mathrm{E}}\right)_{\psi_2}=\left(\frac{\partial\gamma}{\partial \mathrm{E}}\right)_{\psi}\right]_{\mathrm{X},\,\beta-1,\,\psi_1,\,s}$$

when $\left(\frac{\partial\gamma}{\partial\psi}\right)_{\mathrm{E},\,\mathrm{X},\,\beta-1,\,\psi_1,\,s}$ is zero, as it must be when ψ is an extensive variable and the bulk phases are finitely great. Therefore the value for $\left(\frac{\partial\gamma}{\partial \mathrm{E}}\right)_{\mathrm{X},\,\beta-1,\,\psi_1,\,\psi_2}$ is independent of the exact pair of extensive variables ψ_1 and ψ_2

that are kept constant. A similar result must also hold for the sum of the terms on the right-hand side of the electrocapillary equation. The individual terms on the right-hand side do depend, however, on the particular extensive variables that are kept constant. Three alternatives of interest are :—

(i.) $\psi_1=q_L$; $\psi_2=q_M$. For the system mercury–aqueous solution dq may conveniently refer to the change in the number of mols of mercurous ion in phases I. and II., together with their interphases, and dq_M to the change in the corresponding number of mols of hydroxyl ion.

(ii.) $\psi_1=V_1$; $\psi_2=V_2'$.

(iii.) $\psi_1=V_1$; $\psi_2=q_L$, where dq_L has been defined above.

Each of these three alternatives can be made to yield a picture of the structure of the interphase, but it is necessarily a less complete picture than would be obtained by considering the details of the molecular interactions. This is to be expected of the quantities used in pure thermodynamic theory. The first alternative corresponds to expansions at constant quantities of L and M in phases I. and II. together with their interphases, and for this alternative let $\mathcal{T}^*_r$ be denoted by ${}^{(i)}\mathcal{T}^*_r$. By definition ${}^{(i)}\mathcal{T}^*_L=0$, and ${}^{(i)}\mathcal{T}^*_M=0$. The relationships of ${}^{(i)}\mathcal{T}^*_r$ terms to the structure of the interphase is worked out at the end of this section.

It is possible to equate $\left(\frac{\partial\gamma}{\partial E}\right)_{s,\,X,\,\beta-1,\,q_L,\,q_M}$ to a single ${}^{(i)}\mathcal{T}^*$ term if constancy of X, $\beta-1$, and E implies constancy of all intensive variables.

Let a normal to an optical boundary in the interphase generate a surface by describing a closed curve on the optical boundary. If two surfaces be obtained by normal expansion and normal contraction of the optical boundary through fixed radial displacements $+\Delta r_1$ and $-\Delta r_2$, these two surfaces, together with the surface generated by the normal to the optical boundary, will enclose an element of volume. If the two displaced boundaries occupy positions that correspond, in the undisplaced system, to boundaries in the homogeneous regions of phases I. and II. respectively, this element of volume

may be said to contain the interphase together with unknown quantities of phases I. and II. The total number of particles in it may be expressed in mols per unit surface area enclosed on the optical boundary. After a surface expansion at constant intensive variables, the surface concentration of particles in an element of volume included between the radial displacements $+\Delta r_1$ and $-\Delta r_2$ from the new optical boundary will be the same as they were for the original optical boundary. Per unit increase of surface area of the optical boundary these quantities of the different chemical components will have to enter the volume between the two boundaries fixed with respect to the optical boundary. Let the element of volume contain $n_1 \ldots n_r \ldots n_c$ mols of components $1 \ldots r \ldots c$ per unit surface area of the optical boundary, and let the molar fractions of these components in the homogeneous bulk of the phases I. and II. be denoted by ${}^1x_1 \ldots {}^1x_r \ldots {}^1x_c$ and ${}^2x_1 \ldots {}^2x_r \ldots {}^2x_c$ respectively. Then for any component j

$$n_j = \lambda_1 {}^1x_j + \lambda_2 {}^2x_j + {}^{(i)}T^*_j, \quad .$$

where λ_1 and λ_2 are two constants. If, therefore, the element of volume were to be analysed so that the values for each of the n_j terms ($j=1 \ldots r \ldots c$) are known, as well as the composition of the bulk phases, two constants are needed to determine all the ${}^{(i)}T^*$ terms. Since $d\mathrm{N}_\mathrm{L}$ and $d\mathrm{N}_\mathrm{M}$ are zero for the expansion at all intensive variables constant, ${}^{(i)}T^*_\mathrm{L}=0$ and ${}^{(i)}T^*_\mathrm{M}=0$. These two conditions allow the constants λ_1 and λ_2 to be determined, and so values can be assigned to all the remaining ${}^{(i)}T^*$ terms. Thus, when r is great and $x<<$s, the electrocapillary equation becomes

$$\left[\left(\frac{\partial\gamma}{\partial \mathrm{E}}\right)_s = +\sum_1^c {}^{(i)}T^*_r \zeta_r \left(\frac{\partial \mathrm{E}_r}{\partial \mathrm{E}}\right)_s\right]_{\mathrm{X},\ \beta-1,\ q_\mathrm{L},\ q_\mathrm{M}} \quad . \quad . \quad (13)$$

For any single component r it is always possible to find a boundary in the interphase where $\Gamma_r = {}^{(i)}T^*_r$, where Γ_r is Gibbs's expression for the superficial density of component r at the given boundary. In general each component will have to have its Γ referred to a different boundary in order to keep it equal to the corresponding ${}^{(i)}T^*$.

The Gibbs Form of the Electrocapillary Equation.

To transform the electrocapillary equation to the Gibbs form the terms

$$\left(\frac{\partial q}{\partial s}\right)_{E_r,\, X,\, \beta-1,\, \psi_1,\, \psi_2}$$

must be expressed in terms of Gibbs's Γ_r terms, as follows :—

Let m_r denote the total mass in phases I. and II. and their interphases of one of the components r. Then

$$m_r \equiv V_1\,{}^1C_r + V_2'\,{}^2C_r + \int \Gamma_r\, ds, \quad . \quad . \quad . \quad (14)$$

if V_1, V_2', and s are defined as above and ${}^1C_r$ is the concentration of component r in the homogeneous bulk of phase I. ; ${}^2C_r$ the corresponding concentration in phase II. ; Γ_r the " superficial density " of the same component in the interphase as defined by Gibbs [18], *i. e.*, the excess of m_r per unit of s over the value it would have if the concentrations ${}^1C_r$ and ${}^2C_r$ continued up to the boundary defining s.

The integration of $\Gamma_r\, ds$ is taken over the whole boundary of each of phases I. and II., allowing for variations of Γ_r for reasons given below. It follows from the laws of electrolysis, and from the fact that component r can only be introduced into the space containing m_r by flowing charge in the circuit to which E_r and q_r correspond, that

$$\frac{dq_r}{dm_r} = -\zeta_r, \quad . \quad . \quad . \quad . \quad . \quad . \quad . \quad (15)$$

where ζ_r is the electrochemical equivalent of component r as defined above. If expression (14) is differentiated with respect to s, and combined with equation (15), the result is

$$\frac{dq_r}{ds} = -\zeta_r\left[\Gamma_r + \int \frac{d\Gamma_r}{ds}\, ds + \frac{d({}^1C_r V_1 + {}^2C_r V_2')}{ds}\right] \quad . \quad (16)$$

$$= -\zeta_r[\Gamma_r + I(r)], \quad . \quad . \quad . \quad . \quad . \quad . \quad . \quad . \quad (17)$$

where $I(r)$ is defined by equation (17) and represents

a set of correction terms. Thus the Gibbs form of the general electrocapillary equation is

$$\left[\left(\frac{\partial\gamma}{\partial \mathrm{E}}\right)_s\left[1-\left(\frac{\partial p_1}{\partial\gamma}\right)_s\left(\frac{\partial \mathrm{V}_1}{\partial s}\right)_{p_1}\right]\right. = \left.\sum_1^s \zeta_r(\Gamma+\mathrm{I}(r))\left(\frac{\partial \mathrm{E}_r}{\partial \mathrm{E}}\right)_s\right]_{\mathrm{X},\,\beta-1,\,\psi_1,\,\psi_2} \quad . \quad . \quad (18)$$

The correction terms may now be considered. Equations (11) and (18) contain several correction terms analogous to those discussed in the previous papers. Although these terms are in most cases negligible, they are of considerable philosophical interest. The terms are made up of items that fall into three classes :—(i.) those which are independent of the shape of the apparatus and depend only on the definition of the boundary defining Γ, γ, and s, and on the nature of the free spherical interphase concerning which information is desired ; (ii.) those which depend on the nature and extent of the other interphases between phases I. and II. and their respective containing walls; and (iii.) those which represent changes within phases I. and II., and which are proportional to V_1 and V_2'. By changing the shape of the apparatus the items in any one class can be made to vary independently of the other items, while the complete equation remains valid. This must mean that the complete equation is compounded of three separate equations, one for each class of item. Apart from this general argument, however, no means has been found of separating the three equations without introducing quantities which are inaccessible, even ideally, to experiment. It is possible that the reason lies in an indeterminacy like that already mentioned in connexion with potential differences between unlike phases and with internal pressures. Thus surface work may only have a physical significance if it refers to a complete phase boundary, which can never be entirely homogeneous if means are provided for doing work on it. Some of the items in classes (ii.) and (iii.) have already been discussed in the previous papers. Three effects not encountered there are : (*a*) Electrostriction, *i. e.*, a change in internal pressure caused by a change in electrical potential. This affects

$$\left(\frac{\partial \mathrm{V}_1}{\partial s}\right)_{p_1,\,\mathrm{X},\,\beta-1,\,\psi_1,\,\psi_2}$$

and some of the terms included in $I(r)$. (*b*) Passage of charge to the interphases between phases I. and II. and their containing walls. Thus phases I. and II. must be considered as forming a condenser whose capacity is very large at their free common interphase in comparison with their capacity elsewhere. The terms $q_1 \ldots q_r \ldots q_c$ must supply all the charge, *i. e.*, the large amount for the 1–2 interphase and the small amount for the other interphases, but the presence of this small extra amount of charge only affects

$$\left(\frac{\partial q_r}{\partial s}\right)_{E,\, X,\, \beta-1,\, \psi_1,\, \psi_2}$$

if, at any potential difference, the amount of charge on the interphases other than the 1–2 interphase alters when s is altered. In a precisely similar manner Γ_r for any component will not be confined to the 1–2 interphase, but will have a definite value at each point on the surface of phases I. and II., so that the total mass absorbed is $\int \Gamma_r ds$ and not $\Gamma_r s$; but again, it is only the change of $\int \Gamma_r\, ds$ with s that enters into the electrocapillary equation. (*c*) In the general case, expansion at constant E_r will cause a change in Γ_r; the resulting term,

$$\int \left(\frac{\partial \Gamma_r}{\partial s}\right)_{X,\, \beta-1,\, \psi_1,\, \psi_2} . ds \quad ,$$

in equations (16) and (18) may be quite large.

All such effects have been examined, and it has been found that, with certain exceptions, they are very small under the usual experimental conditions. They become important, however, if the thickness of the interphase is comparable with its radius of curvature. Only the exceptions will be further considered, so that in what follows the negligible effects will be tacitly neglected. The exceptions, such as (*c*) above, affect chiefly the term $I(r)$ in equation (18), which is given by

$$\left[I(r) = \left\{ \int \left(\frac{\partial \Gamma_r}{\partial s}\right) ds + \frac{\partial ({}^1C_r V_1)}{\partial s} + \frac{\partial ({}^2C_r V_2')}{\partial s} \right\} \right]_{X,\, E,\, \beta-1,\, \psi_1,\, \psi_2}$$

If the effects of electrostriction are negligible, as they are for small bulk phases where, further, $x << r$, the constancy of all intensive variables, which can hold if $1/r \to 0$, means that ${}^{1}C_r$ and ${}^{2}C_r$ remain constant during the expansion, as will also the values of Γ_r. If, therefore, ψ_1 and ψ_2 refer to V_1 and V_2' constant, this term vanishes, so that the electrocapillary equation becomes

$$\left[\left(\frac{\partial\gamma}{\partial E}\right)_s = +\sum_1^c \zeta_r \Gamma_r \left(\frac{\partial E}{\partial E}\right)_s\right]_{X,\,\beta-1,\,V_1,\,V_2'} \quad . \quad . \quad (19)$$

This equation, in which the volume-correction term vanishes identically since V_1 is kept constant, is valid for every boundary, and a convenient boundary to choose is the optical boundary which is used in the measurement of γ. If the independent variables are the group X, s, E, $c-2$ of the E_r terms, and two q terms, it is necessary to allow one of the E_r terms, say E_j, to vary, and along with it the two q terms, q_L and q_M, whose electromotive forces E_L and E_M are determined by E_j; all the other E terms must be constant in order to keep ${}^{1}C_r$ and ${}^{2}C_r$ constant and eliminate the correction terms. Thus it is impossible to reduce the right-hand side of the electrocapillary equation to the sum of less than three ${}^{(ii)}T^*$ terms, since only $c-3$ of the $\left(\frac{\partial E_r}{\partial E}\right)_s$ terms can be equated to zero, and only $c-2$ to unity. This condition shows that the right-hand side of equation (19) is a linear function of not less than three Γ terms. If the position of the boundary of reference is altered, each of the three terms is altered in such a way as to leave the total linear function unaltered. When the small correction terms are negligible, the Γ_r's may be shown to be equal to the ${}^{(ii)}T_r^*$'s by reference to equations (14) to (17). Both depend upon the position taken for the phase boundary, which affects ${}^{(ii)}T^*$ owing to the surface expansion being at V_1 and V_2' constant. Equation (19) may also be converted to the following form by making E successively $E_1, E_2 \ldots E_{c-2}$, and adding

$$\left[\begin{array}{c} d\gamma = +\sum_1^c \zeta_r \Gamma_r dE_r \\ = -\Sigma \Gamma_r d\mu_r \end{array}\right]_{s,\,X,\,V_1,\,V_2'} , \quad . \quad . \quad (20)$$

which is another familiar form due to Gibbs. It is interesting to note that only $c-2$ of the $d\mu_r$ terms are independent.

The third alternative is to express the electrocapillary equation at ${}^{(iii)}T^*_{L}=0$ and $d\mathrm{V}_2'=0$. This is of interest when the component L occurs in phase I., and has a negligible concentration in phase II. In this case V_1 cannot be independently controlled, and so

$$\left[\mathrm{I}(r)={}^{1}\mathrm{C}_r\left(\frac{\partial \mathrm{V}_1}{\partial s}\right)\right]_{\mathrm{E},\,\mathrm{X},\,\beta-1,\,q_{\mathrm{L}},\,\mathrm{V}_2'}.$$

In this case

$$\left(\frac{\partial \mathrm{V}_1}{\partial s}\right)_{\mathrm{E},\,\mathrm{X},\,\beta-1,\,q_{\mathrm{L}},\,\mathrm{V}_2'}$$

is determined by the choice of the phase boundary, and is zero for the boundary where $\Gamma_{\mathrm{L}}=0$. For any other boundary a distance δ from this one in the direction of phase I.

$$\left(\frac{\partial \mathrm{V}_1}{\partial s}\right)_{\mathrm{E},\,\mathrm{X},\,\beta-1,\,q_{\mathrm{L}},\,\mathrm{V}_2'}=\left(1-\frac{{}^{2}\mathrm{C}_{\mathrm{L}}}{{}^{1}\mathrm{C}_{\mathrm{L}}}\right)\delta\approx\delta, \quad . \quad . \quad (21)$$

since ${}^{2}\mathrm{C}_{\mathrm{L}}$ is negligible, and thus $\mathrm{I}(r)={}^{1}\mathrm{C}_r\delta$.

This may be proved as follows :—

Since $m_{\mathrm{L}}={}^{1}\mathrm{C}_{\mathrm{L}}\mathrm{V}_1+{}^{2}\mathrm{C}_{\mathrm{L}}\mathrm{V}_2'+\Gamma_{\mathrm{L}}s$, and m_{L} is constant,

$$\left(\frac{\partial \mathrm{V}_1}{\partial s}\right)_{\mathrm{E},\,\mathrm{X},\,\beta-1,\,\psi_1,\,\psi_2}=-\frac{\Gamma_{\mathrm{L}}}{{}^{1}\mathrm{C}_{\mathrm{L}}}. \quad . \quad . \quad (21\,a)$$

But $\Gamma_{\mathrm{L}}=-({}^{1}\mathrm{C}_{\mathrm{L}}-{}^{2}\mathrm{C}_{\mathrm{L}})\delta$ by definition, provided that δ is small compared with the radius of curvature of the interphase ; and so it follows that equation (21) is correct. The constancy of all the intensive variables that have been postulated is only possible for a virtually flat interphase, so that constancy of p_1 is implied. However,

$$\left(\frac{\partial \mathrm{V}_1}{\partial s}\right)_{p_1,\,\mathrm{X},\,\beta-1,\,\psi_1,\,\psi_2}$$

does not remain zero for the boundary $\Gamma_{\mathrm{L}}=0$, since one extensive variable, E_i, is allowed to vary, and the volume concentration ${}^{1}\mathrm{C}_{\mathrm{L}}$ will not remain constant, so that (see 21 *a*)

$$\left(\frac{\partial \mathrm{V}_1}{\partial s}\right)_{p_1,\,\mathrm{X},\,\beta-1,\,\psi_1,\,\psi_2}$$

is not equal to $\frac{\Gamma_L}{{}_1C_L}$. Thus the volume correction does not vanish identically in this case as it did for alternative (ii.), but for virtually flat interphases where $x<<r$ the electrocapillary equation reduces to

$$\left[\left(\frac{\partial\gamma}{\partial E}\right)_s = -\sum_1^c \zeta_r \Gamma_r \left(\frac{\partial E_r}{\partial E}\right)_s\right]_{X,\,\beta-1,\,V_2',\,q_L} \quad . \quad . \quad . \quad (22)$$

where all the Γ_r's refer to the boundary $\Gamma_1=0$. Equation (22) could have been obtained as a special case of equation (19), since the extensive variables held constant are trivial in both equations. It may be shown directly, or by taking equation (21) as a special case of equation (19), that the term in the right-hand side must be a linear function of not less than two Γ terms. It should be noted that γ has a value that depends on the position of the optical boundary, and that this boundary does not in general coincide with the boundary $\Gamma_L=0$.

Summary.

(1) A generalized apparatus for the thermodynamic consideration of electrocapillarity has been devised which involves only the use of externally observable work terms.

(2) By means of it a general electrocapillary equation has been derived which includes the Lippmann and Gibbs equations as special cases, and which is capable of being applied to any electrocapillary problem that is soluble by thermodynamic methods.

References.

(1) S. R. Craxford, O. Gatty, and J. St. L. Philpot, Phil. Mag. (7) xvi. p. 849 (1933).
(2) S. R. Craxford, O. Gatty, and J. St. L. Philpot, Phil. Mag. (7) xvii. p. 54 (1934).
(3) G. Lippmann, *Ann. Chim. Phys.* (5) v. p. 494 (1875).
(4) A. Frumkin, *Z. physikal. Chem.* ciii. p. 55 (1922).
(5) J. St. L. Philpot, Phil. Mag. (7) xiii. p. 775 (1932).
(6) S. R. Craxford (to be published shortly).
(7) E. A. Guggenheim, J. Phys. Chem. xxxiii. p. 842 (1929); *ibid.* xxxiv. p. 1540 (1930).
(8) O. Stern, *Z. Elektrochem.* xxx. p. 508 (1924).
(9) J. W. Gibbs, 'Collected Works,' i. p. 331 (London, 1928).
(10) E. Warburg, *Ann. Physik*, xli. p. 1 (1891).
(11) J. J. Thomson, 'Applications of Dynamics to Physics and Chemistry,' p. 191 (London, 1888).

(12) J. A. V. Butler & C. Ocrent, J. Phys. Chem. xxxiv. p. 2286 (1930).
(13) A. Frumkin & A. Gorodetzkaja, *Z. physikal. Chem.* (A) cxxxvi. p. 451 (1928).
(14) M. Andauer & E. Lange, *Z. physikal. Chem.* Bodenstein Festband, p. 247 (1931); *ibid.* (A) clxii. p. 241 (1932).
(15) S. R. Craxford, Phil. Mag. (7) xvi. p. 268 (1933).
(16) F. O. Koenig, J. Phys. Chem. xxxviii. p. 111 (1934).
(17) A. G. Samarcev, *Z. physikal. Chem.* (A) clxviii. p. 45 (1934).
(18) J. W. Gibbs, 'Collected Works,' i. p. 229 (London, 1928).

The Physical Chemistry Laboratory,
Balliol College and Trinity College, Oxford.

LXXX. *On the Heat Conductivity of Simple Cubical Crystals.*

By M. Blackman, *M.Sc., Ph.D., Beit Scientific Research Fellow, Imperial College, South Kensington* *.

§ 1. THE problem as to whether an ideal crystal has a finite heat conductivity has been a point of controversy for a long time; Born † and Debye ‡ recognized that a lattice with harmonic vibrations only would have an infinite heat conductivity, since there is no possibility for a transfer of energy when the normal vibrations are not coupled; the introduction of anharmonic terms (in particular of terms in the Energy expression, of the third order in the amplitude) gave the required coupling, which was utilized by Debye § in the first theory of the heat conductivity of crystals.

Debye showed that in order to have a stationary condition in a crystal through which a heat stream is passing, a temperature gradient is essential; otherwise the coupling between the vibrations automatically ensures a return to a state of thermal equilibrium. The theory produces a finite heat conductivity for the crystal. Debye was able to deduce that the heat conductivity should be inversely proportional to the temperature, which agrees with the experimental results.

Debye's arguments were in part not fully justified, as was shown by Ornstein and Zernike ‖: they attempted

* Communicated by the Author.
† M. Born, *Phys. Zeitschr.* xv. p. 191 (1914).
‡ P. Debye, 'Vorträge über die kinetische Theorie, etc.,' p. 43. Teubner (1914).
§ P. Debye, *loc. cit.*
‖ L. S. Ornstein and F. Zernike, *Proc. Amst. Acad.* xix. p. 1295 (1915).

a correct discussion for the case of a linear elastic continuum and found an infinite heat conductivity.

The whole problem was thoroughly investigated in an important paper by Peierls * (following the earlier work of Pauli †), who considered the lattice and the continuum in the three-dimensional as well as in the one-dimensional case.

We shall give a short discussion of the paper in order to emphasize the main points. The purpose of this paper is to show that for the NaCl crystal type a striking relation between the heat conductivity and the mass ratio of the ions can be deduced from Peierls's theory; this relation was discovered experimentally by Eucken and Kuhn ‡.

§ 2. Peierls establishes first the existence of an H theorem for the heat conductivity. He proceeds by considering the fluctuation in the distribution of the Energy between the various normal vibrations of the lattice, by a modification of the Planck-Fokker fluctuation theory.

If

$$W(E_1, E_2 \ldots)\, dE_1 dE_2 \ldots$$

is the probability of a condition in which the jth normal vibration has an energy between E_j and $E_j + dE_j$, then the change of W with time is, on the above theory,

$$\Delta W = -\sum_j \frac{\partial}{\partial E_j}(\overline{\Delta E_j} \cdot W) + \tfrac{1}{2}\sum_{jj'}(\overline{\Delta E_j \Delta E_{j'}} \cdot W), \quad . \quad (1)$$

where $\overline{\Delta E_j}$ is the mean value of the change in the energy in time τ due to the perturbation.

The evaluation of E_j and ΔE_j is accomplished by considering the perturbation of the normal coordinates of the lattice due to the introduction of anharmonic terms in the energy. The main result of this calculation is that ΔE_f increases linearly with the time, when

$$\nu_f + \nu_{f'} + \nu_{f''} = 0, \quad . \quad . \quad . \quad . \quad . \quad . \quad (2\,a)$$

where

$$f + f' + f'' = \begin{cases} 0, & . \quad . \quad . \quad . \quad . \quad . \quad (2\,b) \\ \pm 2\pi, & . \quad . \quad . \quad . \quad . \quad (2\,c) \end{cases}$$

* R. Peierls, *Ann. d. Phys.* (5) iii. p. 1055 (1929).
† W. Pauli, *Verh. d. Deutsch. Phys. Ges.* (3) vi. p. 10 (1925).
‡ A. Eucken and G. Kuhn, *Zeits. f. phys. Chemie*, cxxxiv. p. 193 (1928).

and ν_f is the frequency of a normal vibration characterized by the value of f, which varies from $-\pi$ to $+\pi$.

Hence the processes which are responsible for an energy transfer are such in which three waves take part, two waves being, however, allowed to interact only with a particular third one.

Having found the necessary condition for an interchange of energy, the next step is to find whether these conditions are sufficient for the existence of an H theorem. This would then mean that any disturbance of the system would be smoothed out again if the system be left to itself, *i. e.*, it would resume its original state as before the disturbance—a condition which is obviously necessary for the existence of a finite conductivity. The analysis shows that of the conditions (2), only 2 (*a*) and 2 (*c*) fulfil the conditions for the existence of the H theorem, whereas 2 (*a*) and 2 (*b*) taken together do not *. The former processes are called by Peierls "Umklapp" processes, and it is these that are primarily responsible for the heat conductivity.

In view of the importance attached to any theory of heat conductivity from a physical point of view, it is, perhaps, not superfluous to pay some attention to the physical meaning of the "Umklapp" processes. The interpretation of these processes which is given by Peierls is that two waves in a crystal die down, giving rise to a third wave (the frequencies being determined by (2)). If we consider two waves moving in a particular direction and interacting to produce a third, then we see that, if the third wave moves in the same direction the energy carried in that direction is unaltered; on the other hand, if the third wave travels in the opposite direction this energy is certainly decreased. Obviously only the latter processes, *i. e.*, such that can remove energy from the main stream, are responsible for the production of a temperature gradient, and hence for the finite size of the heat conductivity. These are the "Umklapp" processes.

The second part of the paper is concerned with the actual calculation of the heat-conductivity formula. The treatment is here somewhat different, because it is necessary to consider wave packets and not waves

* For thermal equilibrium both processes 2 (*b*) and 2 (*c*) are of course necessary.

themselves in order to define a temperature distribution varying over the crystal. For the details of the calculation we refer to the original paper; it suffices to say that the theory gives the right dependence of the heat conductivity on the temperature, although an explicit evaluation of the heat conductivity as a function of the molecular properties was not possible.

§ 3. The discussion of the resonance relations (2) is important for the purpose of this paper. These are

$$\nu_f \pm \nu_{f'} \pm \nu_{f''} = 0,$$

$$f + f' + f'' = \begin{cases} 0, \\ \pm 2\pi \end{cases}$$

for the one-dimensional case, and corresponding formulæ for the three-dimensional case; for the present we will discuss the above only.

For the one-dimensional ionic lattice with two ions of different masses the general expression for the frequency is

$$\nu_f = \frac{\nu_0}{\sqrt{2}} \sqrt{1 \pm \sqrt{1 - \frac{Mm}{\left(\frac{M+m}{2}\right)^2} \sin^2 f}},$$

where M, m are the masses, ν_0 the maximum frequency, and $f = \frac{\pi k}{N}$ (where k varies from 1 to N).

In the case of equal masses we have

$$\nu_f = \nu_0 \cdot \begin{Bmatrix} \sin \frac{f}{2} \\ \cos \frac{f}{2} \end{Bmatrix}.$$

The influence of the mass difference is to cause the frequency curves to split up into two parts, usually termed acoustical and optical branches.

Returning to the above conditions, and taking the case of equal masses with $\nu_f = \nu_0 \sin \frac{f}{2}$, we see that the condition 2 (a) leads to

$$\sin \frac{f}{2} + \sin \frac{f'}{2} - \sin \cdot \frac{f + f'}{2} = 0.$$

This can be fulfilled only if $f = -f'$. This means that there are only two vibrations taking part, since $\nu_0 = \nu_{2\pi} = 0$. This can also be shown graphically, as was done by Peierls.

Now this solution is insufficient for the existence of an H theorem, and is of no consequence for the heat

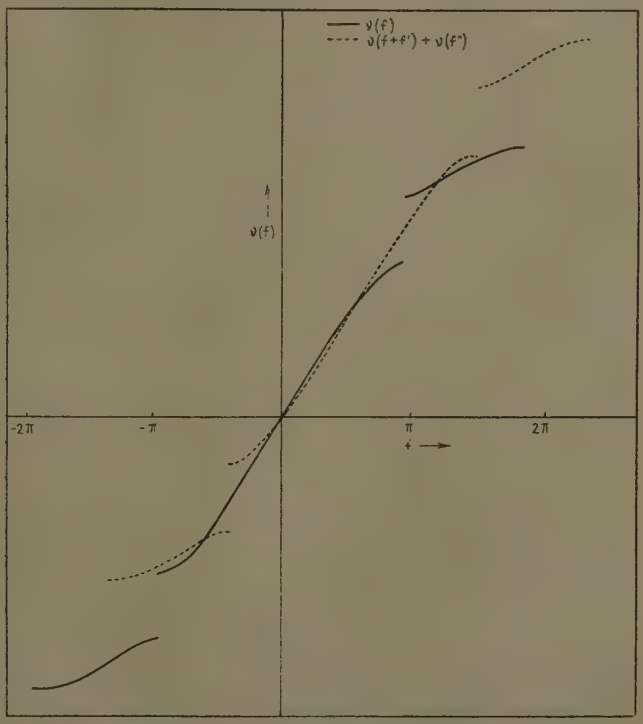

Graphical solution of the resonance conditions.

conductivity. It is necessary to consider the fourth-order energy terms in order to obtain a finite conductivity for this case.

When, however, we extend Peierls's treatment to the case of unequal masses, we obtain solutions which are not trivial. This can be best shown graphically in the figure.

The number of solutions depends on the mass ratio, becoming zero for equal masses.

Now the size of the heat conductivity depends very much on the nature of the above processes. The more types of processes there are which lead to an energy transfer the lower is the heat conductivity (other things being equal). In the one-dimensional lattice we have the fact that the existence of processes which are responsible for the heat conductivity, and where only three waves take part, depends on the nature of the frequency spectrum, and hence on the mass ratio. We should, therefore, expect a very much lower heat conductivity for a lattice of different masses where the third order energy terms suffice to bring about the heat conductivity than for a lattice of equal masses where we have to go to fourth terms in the energy. In other words, we should expect the heat conductivity to be a maximum when the masses were equal, falling off rapidly as the mass ratio differs from unity.

This statement must, however, be modified, because we do not obtain solutions of (2) over the whole range of the mass ratio. There is, firstly, a small region around $\frac{m}{M}=1$ where the number of solutions is too small to be of importance. Then beyond a certain point $\left(\frac{m}{M}>3\right)$ we do not obtain any solutions except the trivial ones. Hence, although a drop in the heat conducting is to be expected, when the mass ratio varies from unity, an increase should occur for large mass differences.

The above analysis has been carried through on the assumption that the mass difference was the only factor responsible for the splitting of the frequency branches. This is not true in general; any factor which distinguishes the one ion from the other can cause this splitting; for instance, if the forces between the particles are taken into account which do not adjoin each other this will also have the effect of splitting the frequency branches, provided that these additional forces are different for different ions.

In the one-dimensional case the effect is, however, very small, and will not alter the essential points made above.

§ 4. In the three dimensional case the position is slightly different, for we have here the coupling between the three main frequency branches *, for the case of equal masses ; this enables waves belonging to different branches to interact, and hence, in general, there will be, owing to this fact, a finite heat conductivity for crystals. The interaction between waves belonging to the one-frequency branch is forbidden, just as in the one-dimensional case : this can easily be seen from a model in the two-dimensional case.

If we take the masses of the ions to be different, each of the three frequency branches splits up into two parts, and then, just as in the one-dimensional case, the interaction of waves belonging to the acoustical and the optical branches also contribute to the dissipation of energy.

We should, therefore, come to the same conclusion, as in the one-dimensional case, that the heat conductivity should have a maximum value when the masses are equal, although the maximum should not be as sharp as in the one-dimensional case. Besides a broad maximum, we should also expect that for very large mass ratios the heat conductivity should rise again, the exact point where this sets in depending, however, on the particular nature of the spectrum.

Here again we must remember that the mass difference is certainly not the only factor causing the splitting up of the frequency branches ; but if we can keep the other factors more or less constant (as they will be in practice), they do not play a very important part unless the splitting they produce is very large ; there are reasons (from optical data) for concluding that this effect will be more or less constant for most of the alkali halides.

The estimation of the height of the maximum is not easy, and only a rough determination has been made. Assuming that both processes are equally effective, as far as the heat conductivity is concerned, both general reasoning and a rough estimation from Peierls's calculation would yield a factor of two : this, under the conditions that the spectrum is, apart from the splitting up of the branches, exactly similar, and the anharmonic constants, etc., the same.

* M. Born, ' Atomtheorie des festen Zustandes ' (Berlin, 1925).

§ 5. When we come to a quantitative comparison with experiment, we must arrange the substances in such a way that the frequency distribution is varied continuously from substance to substance, and, if possible, also the anharmonic factor. The first condition would be fulfilled if we keep the positive ion fixed and vary the negative ion, *e. g.* the potassium halide series. Here the spectrum is made continuously smaller. The anharmonic factor β would probably be not very different, as the expansion coefficients are all of the same order.

We should expect that in this case the maximum might show up above the other effects. The experimental results, taken from Eucken and Kuhn's paper, are rather striking :—

Substance.	λ (273° K.).	λ (83° K.).	$\frac{\lambda_{83}}{\lambda_{273}}$.
NaF	*0·0252*	*0·1243*	4·94
NaCl	0·0238	0·0902	3·78
NaBr	0·0058	0·0124	2·15
KF	0·0169	0·0573	3·38
KCl	*0·0245*	*0·1381*	5·71
KBr	0·0087	0·0226	2·59
KJ	0·0073	0·0304	4·14
RbCl	0·0047	0·0073	1·54
RbBr	*0·0091*	*0·0156*	1·72
Rb J	0·0077	0·0139	1·79

Besides the striking maximum which always occurs in the neighbourhood of $\frac{m}{M}=1$, it will be seen that the temperature coefficient of the heat conductivity also has a maximum at the same point. The abnormally small values recorded for the rubidium salts and potassium bromide are attributable to the presence of impurities ; these do not suffice, however, to wipe out the maximum.

§ 6. We should expect the effect of the anharmonic terms of higher order to become prominent at high temperatures. These give rise to processes in which four (or more) quanta take part, and add a term in the

heat resistance proportional to T^2. There is actually an effect, due to the increase in the specific heat, which will tend to decrease the resistance, so that in the general case we may have an effect in either direction.

The experimental results in the case of KCl, NaCl, etc., show that the resistance rises faster as the temperature, so that we may disregard the specific heat effect. In this case we should expect that the case of equal masses would again be exceptional * ; because we have relatively few " Umklapp " processes, we should expect the additional processes to have a relatively larger effect than in other cases, *i. e.*, we should expect the temperature coefficient of the heat conductivity to be largest for $\frac{m}{M}=1$.

The fact that the experimental results confirm this conclusion is an additional confirmation of the correctness of the original interpretation.

We should not expect any particular regularity for the absolute value of the coefficient of the T^2 terms in the resistance. If

$$W=\alpha T(1+\beta T^2),$$

it is β which shows the maximum, not $\alpha\beta$.

§ 7. Any explanation of the above effects leads to the rule that the more complex the spectrum of a crystal is the smaller is its heat conductivity. This was realized also by Eucken and Kuhn, who have tabulated experimental data supporting this point.

Furthermore, we would expect from Debye's or Peierls's theory that the anharmonic factor would be important for the quantitative size of the heat conductivity. Actually Peierls's theory leads to something of the order $\frac{1}{\beta^2}$, where β is a mean anharmonic constant. As $\beta=0$ would mean an infinitely high heat conductivity, we should naturally expect such substances to show an abnormally high heat conductivity ; in general a very small value of β goes with a very tight binding between the particles and a small expansion coefficient. The best

* The existence of this effect was suggested to me by Dr. Peierls.

example would be diamond, but, unfortunately, the measurements at ordinary temperatures lie in a region of $T << \theta$ (θ=Debye temp.), and here a comparison with other substances is hardly likely to be justified.

Summary.

The theory of heat conductivity of crystals, due to Peierls, has been shown to account very simply for the remarkable regularity in the heat conductivity of the alkali halides discovered by Eucken and Kuhn.

The above paper was started in Göttingen during my stay there, as Queen Victoria Scholar of the University of South Africa, and completed at the Imperial College. I should like to express my thanks to Prof. M. Born and to Dr. E. Teller for their interest and encouragement. I am also indebted to Dr. R. Peierls for very helpful discussions and for reading the manuscript.

LXXXI. *The Ignition of Gaseous Mixtures by the Corona Discharge.* *By* Robert W. Sloane, *B.Sc., M.A., Thomson Experimental Scholar, The University, Glasgow**.

Introductory.

IGNITION of inflammable gaseous mixtures by sparks and by break arcs has been investigated by many workers [1], [2], but only passing references have been made to ignition by the corona discharge. Thornton [3] states, in connexion with a brush discharge, that "gaseous mixtures cannot be fired by such a discharge or by the more active discharge from needle-points at extra high pressure unless a definite spark passes." On the other hand, Morgan [4] records that the brush discharge between the secondary terminals of an induction coil may produce ignition.

The current in a discharge may be limited so that the discharge takes the form of a corona either by suitable arrangement of the form and size of the gap or by the use of high-resistance electrodes. Metal electrodes

* Communicated by Prof. E. Taylor Jones, D.Sc., F.Inst.P.

with a high resistance elsewhere in the circuit do not constitute an equivalent arrangement, because the capacity of the electrodes may be discharged by a spark. In this paper cases of ignition of coal-gas–air mixtures by transitory discharges from dielectric surfaces and by steady corona discharges are recorded.

Part I.—Ignition by Transitory Corona Discharges.

In the first experiments insulating surfaces were charged by contact with charged metal surfaces. A condenser (fig. 1), consisting of two ebonite plates C, D, ·16 cm. thick, in contact between two brass plates A, B, was connected across the poles of a Wimshurst machine in parallel with an electrostatic voltmeter. When the

Fig. 1.

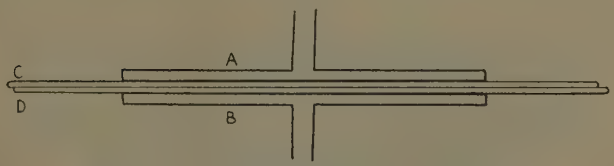

Method of charging surfaces of ebonite plates.
A, B, brass plates; C, D, ebonite plates.

condenser was charged, and A and B removed, charges remained on the outer surfaces of C and D, held by their mutual attraction. If the original potential difference V across the condenser exceeded a particular value (about 6000 volts), a discharge took place from the charged sides of C and D to the air when these dielectric plates were separated. If the charged surfaces were now brought together another small discharge was sometimes obtained, but it was always possible to obtain a discharge from the insulating surface to a conductor.

The quantity acquired by one of the plates charged in this way, when V was less than 6000 volts, was found, in every case, to be much less than the value calculated from potential and capacity, and did not vary in any regular manner with the potential. The amount of charge left, after the discharge at separation, on a plate which had been more highly charged seemed equally

fortuitous. Neither did the charge acquired by the ebonite plates from brass disks of various sizes (diameters 2, 4, 6, 8, and 10 cm.) at any one difference of potential vary regularly with the areas of the disks.

It would appear that no definite surface density could be obtained on an insulating surface charged in this way. This is no doubt due to the fact that the various surfaces make contact at a few points only. Unsuccessful attempts were made to overcome this difficulty, first by using mercury contacts with the dielectric, and later by using sheets of a compressible dielectric and forcing the metal disks against them. The method was abandoned because it was not found possible to ignite a coal-gas–air mixture by any discharge of electrification so obtained in which only dielectrics were concerned, although these discharges were both audible and visible. A discharge from the charged insulating surface to a conductor can, however, ignite a coal-gas–air mixture.

Fig. 2.

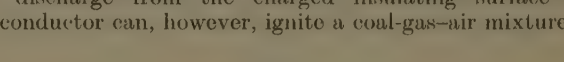

A, B, brass rods; C, D, tubes of dielectric or high resistance material.

The system of fig. 1, which has been considered as a condenser, may also be regarded as a high resistance. If a current flows through this resistance it must cross the adjacent surfaces of C and D. If the current continues to flow when these surfaces are separated by an air-space a discharge must pass through the air between them. If the conductors A and B are in the form of rods and the insulators C and D in the form of tubes closed at one end and slipped over the rods (fig. 2), the system is a pair of high-resistance electrodes. The advantage of the arrangement is that it allows investigation to be made of a discharge between the dielectric surfaces without changing the contacts between A and C and B and D.

Two such electrodes were used as the poles of a Wimshurst machine. Pairs of tubes of paraffin wax, ebonite, glass, white fibre, lignum vitæ, teak, mahogany, oak, greenheart, hemlock, plane tree, maple, and white-wood were tried for C and D.

In every case, except in the case of paraffin wax, it was possible to produce a discharge between the "insulating" surfaces. At short gap lengths, 1 to 10 mm., depending on the material, this discharge was one or two millimetres wide. The visible parts of the discharge were a blue glow close to the cathode and a redder, slightly narrower glow extending from the anode to within a short distance of the luminosity at the cathode. When the gap was lengthened the discharge narrowed, and, if the dielectric did not break down, it ultimately resembled a faint brush discharge. Neither the discharge between glass electrodes nor that between ebonite electrodes ignited a coal-gas–air mixture admitted to the gap from a Fisher burner. When white fibre or lignum vitæ was used ignition was obtained when the glow was sufficiently long (12 to 18 mm.). In the case of the

Fig. 3.

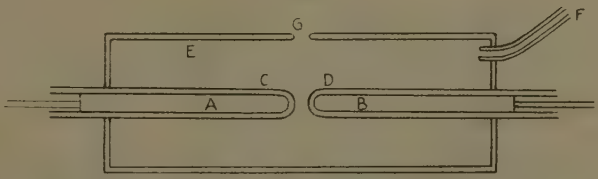

A, B, conducting rods; C, D, tubular glass electrodes; E, oven; F, delivery tube for gas; G, opening for thermometer.

other woods no ignition by the discharge took place. The wooden electrodes became punctured before a gap-length of 12 mm. was reached. In every case the spark at breakdown of the electrode material produced ignition.

The current carried by such a discharge between dielectrics will vary, *ceteris paribus*, with the total resistance of the electrodes, and the concentration of the discharge, and the area of the electrodes used by the discharge will vary with the specific resistance of the electrodes. The specific resistance of glass decreases rapidly with rise of temperature. When the experiment just described was repeated with glass electrodes heated to 100° C. the discharge (8 mm. long) produced ignition. More accurate results of this type were obtained with the apparatus described in the following paragraph.

A and B (fig. 3) are carbon rods with brass rods screwed

into them. C and D are tubes of soda glass 12 cm. long, 1·14 cm. wide, and ·16 cm. thick, painted with "Aquadag" colloidal graphite on the inside at the closed end to make good contact with A and B. E is a cylindrical oven of unglazed earthenware 18 cm. long and 5 cm. in diameter. C, D, and the glass tube F are sealed in with plaster of Paris. G is a circular hole of diameter ·7 cm. Round the oven is wound a heating coil which will maintain the oven at 250° C. when the current is 1·25 amp. A and B were connected across the secondary of an induction coil and F led, through a stopcock and a safety packing of wire gauze, to a large gas-container.

Fig. 4.

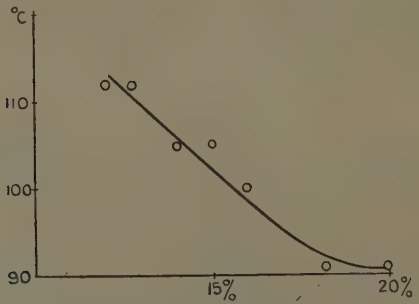

Temperature of glass electrodes for ignition of coal-gas-air mixtures.

Observations were taken in the following manner. A mixture of coal-gas and air was made up in the gas-container. The oven was heated to about 120° C., the temperature being read on a thermometer inserted in the hole G; the heating current was switched off and, when the thermometer reading had steadied at, say, 125° C., the thermometer was replaced by a cork. The interrupter was started, the primary current of the coil was switched on, and the mixture was allowed to flow into the oven, the outlet from which was the small space round the cork. If the gas-mixture in the oven became ignited (as shown by the cork being blown out) the experiment was repeated at a lower temperature. If ignition did not take place the experiment was repeated at a higher temperature. The whole process was repeated

until an " ignition " and a " no ignition " were obtained at not more than three degrees apart. The experiment was carried out with gas-mixtures of different concentration.

The gap-length, 5 mm., and the primary current were constant throughout. The amount of energy taken from the secondary circuit was small, and varied little with the temperature of the electrodes, so that the peak-potential across the leads to the electrodes, 45 kv., was constant.

Fig. 5.

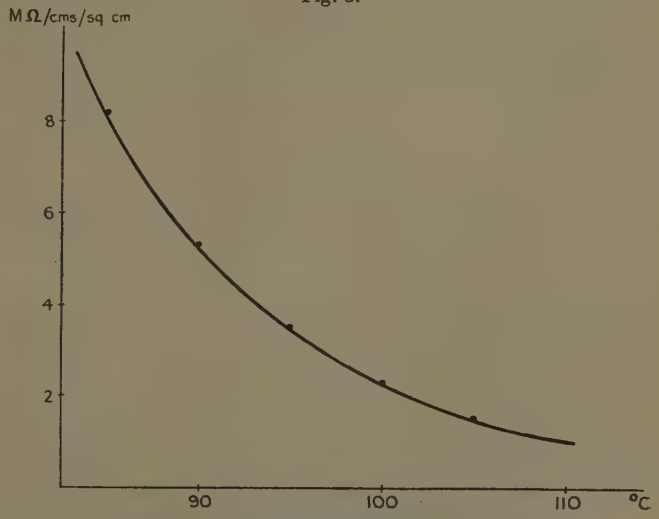

Variation of specific resistance of glass electrodes with temperature.

Fig. 4 shows the lowest temperature at which the discharge used in this experiment would ignite 12 to 20 per cent. coal-gas–air mixtures.

The Variation of the Resistance of Glass with Temperature.

The two glass tubes used in the ignition experiments were mounted so as to dip into mercury, and filled with mercury to the level of the mercury in the vessel. A 1000-volt D.C. generator and a Gambrell galvanometer were connected across the mercury electrodes inside

the tubes, so that the resistance of the glass tubes was in series with the generator and galvanometer. The mercury was heated by a Bunsen flame. In fig. 5 the specific resistance of the glass in millions of megohms/cm./sq. cm., calculated from the galvanometer readings, the galvanometer constant, and the dimensions of the tubes, is plotted against the temperature of the mercury, which will be the temperature of the glass, since the heating was slow.

Fig. 6.

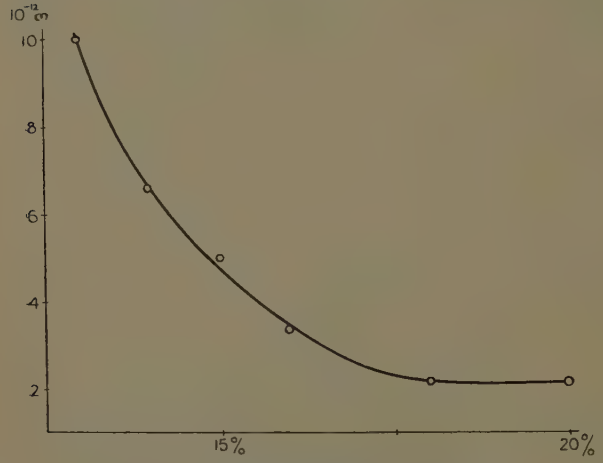

Electrode conductivity required for ignition of coal-gas-air mixtures.

In fig. 6 the abscissæ are taken from the smooth curve in fig. 4, and the ordinates are the reciprocals of the ordinates of fig. 5, the points being taken at the same temperatures on the two graphs. This graph, therefore, gives some indication of the manner in which the igniting power of the discharge varies with the conductivity of the electrodes.

The Potential across the Discharge.

The potential difference across a discharge between glass electrodes cannot be measured directly. Even if the potential were steady and the current known, the

potential across the discharge cannot be deduced, because the form of the lines of flow through the glass, and, therefore, the resistance of the glass, is unknown. The following experiment is an attempt to overcome this difficulty.

A steady potential was maintained across the electrodes by a condenser charged with an induction coil through a diode valve, and could be measured by a sphere-gap. A galvanometer was connected in series with the glass gap. As in the ignition experiments, the temperature of the glass could be varied.

Let E be the potential difference across the condenser, e the potential difference across the discharge, i the steady current flowing, and R_1 the resistance of the glass at θ_1° C. Then

$$E = R_1 i + e.$$

TABLE I.

i.	θ_1.	θ_2.	E.	E′.	k.	e.
divs.	° C.	° C.	kv.	kv.		k.v.
1·0	90	97	24·0	20·0	$\frac{27}{12}$	17·0
1·2	98	108	25·3	20·0	$\frac{13}{6}$	15·5
2·2	103	107	25·3	22·8	$\frac{110}{65}$	17·7

The gap-width was 5 mm.

Let R_2 be the resistance of the electrodes at θ_2° C., and let E′ be the value to which E has to be adjusted, so that i is the same as before. Then

$$E' = R_2 i + e;$$

and if

$$\frac{R_1}{R_2} = k,$$

then

$$e = \frac{E - kE'}{1 - k}.$$

It seems reasonable to assume that k is approximately equal to the ratio of the specific resistances of the glass at θ_1 and θ_2. The results of these measurements are given in Table I.

The accuracy is not high, but seems sufficient to indicate that the maintenance potential for this discharge is approximately equal to the sparking potential.

The Quantity carried by One Discharge.

In the apparatus used in the ignition experiments a ballistic galvanometer, shunted by a Leyden jar, was inserted in series with the glass gap, and a Meiklejohn hand interrupter was substituted for the trembler interrupter of the coil. The primary current was adjusted so that the secondary peak potential was the same as in the ignition experiments. When the primary current

Table II.

Temperature.	Galvanometer deflexion.	q.	j.
° C.		microcoulombs.	joules.
90.....	110	·16	·0027
93.....	110	·16	·0027
97.....	115	·17	·0029
102.....	120	·18	·0030
109.....	130	·19	·0032

was broken the galvanometer deflexion gave the quantity which flowed round the secondary circuit, that is, the quantity carried by the discharge. During the experiment the electrodes were at temperatures within the range covered in the ignition experiments. The results are given in Table II.

q is the quantity in microcoulombs, j the energy dissipated in the discharge, i. e., $j=q$ V. 10^{-3} joules. The gap-width was 5 mm., and V, the potential across the discharge, was assumed to be 17 kv.

In fig. 7 the energy dissipated in the discharge, estimated in the above manner, is plotted against percentage of coal-gas in the coal-gas–air mixture, which the discharge will just ignite.

Heating of the Gas.

The ends of the glass electrodes were enclosed in an air-tight ebonite chamber forming the bulb of a dilatometer connected with an open manometer containing water or oil. When the primary current was broken a discharge passed inside the chamber, and caused the liquid in the manometer to move. The difference of levels produced in the manometer is due to three separate effects, viz., the pressure-wave from the discharge, the change of volume due to chemical change, and the change of volume due to the heating of the enclosed air. If the zero be read at the end of the experiment, the

Fig. 7.

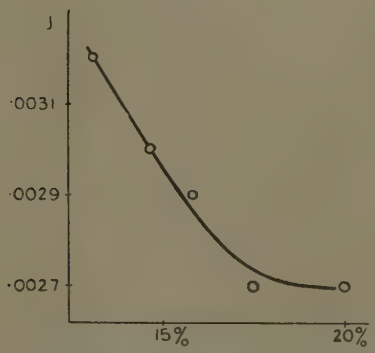

Least igniting energy for coal-gas-air mixtures.

chemical effect, which is permanent, may be ignored. The heating effect was estimated in two ways. First, by measuring the comparatively slow change of volume as the thermometer cooled to its new zero after the sudden change due to the pressure-wave had disappeared; second, by using an oil in the manometer too viscous to move under the impulse of the pressure-wave. It moved only under the pressure due to the less transient heating effect.

The change in level of the liquid in the manometer tube, observed through a graticulated microscope, was always of the order of ·06 mm., corresponding to a change of volume at constant pressure of ·2 c.mm. Thus

the quantity of energy that appears as heat after one discharge is about $6 \cdot 10^{-5}$ joules. This is 2 per cent. of the total energy dissipated in the discharge, most of which is, no doubt, absorbed as heat by the electrodes.

Part II.—Ignition by Steady Corona Discharges.

A steady high potential was maintained by charging a smoothing circuit from a "36-inch" induction coil through a large diode valve. The smoothing circuit consisted of a capacity of ·01 mfd. and one of ·1 mfd. in parallel, with a large self-inductance connected between them. The potential could be measured by a sphere gap in series with a high resistance (a short length of string), and a microamperemeter was connected in series with the test gap. The positive terminals of the secondary, of each condenser, and of each gap were connected to earth, and the whole high potential (negative) system was sheathed in paraffin wax with only the electrodes at the gaps protruding. The ends of slate rods formed the electrodes of the test gap. A steady current passed between these electrodes when the primary current had a suitable value.

When the discharge was running, gas was allowed to flow from a Fisher burner below the gap. If the discharge failed to ignite the gas the primary current was increased until ignition occurred. If the gas ignited immediately, the current was reduced until the discharge failed to ignite the gas, and was then increased as before. The least discharge-current required to cause ignition was read on the microamperemeter, and the earthed sphere of the sphere gap was moved forward until a spark passed. The primary current was then switched off, and the sphere- and test-gap lengths measured. The experiment was repeated with different test-gap lengths.

The mixture escaping from the burner contained an excess of coal-gas, so that, on mingling with the air, it would contain at some part the most easily ignitable mixture.

In the first experiments the test-gap electrodes were slate rods, 5 mm. in diameter, with rough hemispherical ends. Their total resistance, measured when the ends were smeared with "Aquadag" and bound with wire, was 13·5 megohms. Their effective resistance, measured

when the rounded ends were touching and wire contact was made at the other ends, was 200 megohms.

The results obtained by the method just described are shown in Table III.

These are typical results, but they are not repeatable with more than 20 per cent. accuracy because of a certain electrode effect. When the discharge was started it took place between the ends of the electrodes, but soon, within a few seconds if the electrodes had been used recently, the discharge left the end of the cathode and proceeded from an area on the side of the rod. and moved farther and farther up the rod. While this happened the current flowing might rise, or fall, or show no change,

TABLE III.

Slate gap.	Least igniting current.	Sphere gap.
mm.	microamp.	mm.
2·8	300	4·7
4·3	300	6·7
5·5	190	6·9
8·3	150	8·8

depending, no doubt, on the area of cathode used by the discharge. Owing to this variable concentration of the discharge it is obviously impossible to estimate the effective resistance of the electrodes in any particular case, and it is, therefore, impossible to find the potential across the discharge. New slate electrodes, 3·5 mm. in diameter, tapered at an angle of 30° to hemispherical ends about 1·5 mm. in diameter, proved no more satisfactory. Least igniting currents were of the same order with the new electrodes as with the old. For instance, with a slate gap 5·2 mm. long a current of 280 microamp. lit the gas from the burner.

It seems that, though high-resistance electrodes are convenient for the production of corona, metal point electrodes must be used if more accurate measurements are to be made. A few measurements were taken by

a method of this kind and are shown in Table IV. In these experiments metal points (wires 3 mm. long by $\frac{1}{4}$ mm. diameter, with convex ends) were attached to the ends of the slate electrodes and the discharge-current measured as before.

When metal points are used to produce a corona the potential difference across them can be measured directly by an electrostatic voltmeter, provided that a high resistance is connected in series with the voltmeter so that the capacity of the instrument cannot discharge suddenly across the gap. In this way it was found that the potential difference across a discharge 3 to 4 mm

TABLE IV.

Point gap.	Least igniting current.	Sphere gap.
mm.	microamp.	mm.
3·0	330	3·70
4·4	300	3·30
6·0	320	3·95

long, the current being 350 microamp., was about 2500 volts.

Summary.

1. It was not found possible to ignite any coal-gas–air mixtures by the discharge of electricity between the surfaces of good insulators such as paraffin wax, ebonite, or cold glass.

2. It is possible to ignite inflammable coal-gas–air mixtures by the discharge of electricity between the surfaces of less good insulators such as white fibre, glass at 100° C., or slate.

3. Mixtures of 12 to 20 per cent. coal-gas in air may be ignited by the induction-coil discharge between glass electrodes at about 100° C. 5 mm. apart when the total energy of the discharge is about ·003 joules.

4. A steady corona discharge between slate electrodes 3 or 4 mm. apart carrying a current of about 300

microamp. will ignite the most easily ignited coal-gas–air mixture.

5. The steady corona discharge between metal points 3 to 6 mm. apart will ignite the most easily ignited coal-gas-air mixture when the current is greater than 300 microamp.

Acknowledgments.

I am indebted to the Research Department of Imperial Chemical Industries, Ltd., for suggesting this problem, for interest in the work, and for a personal grant. To Prof. E. Taylor Jones I owe thanks for the facilities for the experiments and for help and encouragement.

References.

(1) Morgan, 'Fuel in Science and Practice,' xi. p. 452 (1932) (with references).
(2) Taylor Jones, 'Induction Coil,' chap. viii. (1932) (with references).
(3) B. A. Report, 1914, p. 513.
(4) Journ. Inst. Elect. Eng. liv. p. 254.

Cf. also Tchang Te-Lou, *Comptes Rendus*, cxcviii. p. 542 (1934), and Lewis and Kreutz, Journ. of Chem. Physics, i. no. 1 (1933).

LXXXII. *The Displacement and Deformation of an Elastic Bar.* *By* E. H. Bateman, *M.A.**

1. THE internal stresses in a network of elastic bars under the action of known external forces may be obtained directly from the partial derivatives of the strain energy or work of deformation with respect to the unknown moments†. It may also be shown that if the deformation is caused by known displacements instead of, or in addition to, known external forces, a similar method of analysis is applicable, provided that the work of displacement can also be expressed in terms of the unknown moments. The method depends on the equality between the work of deformation and the work of displacement for each unit of the network system.

* Communicated by the Author.

† E. H. Bateman, "The Strain Energy Method in Elastic Network Analysis," Phil. Mag. xvii. p. 1004 (May 1934).

Thus, if AB is an elastic bar acted on by end moments α, β, and by any system of transverse loading T, the strain energy is

$$W=f(\alpha, \beta, T) \quad . \quad . \quad . \quad . \quad . \quad . \quad (1)$$

and the external work of displacement is

$$V=\tfrac{1}{2}.\alpha.\theta_\alpha+\tfrac{1}{2}.\beta.\theta_\beta+\tfrac{1}{2}.T.\Delta_T, \quad . \quad . \quad . \quad (2)$$

where θ_α and θ_β are the displacements of the end moments α and β, and Δ_T is the effective displacement of the transverse loading system. If, now, small increments $\delta\alpha$ and $\delta\beta$ are applied, the corresponding increments of strain energy and of external work are

$$\delta W=\frac{\partial W}{\partial \alpha}.\delta\alpha+\frac{\partial W}{\partial \beta}.\delta\beta,$$

$$\delta V=\alpha.\delta\theta_\alpha+\beta.\delta\theta_\beta.$$

But since α is proportional to θ_α, and β is proportional to θ_β,

$$\alpha.\delta\theta_\alpha=\theta_\alpha.\delta\alpha \quad \text{and} \quad \beta.\delta\theta_\beta=\theta_\beta.\delta\beta;$$

thus $$\delta V=\theta_\alpha.\delta\alpha+\theta_\beta.\delta\beta.$$

But $\delta V=\delta W$; hence

$$\frac{\partial W}{\partial \alpha}=\theta_\alpha \quad \text{and} \quad \frac{\partial W}{\partial \beta}=\theta_\beta. \quad . \quad . \quad . \quad . \quad (3)$$

Now, since the final object of the analysis is to find the moments caused by known displacements, we adopt the convention that θ_α and θ_β are independent of α and β, so that, referring to (2),

$$\frac{\partial V}{\partial \alpha}=\tfrac{1}{2}.\theta_\alpha \quad \text{and} \quad \frac{\delta V}{\partial \beta}=\tfrac{1}{2}.\theta_\beta. \quad . \quad . \quad (4)$$

Hence, on this assumption, we have from (3) and (4)

$$\frac{\partial}{\partial \alpha}(W-2V)=\frac{\partial}{\partial \beta}(W-2V)=0, \quad . \quad . \quad (5)$$

and for a network system formed by n elastic bars it follows that

$$\frac{\partial U}{\partial \alpha}=\frac{\partial U}{\partial \beta}=\ldots=0, \quad . \quad . \quad . \quad . \quad . \quad (6)$$

where $U=\Sigma^n(W-2V)$.

Here the purpose of the summation is to allow algebraic simplification before the operation of partial derivation,

and equation (6) does not define the principle of minimum strain energy, though the theorem follows from it if the unknown moments are reduced in number to the degree of indeterminacy of the network.

2. The expression for V given in (2) must be modulated to a more convenient form for use in (5), since the angles θ_α and θ_β are formed by the combination of angular and transverse displacements indicated in the figure.

Here θ_A and θ_B are the angles of rotation of the tangents at A and B, measured from their original position and the rotation of the line AB in taking up the position A′B′ is $\phi=(\Delta_B-\Delta_A)/l$, where $\Delta_A=AA'$, $\Delta_B=BB'$.

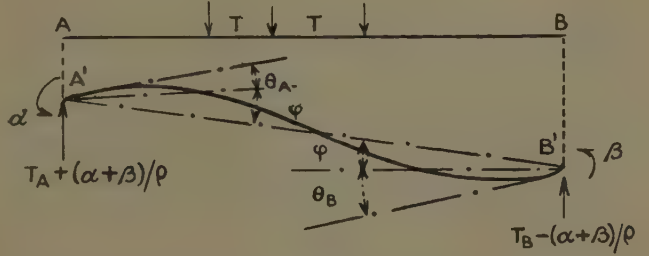

Then the work of displacement is the work of rotating the end moments plus the work of translation, so that

$$\begin{aligned}V=&\tfrac{1}{2}\alpha(\theta_A+\phi)+\tfrac{1}{2}\beta(\theta_B+\phi)\\&-\tfrac{1}{2}.\phi(\alpha+\beta)-\tfrac{1}{2}.\Delta_A(\alpha+\beta)/l+\tfrac{1}{2}.\Delta_B(\alpha+\beta)/l\\&+\tfrac{1}{2}.T.\Delta_T-\tfrac{1}{2}.T_A.\Delta_A-\tfrac{1}{2}T_B.\Delta_B\\=&\tfrac{1}{2}.\alpha(\theta_A+\phi)+\tfrac{1}{2}.B(\theta_B+\phi)+C,\end{aligned}$$

which is equivalent to (2), and may be written

$$2V=\alpha\theta_A+\beta\theta_B+(\alpha+\beta)(\Delta_B-\Delta_A)+C, \quad . \quad . \quad (7)$$

where C is independent of α and β.

The corresponding expression for the strain energy of deformation is

$$W=\{\alpha^2-\alpha\beta+\beta^2-\alpha(2a+b)+\beta(a+2b)\}.l/6EI+C', \quad (8)$$

where E is Young's Modulus, I is the relevant moment of inertia, a, b are the end moments which would be

produced at A and B by the transverse loading if the ends of the bar were fixed in position and direction, and C′ is independent of α and β *.

3. The method may be illustrated by its application to a simple case. Thus, if AB is a cantilever fixed A and the deflexion at B is Δ, we have

$$\beta=0, \quad \Delta_A=0,$$

and

$$W-2V=\{\alpha^2-\alpha(2a+b)\}.l/6EI-\Delta.\alpha/l+\alpha\theta_A+\text{const.}$$

Derivation with respect to α gives

$$0=(2\alpha-2a-b).l/6EI-\Delta/l+\theta_A, \quad . \quad . \quad . \quad (9)$$

which is a general relation for the deformation of a cantilever.

From this equation may be deduced the deflexion at the end of a cantilever for any system of loading; for example, if the deflexion is due to a load P at B, we have $a=b=0$, $\alpha=P.l$, and we find $\Delta=Pl^3/3EI+l\theta_A$; or, if there is an applied load ω per unit length, $a=b=\omega l^2/12$, $\alpha=\omega l^2/2$, and we find $\Delta=\omega l^4/8EI+l\theta_A$.

4. It may also be of interest, in further illustration of the method, to obtain the two following well-established results:—

First we note that equations (5), if applied to (7) and (8), are, in fact, the slope deflexion equations

$$\left.\begin{aligned}0&=(2\alpha-\beta-2a-b).l/6EI-\theta_A-(\Delta_B-\Delta_A)/l,\\ 0&=(2\beta-\alpha+a+2b).l/6EI-\theta_B-(\Delta_B-\Delta_A)/l.\end{aligned}\right\} \quad (10)$$

Secondly, the theorem of three moments for a continuous girder is defined at once by an equation of the form (6), $\dfrac{\partial U}{\partial\beta}=0$, where U is the sum, $\Sigma(W-2V)$, for two consecutive sections AB and BC, for which there is continuity of bending moment, β, at B.

5. As a final example we derive an expression for the deflexion at any point in a simply supported beam, ABD,

* E. H. Bateman, "The Strain Energy of an Elastic Bar," Phil. Mag. xvi. p. 1128 (Dec. 1933).

for any system of transverse loads. The beam is supported at A and D, and the deflexion of B in a direction at right angles to AD is Δ. The bending moment at B is β; the end moments acting on AB and BD may, therefore, be written $0, \beta$; $-\beta, 0$, and

$$\begin{aligned} U &= (W - 2V) \\ &= \{\beta^2 + \beta(a+2b)\} . l_1/6EI + \{\beta^2 + \beta(2c+d)\} . l_2/6EI \\ &\quad - \Delta . \beta(l_1+l_2)/l_1 l_2 + \text{const.}, \end{aligned}$$

where $l_1 = AB$, $l_2 = BD$, and (a, b) and (c, d) are the end fixing moments for AB and BD as defined in paragraph 2.

Then $\dfrac{\partial U}{\partial \beta} = 0$ becomes

$$0 = (2\beta + a + 2b) . l_1/6EI + (2\beta + 2c + d) . l_2/6EI - \Delta(l_1+l_2)/l_2 l_2, \quad . \quad . \quad (11)$$

which is a general relation for the deformation of a simply supported beam.

If the deflexion is caused by a load P at B,

$$a = b = c = d = 0,$$

$$\beta = P . l_1 l_2/(l_1 + l_2),$$

and we find

$$\Delta = \frac{P l_1^2 l_2^2}{3EI(l_1+l_2)} .$$

If the deflexion is caused by a uniform load ω per unit length,

$$a = b = \omega l_1^2/12, \qquad c = d = \omega l_2^2/12, \qquad \beta = \omega l_1 l_2/2,$$

and we find

$$\Delta = \omega l_1 l_2 (l_1^2 + 3 l_1 l_2 + l_2^2)/24 . EI.$$

The method also leads directly to the complete solution of any problem involving fixed ended or continuous beams.

6. In the analysis of a network of elastic bars this system enables a solution to be developed by a method of partial derivatives if, owing to the existence of applied displacements or the redundancy of supports, the strain-energy method is inapplicable.

LXXXIII. *Negative Ions of Iodine.*—Part II. *Ion Beams*.*
By JOHN SPENCER-SMITH, *Ph.D., Department of Physics, Queen's University, Belfast.*†

IT has been shown in a previous paper ‡ that probe measurements in the glow-discharge and low-voltage arc in iodine vapour indicate that negative ions are present in numbers closely equal to those of the positive ions. These measurements do not, however, give any direct information as to the nature of the ions, and it is also desirable to obtain confirmation of the probe results by some independent method. It was, therefore, decided to attempt to draw ion beams out of the discharge into an evacuated chamber, and there to submit them to magnetic analysis. This has been carried out in two stages: first, separation of electrons from negative ions by small magnetic fields, and, second, analysis of the ion beam itself by stronger fields. A similar analysis has been performed incidentally for the positive ions from the glow-discharge, and some rough measurements have been made of the absorption of the negative ions and electrons in iodine (I_2) vapour. From the work of Hogness and Harkness § we should expect the ions I^-, I_2^-, and I_3^- to be present; all three have been found, together with the corresponding positive ions, and, in the negative sections of the discharge, I^{++}.

1. *Magnetic Analysis.*

The apparatus used is shown in fig. 1. It consisted of a discharge-tube A of Type I.‖, 4 cm. in diameter, connected by a side-tube, 1 cm. in diameter and 1 cm. long, to a bulb B, 8 cm. in diameter. All metal parts, except the tungsten seals through the pyrex and molybdenum wire leads, were of nichrome. A metal cylinder C with a central tube 0·2 cm. in diameter fitted closely into the

* This paper includes part of a thesis submitted to the University of London for the degree of Doctor of Philosophy.

† Communicated by Prof. K. G. Emeléus, M.A., Ph.D.

‡ Spencer-Smith, Phil. Mag. xix. p, 806 (1935). This will be referred to subsequently as Part I.

§ Hogness and Harkness, Phys. Rev. xxxii. p. 784 (1928).

‖ Spencer-Smith, *loc. cit.*

connecting tube. Immediately behind C was a metal plate D pierced with a 0·2 cm. hole in line with that in C. The Faraday cylinder E was in line with C and D, and a second Faraday cylinder F was placed above * E, so that particles passing through C and D and received on F would have been deviated through an arc of mean radius 12·5 cm. The bottom of B tapered into a wide tube J. The system could be exhausted by a three-stage mercury

Fig. 1.

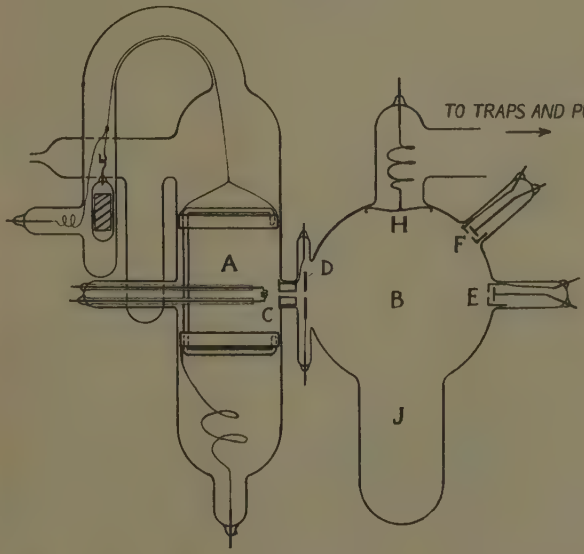

diffusion pump connected to it through two large liquid-air traps with a tap of 2 cm. clearance in the barrel between them. The inside of B was heavily sputtered with platinum, to which contact was made by the spring H. A tungsten filament was mounted opposite C in A, to give alternatively a beam of electrons for calibration purposes, or to serve as the cathode of a low voltage arc. The iodine was prepared as described in Part I., except that in some experiments the iodine distillation train was exhausted by a separate pumping train, and contact

* Or, in cases, below E.

between it and the main discharge system finally made by breaking a thin glass internal seal *in vacuo*.

For work with electrons the earth's magnetic field was balanced out by Helmholtz coils, the current in which was adjusted to an optimum value by having A and B exhausted, and bringing an electron beam from the filament in A on to the inner collector of E. In addition to the compensating coils, a vertical pair of Helmholtz coils was mounted beside B for deflecting electrons off E on to F. For deflecting negative or positive ions an electromagnet was mounted with its poles against B; this gave fields up to 2000 gauss, but they were not uniform throughout the bulb. A was shielded from the electromagnet by soft iron, imperfectly for the larger fields, as shown by some visible disturbance of the main discharge. To maintain the pressure in B below 10^{-4} mm. whilst that in A was of the order of 0·2 mm., J was cooled in liquid air and B continually exhausted by the pump.

The first stage in the analysis consisted in the separation of the negative ions and electrons. Running a glow-discharge in A, a mixed beam from any desired part of the discharge was drawn into C by making it a few volts positive to the space-potential in the discharge in its neighbourhood, previously located by the Langmuir method, using C itself as probe. The beam was further accelerated towards D, and its composition (all ions; electrons) found by deflecting the electrons away from E by a small magnetic field insufficient to affect the ions.

There are several difficulties in this method. First, there was of necessity some gas in the channel in C, so that the composition of the beam when it entered B was not necessarily the same as when it left A. Second, it was found that, although the ion beams were well focussed, the electron beams were slightly divergent and could not be received entirely through the front apertures in E and F. Both parts of E and F, case and inner electrode, were, therefore, used simultaneously as collectors. Third, the presence of the comparatively large positively charged surface of C has a disturbing effect on the main discharge in A, even before an arc strikes to it. It was usually possible to work with a potential across the sheath on C not greater than 10 volts. With C negative and drawing positive ions, a very much smaller disturbance resulted. For these reasons the data obtained for the

relative numbers of electrons and negative ions are to be regarded as confirmatory of those obtained in Part I. rather than as furnishing more accurate data.

Typical curves for the current to E are shown in fig. 2. In the upper curve the current for zero field is that of electrons and negative ions combined; this falls rapidly to a constant value for fields greater than 25 gauss. That the latter is correctly attributed to negative ions is shown by the lower curve, which represents the current to E with A and B both evacuated, and electrons drawn to C from

Fig. 2.

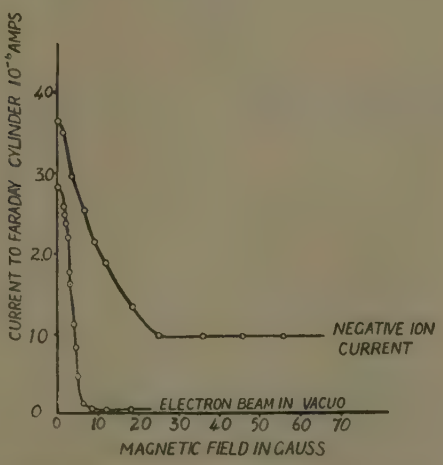

Separation of electron and negative ion currents.

the filament; this falls to practically zero for fields of more than 10 gauss. It will be noticed that the ion currents are large enough to be readily measured with a galvanometer; it was found desirable to use an electrometer only for the positive ions and for certain of the absorption measurements. Some idea of the disturbing effect of C * is given by the ratio (R) of the negative ion and total negative currents to E for different parts of the

* Secondary emission from E will also play some part. D and the sputtered Pt. and E (apart from the small p.d. in the galvanometer lead) were all at earth potential.

discharge and different accelerating potentials. This is tabulated in Table I. for, first, (α) 10 volts across the sheath on C and 60 volts between C and D, and, second, (β) 40 volts across the sheath on C and 180 volts between C and D. In both cases the discharge in A was one at 900 volts, $1{\cdot}2.10^{-3}$ amp./cm.^{2}, and the iodine pressure in A 0·2 mm. This uncertainty is not sufficient, however, to prevent the data from furnishing confirmation of the result reached in Part I. that there are numerous negative ions in the discharge.

Similar measurements were made with a low-voltage arc run between the filament and C as anode, the analysis

TABLE I.

Apparent Ratio of Negative Ion Random Current to Total Negative Random Current in various parts of the Glow-discharge.

Position of channel.	R (α).	R (β).
Negative glow	0·28	0·35
Faraday dark space	0·27	0·38
Positive column	0·21	0·40

being then confined to ions and electrons reaching C in the normal course. Apart from this, the experimental methods and results were essentially the same as for the glow-discharge.

The second stage of the analysis—the separation of the components of the ions beam—was carried out in two ways. In the first, sufficiently large magnetic fields were applied to bring I^-, I_2^-, and I_3^- successively on to F. This was not made much use of, as, on account of the large mass of the ions, it necessitated the use of inconveniently low accelerating potentials to C and D. Larger accelerating potentials, with correspondingly larger magnetic fields, if the latter had been available, would have been undesirable owing to the combined electric and magnetic disturbances of the main discharge. Some measurements were, however, made by this method and served to confirm those obtained by the second method. In this, with

which most of the data were obtained, the various components of the ion beam were bent off E in succession by gradually increasing the magnetic field. The curve showing the current to E as a function of the magnetic field then falls by steps as the field is increased (fig. 3). The magnitudes of the steps gives a measure of the relative intensities of the different types of ions, whose momentum spectrum is given, naturally with rather poor resolution, by the slope of the current-field curve. From the geometry of the apparatus and the magnitudes of the electric and magnetic field the main ions were identified.

Fig. 3.

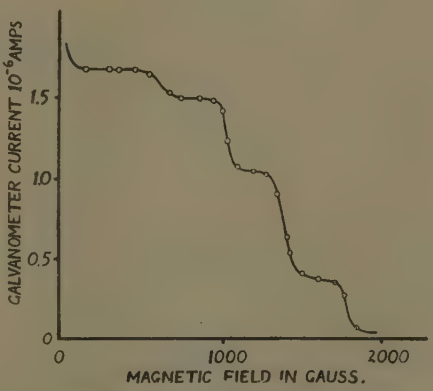

Negative ion current to collector E.

In addition to I^-, I_2^-, and I_3^- peaks, a peak of greater e/m value always appeared when there was an accelerating potential between C and D ; this was attributed to ions I^- formed in the channel in C. No other ions were recorded.

Fig. 4 shows the composition of the ion beam drawn from a glow-discharge at 900 volts, $1{\cdot}5.10^{-3}$ amp./cm.^{2} at 0·2 mm. pressure In the successive positions C was opposite the brightest part of the negative glow, the negative glow and Faraday dark-space boundary, the middle of the Faraday dark space, and the positive column respectively. The accelerating potential on C was 10–16 volts, and between C and D 40 volts. In

fig. 5 the relative values of the ion currents are plotted against position in the discharge. The composition of the beam from a low-voltage arc was found similar to that from the middle of the negative glow.

Fig. 4.

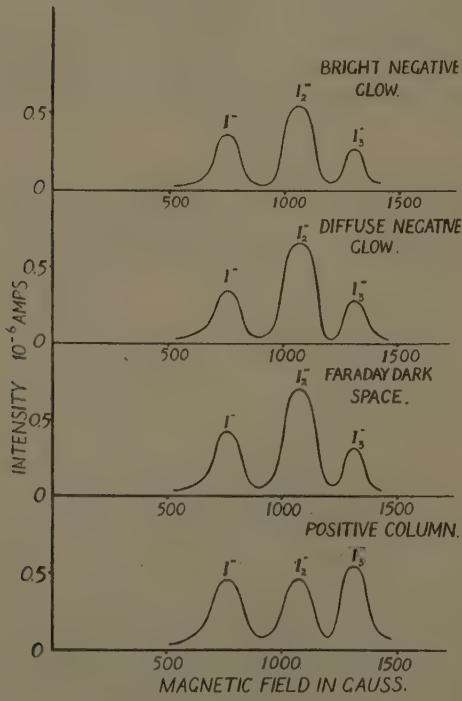

Negative ion mass spectra.

In view of the complicated conditions in the discharge and the very small present knowledge of the properties of negative ions, it is not worth attempting a detailed discussion of these results. Two points are, however, worth comment. First, very many more ions of the normal molecule (I_2^-) have been found than were found by

Hogness and Harkness * ; it is possible that the present experiments represent a nearer approach to some sort of an equilibrium condition, in which the electron temperature plays an important part, than do those in which electron beams are employed. Second, the increase in the amount of I_3^- in the positive column appears far too large to be accounted for in any such way as by secondary collisions in C, and may perhaps be attributed, in the same general manner as above, to a different pseudo-equilibrium in negative glow and positive column, consequent on the different distribution of energy amongst the electrons in the two places.

Fig. 5.

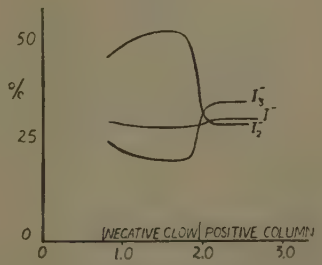

Negative ion distribution. The abscissæ are distances from the cathode in cm.

Positive ion beams were drawn into B with C negative, and subjected to analysis by the second method. There was less disturbance of the discharge with C negative than with it positive, and the beams correspondingly less intense. Typical results are shown in fig. 6 for a glow-discharge in A at 900 volts, $1{\cdot}8.10^{-3}$ amp./cm.^{2}, at a pressure of 0·2 mm. C was held 40 volts negative to the space, and the accelerating potential between C and D was 50 volts. I^{++} occurs in small quantity in the negative glow and Faraday dark space and is absent from the positive column, in accord with spectroscopic observations. By far the strongest peak is that of I_2^+. The relative intensities of the singly charged ions change but little throughout the discharge.

* Hogness and Harkness, *loc. cit.*

2. *Absorption Measurements.*

If B contains gas instead of being evacuated, some ions and electrons will fail to reach E on account of collisions made with the gas molecules in crossing the bulb. Without a fuller description of the behaviour of the particles concerned, the term "collision" is necessarily somewhat vague, but the results obtained are nevertheless of some

Fig. 6.

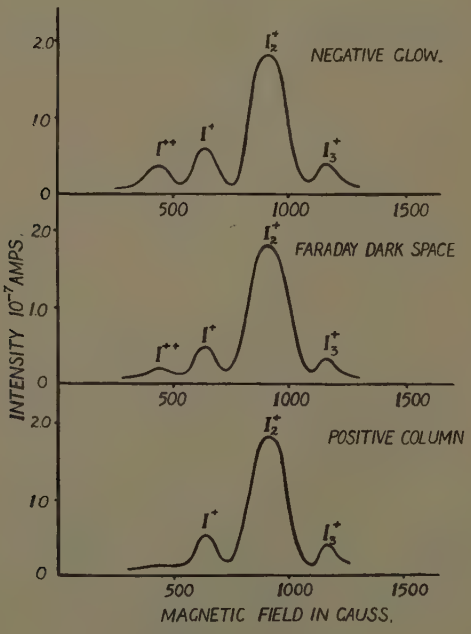

Positive ion mass spectra.

interest. The probability of collision P may be defined as the number of collisions made by a particle in going unit distance (1 cm.) through the vapour at a pressure of 1 mm. at 0° C. The falling off in the strength of a current (I) of particles in going through a distance x at pressure p, reduced to 0° C., will then be given by

$$I = I_0 e^{-Pxp},$$

where I_0 is the initial current. P can be found from the slope of the linear plot of log I against p, if x is known. To measure P for the collisions of electrons and negative ions with neutral iodine molecules (I_2), C was made 7 volts positive to the main discharge in its neighbourhood, and further accelerating potentials of up to 53 volts applied between C and D. For greater accelerating potentials the results were vitiated by the main discharge tending to penetrate into the channel in C. x is about 8 cm. The iodine pressure in B was controlled by having the

Fig. 7.

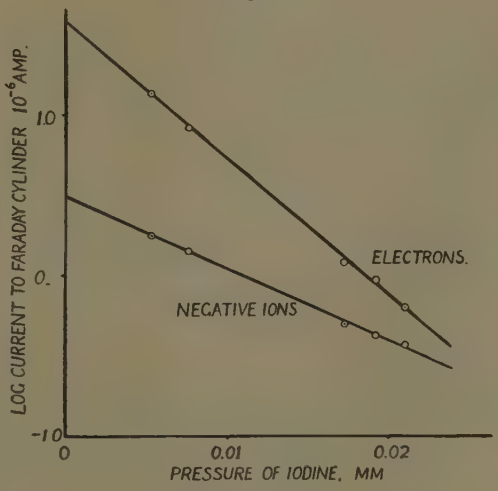

Absorption curves.

tube J and the first liquid-air trap in baths at the same temperature, less than that in B, with the tap between the two traps closed. The electron current and negative ion current to E were measured, as described previously (§ 1), for various pressures of iodine in B and various accelerating voltages. It was assumed, from the data obtained with probes under comparable conditions, that the effect of the initial velocities of the electrons could be allowed for by increasing the measured total accelerating potential across the sheath and between C and D by 1 volt. This, nevertheless, introduces uncertainty into

the results for low electron speeds, and since, in addition, it was not found possible to obtain well-defined beams with this apparatus for accelerating potentials of less than some 10 volts, the data for low-speed particles are not claimed to be very accurate. Typical lines showing the logarithm of the electron and ion currents to E as a function of the pressure in B are shown in fig. 7. The accelerating potential was 30 volts. The results of all the measurements are collected in fig. 8, where P is shown as

Fig. 8.

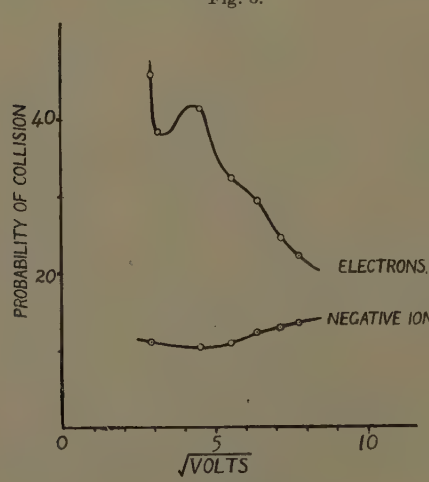

Absorption probabilities.

a function of the speed of the particles expressed in (volts)$^{\frac{1}{2}}$. As mentioned above, the exact course of the curve is uncertain for the slowest electrons and ions. The small collision probability for ions may be explained, following Massey and Smith *, by most of the elastic collisions resulting in small deflexions which would not be detected with the present apparatus. A somewhat similar behaviour of positive ions has been reported †.

* Massey and Smith, Proc. Roy. Soc. A, cxlii. p. 142 (1933).

† Dempster, Phil. Mag. iii. p. 112 (1927); Ramsauer and others, *Ann. d. Physik*, viii. p. 709 (1931).

In view of the complexity of the ion beam, further discussion of its behaviour is unprofitable. The form of the curve for electrons is generally similar to that in a number of other gases *.

Summary.

It has been found possible to draw out from the discharge an intense beam of negative ions and to subject it to magnetic analysis. I^-, I_2^-, and I_3^- have all been found to be present, I_2^- being the commonest ion in the negative glow, whilst all three are present in approximately equal numbers in the positive column. A similar study of the positive ions established the presence of I^{++}, I^+, I_2^+, and I_3^+, I^{++} being absent from the positive column, and I_2^+ by far the most intense in all regions of the discharge studied. The probability of collision between electrons and negative ions of medium speed and neutral iodine molecules has been measured approximately.

Acknowledgments of assistance are made as in Part I. and, in addition, to Dr. H. S. W. Massey, for discussion of the work described here.

LXXXIV. *Note on a Self-checking Notation for Vector Equations and Vector Diagrams.* *By* A. C. Walshaw, *M.Sc., D.I.C.* (*Lecturer in Engineering, Northampton Polytechnic, London*) †.

MANY notations and systems of labelling are used in applied mathematics and engineering science when dealing with vector equations and vector diagrams. They all purpose to be simple shorthand statements in symbolical form of verbal statements regarding vectors. They seek to clarify and to aid in the drawing of vector diagrams.

None of the notations is quite satisfactory, the defect being that neither a vector equation nor a vector diagram is self-checking as to its accuracy. They have to be

* *Cf.* Brode, Revs. Mod. Physics, v. p. 257 (1933).

† Communicated by J. G. Docherty, D.Sc., A.M.Inst.C.E., A.M.I.Mech.E.

checked by referring back to some link mechanism diagram or to some vector equation respectively.

The notation presented in this paper makes both the vector equation and the vector diagram self-checking. It also preserves simplicity and clarifies the equations and diagrams.

The notation is based on a simple shorthand way of writing down a vector equation in symbolical form.

Consider the simple case of two bodies A and B moving at any instant with velocities represented by the symbols V_A and V_B respectively. Then, the notation is, that since the velocity of A relative to B is equal to the velocity of A minus the velocity of B (subtracted vectorially), it is agreed to represent the velocity of A relative to B by the symbol $V_{(A-B)}$,—that is, the velocity equation written in symbols becomes

$$V_{(A-B)}=V_A-V_B,$$

or, rearranged,

$$V_A=V_{(A-B)}+V_B.$$

Fig. 1.

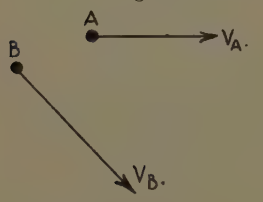

Fig. 2.

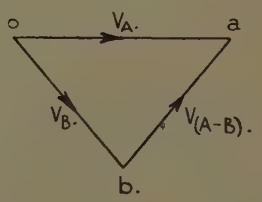

The important point to notice about these last two equations is that the suffixes and signs sum up so as to balance on each side of the equations.

The fact that the adding up of the suffixes on one side of a vector equation must result in the same total as that due to adding up the suffixes on the other side of the equation proves to be the basis of making vector equations and vector diagrams self-checking. For example, in the simple case of the two moving bodies A and B of fig. 1 we get fig. 2 as the velocity diagram for the velocity equation

$$V_A=V_B+V_{(A-B)}.$$

In this it will be seen that the vectors V_B and $V_{(A-B)}$ add vectorially to give V_A, and that the suffixes of the vectors whose arrowheads follow round one way (*oba*) add up to that of the vector going the other way (*oa*).

Similarly fig. 3 is the velocity diagram for the velocity equation

$$V_B = V_A + V_{(B-A)},$$

in which the vectors V_A and $V_{(B-A)}$ must add together vectorially to give V_B. It will be noticed that the suffixes of the vectors whose arrowheads follow round in direction *oab*, add up to that of the vector going round in the other direction (*ob*).

This can be extended to complicated vector equations and vector diagrams, in which the suffix notation renders them both self-checking.

Fig. 3.

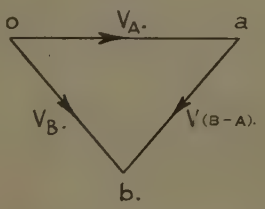

It will have been noticed that the suffix notation demands that for a vector to be completely defined it must have (i.) magnitude, (ii.) direction, (iii.) an arrowhead indicating sense, and (iv.) the arrowhead labelled in the suffix notation.

A slightly more complicated problem, requiring the vector equations and vector diagrams for the velocity and acceleration of the hammer of a piece of mechanism, will illustrate further the application of this notation and show how it renders the vector equations and diagrams self-checking.

Fig. 4 shows the link diagram of the mechanism from which it is required to find the velocity and acceleration of the hammer E relative to the bearing D.

Fig. 5 shows the velocity equation and the velocity diagram in which it will be seen that the suffixes and

Fig. 4.

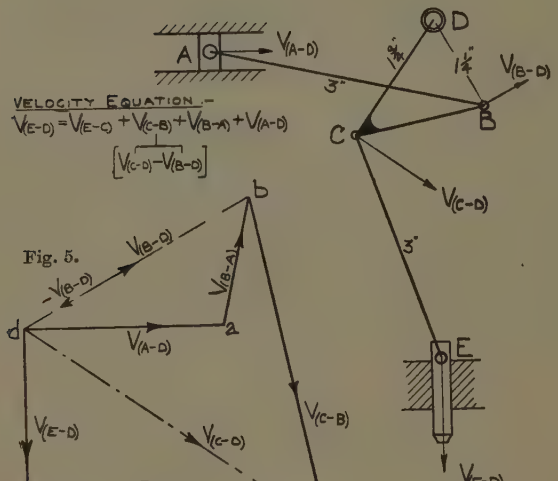

VELOCITY EQUATION :-

$$V_{(E-D)} = V_{(E-C)} + V_{(C-B)} + V_{(B-A)} + V_{(A-D)}$$

$$\left[V_{(C-D)} - V_{(B-D)}\right]$$

Fig. 5.

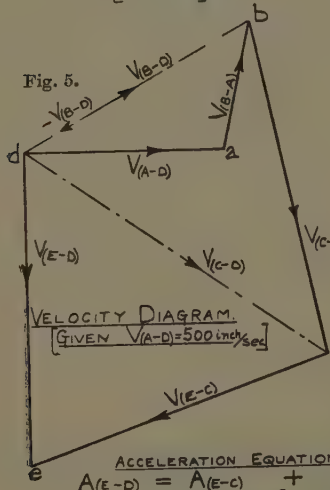

ACCELERATION EQUATION :-

$$A_{(E-D)} = A_{(E-C)} + A_{(C-B)} + A_{(B-A)} + A_{(A-D)}$$

$$\left[{}_cA_{(E-C)} + {}_tA_{(E-C)}\right] \left[\left[{}_cA_{(C-D)} + {}_tA_{(C-B)}\right] - \left[{}_cA_{(B-D)} + {}_tA_{(B-D)}\right]\right] \left[{}_cA_{(B-A)} + {}_tA_{(B-A)}\right]$$

Fig. 6.

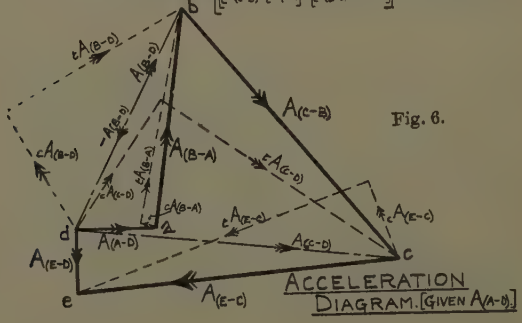

signs on the right-hand side of the equation sum up to balance those on the left, and that in the diagram the suffixes and signs of the vectors whose arrowheads follow round one way balance the sum of those following round the opposite way. The vector equation and vector diagram check themselves therefore merely by adding suffixes.

Fig. 6 shows the acceleration equation and the acceleration diagram for the mechanism. Centripetal and tangential components of acceleration ($_c$A and $_t$A respectively) have been shown both in the equation and in the diagram, and, as in the vector equation and diagram of fig. 5, it will be seen that the acceleration equation and diagram of fig. 6 are self-checking in the same way, merely by adding suffixes.

A further point regarding the suffixes and signs in the vector equations as set down in this notation is that they are found to obey the simple sign rule of algebra,

$$(a-b)=(-b+a)=-(-a+b).$$

One can therefore manipulate and manœuvre the signs and suffixes according to this simple rule.

This follows quite simply from a consideration of the two moving bodies, A and B of fig. 1, which give a vector equation,

$$V_A-V_B=V_{(A-B)}.$$

Multiplying this equation by -1 gives

$$-V_A+V_B=-V_{(A-B)}, \quad . \quad . \quad . \quad . \quad . \quad (a)$$

but

$$-V_A+V_B=V_B-V_A=V_{(B-A)}=V_{-(A-B)}. \quad . \quad . \quad (b)$$

Therefore, from equations (a) and (b)

$$-V_{(A-B)}=V_{-(A-B)}=V_{(B-A)},$$

showing that the sign in front of the vector can be taken in with the suffix and obeying the simple algebraic rule of signs ; so that equation (a) can be written

$$-V_A+V_B=-V_{(A-B)}=V_{-(A-B)}=V_{(B-A)}=V_B-V_A.$$

Any one of these equivalent forms can be used to manipulate and transform a vector equation into a desired alternative ; for instance, it will be seen that in

the velocity equation of fig. 5 the vector $V_{(C-B)}$, giving the velocity of C relative to B, is not known directly, and can only be found by use of the vectors $V_{(C-D)}$ and $V_{(B-D)}$. The suffixes and signs of these latter two vectors can be manipulated and arranged according to the two rules which the suffix notation enunciates, namely :

(i.) That the suffixes and signs on each side of a vector equation must add up to balance each other ; and

(ii.) That the sign in front of a vector can be taken in with the suffix of that vector to obey the simple algebraic rule of signs.

Thus :

$$\begin{aligned} V_{(C-B)} &= V_{(C-D)} + V_{(D-B)} \\ &= V_{(C-D)} + V_{-(B-D)} \\ &= V_{(C-D)} - V_{(B-D)}. \end{aligned}$$

The difference between the two vectors therefore gives $V_{(C-B)}$, and the vector diagram for this equation is seen as the triangle *bdc* in fig. 5.

A similar manipulation for the vector $A_{(C-B)}$ can be seen in the acceleration equation and diagram of fig. 6.

Nov. 1934.

LXXXV. *Internuclear Distance and Vibration Frequency in Diatomic Molecules.* *By* Prof. H. S. Allen, *M.A., D.Sc., F.R.S., and* A. K. Longair, *M.A., B.Sc., University of St. Andrews* *.

A diatomic molecule, or " di-atom " in the terminology of Douglas Clark †, is a molecular group, not necessarily stable in the chemical sense, where only two atoms are present. In this paper we are concerned with empirical relations between the internuclear distance and the fundamental frequency of vibration along the internuclear axis. We employ for the most part the notation and experimental values given in the valuable ' Report

* Communicated by the Authors.

† Douglas Clark, Phil. Mag. xix. p. 476 (1935).

on Band Spectra of Diatomic Molecules' by W. Jevons (1932), and denote by ω_e the frequency (in wave numbers) for vibrations of small amplitude about the equilibrium position, and by r_e the distance between the nuclei in this position. Considerable interest has been taken in the problem of finding a relation between these two quantities, and although no theoretical relation has been established, several attempts have been made to find an empirical formula to fit the numerical data found from the analysis of band spectra.

Birge * and Mecke † independently pointed out that large vibrational frequency is associated with small internuclear distance in different electronic states of a given molecule, and Mecke found that $\omega_0 r_0^2$ was approximately constant for the same molecule. Morse ‡ gave an empirical relation applicable to many states of a given molecule, and also to a number of different molecules :—

$\omega_0 r_0^3 \doteq$ const. (about 3000 Å.^{3}/cm. *i. e.*, $3{\cdot}000 \times 10^{-21}$ cm.^{2}).

He gives figures for 56 states of various molecules, and says that the above equation holds to within a probable error of ± 120 and a maximum deviation of 420. This is about due to the probable error in the recorded values of r_0, for if these values had a probable error of 1·3 per cent., then r_0 would be given to a probable error of 4 per cent. Morse, however, adds a footnote to the effect that:—

"It will be noticed that the molecules for which r_0(calc.) differs markedly from r_0(obs.) are the least symmetric molecules in the list $\left(i.e., \frac{M_1M_2}{M_1+M_2}\right.$ differs considerably from $\left.\frac{M_1+M_2}{4}\right)$. Mulliken has suggested that perhaps the rule holds accurately only where $M_1 \simeq M_2$. The calc. values for the perfectly symmetric molecules O_2, H_2, and N_2 give the most consistent check with experimental values. To apply the rule to very unsymmetric molecules, it may be necessary to introduce an 'unsymmetry factor' of the type $\left[\frac{4\,M_1M_2}{(M_1+M_2)^2}\right]^{\frac{1}{4}}$ into the term $r_0^3\omega_0$."

* Birge, Phys. Rev. (2) xxv. p. 240 (1925).
† Mecke, *Zeit. f. Physik*, xxxii. p. 823 (1925).
‡ Morse, Phys. Rev. (ii.) xxxiv. p. 57 (1929).

C. H. Douglas Clark * was led to examine Morse's results and modify his formula by introducing a factor depending on the "group number." He gave $\omega_e r_e^3 \sqrt{n} = k - k'$ where n is the group number and is defined as the number of "shared electrons," usually as $a+b$ where a is the number of valency electrons in the first atom and b is the number of the second; k is constant for a given molecular period, k' being the correction for an ionized molecule. The constant is characteristic of the period, and the latter is defined by the number of completed shells in the atoms. Thus in a KK molecule each atom has a completed K shell, while in a KM molecule one atom has a completed M shell and the other only a completed K shell.

Badger† has suggested the relation $k_0\ (r_e - d_{ij})^3 = 1{\cdot}86 \times 10^5$, where k_0 is the restoring force on a nucleus in dynes per unit displacement along the internuclear axis and is given by $\omega_e c = 2\pi \left(\frac{k_0}{\mu}\right)^{\frac{1}{2}}$, and d_{ij} is a constant characteristic of the molecular period and "might be called the distance of nearest approach of the two nuclei." Substituting for k_0, it will be found that Badger's formula reduces to $\omega_e (r_e - d_{ij})^{3/2} \sqrt{\mu} = \text{const.}$

Here μ is the "reduced mass" or "effective mass" of the molecule $= \dfrac{M_1 M_2}{M_1 + M_2}$ where M_1 and M_2 are the masses of the nuclei, or $\dfrac{A_1 A_2}{A_1 + A_2} \times 1{\cdot}6489 \times 10^{-24}$ gm. where A_1 and A_2 are the atomic weights of the atoms. c denotes the velocity of light.

The Isotope Effect.

The Theory of Isotopes has met with so much success in the interpretation of band spectra that there can be no possible doubt as to its validity in general. It is found that the vibrational frequency involves the effective mass of the molecule, for ω_e varies as $\mu^{-\frac{1}{2}}$, but the internuclear distance r_e is very nearly, though not quite, the same for isotopic molecules. The reason for the latter statement is that the extranuclear electric field does not depend to any marked extent on the masses of the nuclei. For

* Douglas Clark, Phil. Mag. (7) xviii.p. 459 (1934); Phys. Rev. xlvii. p. 238 (1935).

† Badger, Journ. of Chem. Phys. ii. no. 3 (1934).

example, consider the isotopes H_2 and HD. The values given by Urey and Teal * are such that r_e for H_2 is 0·7398 A. and for HD is 0·7398 A., while ω_e for H_2 is 4415·64 and for HD is 3824·99. These values fit in well with what has just been said, because $\frac{\omega_e(H_2)}{\omega_e(HD)}=1{\cdot}154$ and $\sqrt{\frac{\mu_{HD}}{\mu_{H_2}}}=1{\cdot}154$. It should, however, be noted that R. de L. Kronig † has predicted that "in certain cases the potential energy function for the vibration of the non-rotating molecule is not identical for the two isotopes, the internuclear distance being slightly smaller for the heavier isotope." An example of this has been found by W. W. Watson ‡ in the spectra of CaH and CaD. He concludes that "in corresponding states of these two molecules . . . the variation of the theoretical relations as a function of the mass of the molecule is entirely verified."

A modified Morse Formula involving reduced mass.

From the last paragraph, it will be seen that Douglas Clark's formula, from its very nature, cannot hold for the case of isotopes, because r_e and n remain constant and ω_e varies. In addition, although it fits very well for the KK period and quite well for the KL and KM periods, it is not so satisfactory beyond that. The present writers therefore sought for a formula, which, while fitting the facts almost as well as well as Clark's would also satisfy the isotope condition. It was thought that $\omega_e r_e^3\sqrt{\mu}=$ const. would be suitable, the constant being characteristic of the molecular period. The tables which follow show in the last column the results of calculating this expression, and these may be compared with those due to Morse and Clark given in the preceding columns. The value of Morse's constant is given in 10^{-21} cm.^{2}, and that of Clark in the same units. The molecules are arranged in order of increasing reduced mass, and only the ground states of non-hydride molecules are treated.

* Urey and Teal. Rev. Mod. Physics, vii. no. (1935).
† R. de L. Kronig, *Physica*, i. p. 617 (1934).
‡ W. W. Watson, Phys. Rev. xlvii. p. 27 (1935). See also Holst and Hulthén, 'Nature,' cxxxiii. p. 496 (1934).

In Douglas Clark's papers the mean error is calculated in terms of the internuclear distance r_e. In this paper it is done in terms of the period constant, so that the error will be approximately three times as great. For $\omega_e r_e^3\sqrt{n}$ the mean error, neglecting sign, for the table shown above is 2·66 per cent. For $\omega_e r_e^3\sqrt{\mu}$, excluding lithium, the error is 3·29 per cent., so that the agreement is hardly as good. (Lithium for this formula seems to fall into a different molecular class.) It seems highly probable that

KK Period.

Molecule.	State.	Reduced mass $\mu\times10^{24}$ gm.	ω_e cm.$^{-1}$	$r_e\times10^8$ cm.	Morse $r_e^3\omega_e\times10^{21}$ cm.^{2}	C. H. D. Clark $\omega_e r_e^3\sqrt{n}\times10^{21}$ cm.^{2}	$\omega_e r_e^3\sqrt{\mu}\times10^{23}$ gm.$^{\frac{1}{2}}$ cm.^{2}
Li_2	$^1\Sigma_g^+$	5·771	351·60	2·67	6·691	9·462	16·080
BeO ...	$^1\Sigma^+$	9·498	1487·45	1·328	3·485	9·860	10·750
C_2	$^3\Pi_u$	9·894	1641·55	1·308	3·671	10·390	11·550
BeF ...	$^2\Sigma^+$	10·07	1265·6	1·357	3·163	9·491	10·040
CN	$^2\Sigma^+$	10·67	2068·79	1·169	3·307	9·919	10·800
$B^{10}O$ ..	$^2\Sigma^+$	10·15	1940·49	1·199	3·344	10·030	10·650
$B^{11}O$ ...	$^2\Sigma^+$	10·75	1885·41	1·199	3·249	9·747	10·650
CO	$^1\Sigma^+$	11·31	2167·4	1·146	3·296	10·420	10·960
N_2	$^1\Sigma_g^+$	11·54	2359·60	1·094	3·089	9·770	10·495
NO	$^2\Pi_{reg}$	12·31	1906·5	1·146	2·882	9·519	10·070
O_2	$^3\Sigma_g^-$	13·19	1584·91	1·204	2·777	9·583	10·050

Mean of last column (excluding lithium)=10·602

both these errors are attributable to the error in measuring r_e. In the case of the BO isotopes, the fact that α (a coefficient necessary to calculate r_e) has not been derived from the spectroscopic measurements for $B^{10}O$ does not permit us to give an empirical value of r_e for this molecule. In the table r_e for $B^{10}O$ has been assumed equal to r_e for $B^{11}O$, firstly, because isotope theory predicts that such will be the case, and, secondly, because the respective values of r_0 for these two isotopes agree to within 1 in 3000, so that it is probable that the equilibrium internuclear distances will be very nearly equal. There seems to be some uncertainty as to the value of ω_e for O_2, while in the case of CO the value of α was assumed to be 0·026,

for the sake of getting r_e and bringing this molecule into line with the rest.

Other isotopic molecules for which data are available are H_2 and HD, and although they fall into a period of their own, it might be well to note here that $\omega_e r_e^3 \sqrt{\mu}$ gives constants 1·6295 and 1·629 for these molecules.

KL Period.

Molecule.	State.	Reduced mass $\mu \times 10^{-4}$ gm.	ω_e cm.$^{-1}$	$r_e \times 10^8$ cm.	Morse $r_e^3\omega_e \times 10^{21}$ cm.^{2}	C. H. D. Clark $\omega_e r^3 \sqrt{n} \times 10^{21}$ cm.^{2}	$\omega_e r_e^3 \sqrt{\mu} \times 10^{33}$ gm.$^{\frac{1}{2}}$ cm.^{2}
CP	$^2\Sigma$	14·27	1239	1·558	4·688	14·06	17·700
SiN.....	$^2\Sigma^+$	15·39	1151·68	1·568	4·441	13·32	17·430
PN	$^1\Sigma$	16·04	1337·24	1·487	4·399	13·91	17·620
AlO ...	$^2\Sigma^+$	16·56	977·0	1·614	4·107	12·32	16·710
SiO.....	$^1\Sigma$	16·80	1240·5	1·505	4·231	13·38	17·340
PO	$^2\Sigma$	17·41	1230·64	1·446	3·723	12·35	15·530
SO	$^3\Sigma$	17·6	1123·7	1·489	3·710	12·85	15·580

Mean of last column = 16·844

KM Period.

Molecule.	State.	Reduced mass $\mu \times 10^{24}$ gm.	ω_e cm.$^{-1}$	$r_e \times 10^8$ cm.	Morse $r_e^3\omega_e \times 10^{21}$ cm.^{2}	C. H. D. Clark $\omega_e r_e^3 \sqrt{n} \times 10^{21}$ cm.^{2}	$\omega_e r_e^3 \sqrt{\mu} \times 10^{33}$ gm.$^{\frac{1}{2}}$ cm.^{2}
CaF ...	$^2\Sigma$	21·99	586·7	(1·98)	4·554	13·67	21·350
TiO.....	$^3\Pi$	19·78	1008·12	1·617	4·261	13·47	18·950

Mean of last column = 20·150

In this case, as before, the errors are slightly in favour of Douglas Clark's formula, the actual deviations being 4·32 per cent. and 4·60 per cent. Many more molecules are included in this period than are given by Clark. The data for CP are given by Bärwald, Herzberg, and Herzberg *, those for PN by Curry, Herzberg, and Herzberg †,

* Barwald, Herzberg, and Herzberg, *Ann. d. Physik*, xx. (6) pp. 569–592 (1934).

† Curry, Herzberg, and Herzberg, *Zeit. f. Physik*, lxxxvi. (5–6) pp. 348–366 (1933).

and those for PO by A. K. Sen Gupta *. The other data are given by Jevons.

CaF is included, for although there is some doubt as to the value of r_e it is very probable that it is between 1·96 and 2·00 Å. † The errors are again in favour of Clark—0·7 per cent. against 6 per cent.

LL Period.

Molecule.	State.	Reduced mass $\mu\times10^{24}$ gm.	ω_e cm.$^{-1}$	$r_e\times10^{8}$ cm.	Morse $r_e^2\omega_e\times10^{21}$ cm.^{2}	C. H. D. Clark $\omega_e r_e^3\sqrt{n}\times10^{21}$ cm.	$\omega_e r_e^3\sqrt{\mu}\times10^{33}$ gm.$^{\frac{1}{2}}$ cm.^{2}
Na_2	$^1\Sigma_g^+$	18·96	159·23	3·070	4·606	6·513	19·830
P_2	$^1\Sigma_g^+$	25·58	779·3	1·88	5·180	16·38	26·200
S_2	$^3\Sigma_g^-$	26·45	727·4	1·840	4·530	15·71	23·300
Cl_2	$^1\Sigma_g^+$	28·86	564·9	1·983	4·408	16·49	23·680

Mean of last column = 23·253

This table shows a definite improvement on Clark's formula, having a mean error of only 5·2 per cent. in place of 26·0 per cent. It should be noted that the value of r_e used for sulphur is not that of Jevons, but one given by Badger ‡ in a recent publication, where he re-examined the work of Naudé and Christy, and concluded that $r_e = 1{\cdot}840$ instead of 1·603 Å.

MM Period.

Molecule.	State.	Reduced mass $\mu\times10^{24}$ gm.	ω_e cm^{-1}	$r_e\times10^{8}$ cm.	Morse $r_e^2\omega_e\times10^{21}$ cm.^{2}	C. H. D. Clark $\omega_e r_e^3\sqrt{n}\times10^{21}$ cm.^{2}	$\omega_e r_e^3\sqrt{\mu}\times10^{33}$ gm.$^{\frac{1}{2}}$ cm.^{2}
K_2	$^1\Sigma_g^+$	32·15	92·64	3·91	5·539	7·832	31·410
Br_2	$^1\Sigma_g^+$	65·89	323·86	2·28	3·838	14·36	31·150

Mean of last column = 31·280

* A. K. Sen Gupta, Proc. Phys. Soc, xlvii. p. 247 (1935).
† Harvey, Proc. Roy. Soc. A, cxxxiii. p. 336 (1931).
‡ Badger, Phys. Rev. xlvi. (11) pp. 1025-6 (Dec. 1934).

The above table is interesting. Potassium and bromine come at different ends of the period, diverge greatly in the values of μ, r_e, and ω_e, yet give constants with a mean error of only 0·83 per cent. for the new formula as compared with 29 per cent. for the other formula.

NN Period.

Molecule.	State.	Reduced mass $\mu\times10^{24}$ gm.	ω_e cm.$^{-1}$	$r_e\times10^8$ cm.	Morse $r_e^3\omega_e\times10^{21}$ cm.^{2}	C. H. D. Clark $\omega_e r_e^3\sqrt{n}\times10^{21}$ cm.^{2}	$\omega_e r_e^3\sqrt{\eta}\times10^{33}$ gm.$^{\frac{1}{2}}$ cm.^{2}
I_2	$^1\Sigma_g^+$	104·65	214·26	2·660	4·032	15·10	41·260
Te_2	$^3\Sigma$	105·1	250·9	2·85	5 805	20·11	59·520

In the last table we find that the only two molecules available for the NN period do not give consistent results. Reasons are given in the footnote on p. 1040 why it seems probable that I_2 is characteristic of the period, and in this connexion it should be mentioned that the constants for ICl are known, and give values for Morse's and Clark's formulæ of 4·742 and 17·74, and for the new formula 31·890.

Discussion of Results.

It will thus be seen that this formula extends rather farther than Clark's, although its agreement with observation is hardly as good as his in the earlier periods. In addition to this, however, it is of value because relations exist between the period constants which make it possible to forecast approximately constants which are not known from experimental data. Lack of data is, of course, a great handicap, but practically all molecules for which data are known have been included The mean values of the constant for each molecular period are as follows:—

KK period $=10\cdot602\times10^{-33}$ gm.$^{\frac{1}{2}}$ cm.^{2}
LL ,, $=23\cdot253$,, ,, ,,
MM ,, $=31\cdot280$,, ,, ,,

KL ,, $=16\cdot844$,, ,, ,,
KM ,, $=20\cdot150$,, ,, ,,

Now, if we calculate the mean of the constants for KK and LL, this comes to 16·927, which is in very close agreement with the value for KL, and the mean of KK and MM comes to 20·957, which is a good approximation to the value of KM. There is one other case of this—that of the molecules I_2, ICl, and Cl_2, representing the NN, LN, and LL periods. I_2 is 41·260 and Cl_2 23·680, giving a mean of 32·470, while the constant for ICl is 31·890.

It would seem, therefore, that molecules containing atoms in the same horizontal row of the periodic table of elements have the same constant, and that molecules formed of atoms in different rows have a constant which is the mean of the constants characteristic of the respective rows. Thus, if we have molecular periods XX, XY, and YY, then $XY=\frac{XX+YY}{2}$, and if we know any two of these, the third can be calculated.

Further, examination of the constants reveals the fact that these are approximately proportional to the *number of completed electronic shells in the molecule.* KK has two shells, LL four, KL three, etc., so we get

$$\text{KK} \quad \frac{10\cdot602}{2}=5\cdot301,$$

$$\text{LL} \quad \frac{23\cdot253}{4}=5\cdot813,$$

$$\text{MM} \quad \frac{31\cdot280}{6}=5\cdot213,$$

$$\text{KL} \quad \frac{16\cdot844}{3}=5\cdot615,$$

$$\text{KM} \quad \frac{20\cdot150}{4}=5\cdot040.$$

So that, in addition to the rule given above, it even seems possible to forecast the value of the constant simply from the number of completed shells in the molecule*.

* *The case of Iodine and Tellurium.*—These two elements of the same period give widely different constants, but both the rules suggested would seem to indicate that iodine is characteristic of the period, and that, provided the data for Te_2 are correct, the latter is unique in some respect. The constant for ICl points to I_2 being about 40·527, and as it has eight sheils, the rule given above indicates a value of about 42·500, while actually it is 41·260.

At first sight it would seem as if the proposed relation involving reduced mass were incompatible with that suggested by Douglas Clark which contains the group number n. In view of the fact that both relations are empirical and only approximate, it may be well to suspend judgment on this point till some theoretical basis for a relation between internuclear distance and frequency is obtained. As the cube of the internuclear distance is here involved, it is of interest to mention that according to Biltz the "zero atomic volume" for a large number of elements is given approximately by the equation $V=11{\cdot}3a$ c.c., where a is the ratio of the principal quantum number of the outermost orbit to the group number. In general this principal quantum number corresponds to the number of completed shells. Possibly instead of regarding the formula containing n and that containing μ as alternatives, it may be better to regard them as complementary, in the sense that the first deals with a progression from group to group, and the second with a progression from period to period.

Summary.

The relation between internuclear distance r_e and vibration frequency ω_e for diatomic molecules has been expressed by Morse in the formula $\omega_e r_e^3=\text{const.}$, and modified by Clark in the form $\omega_e r_e^3\sqrt{n}=\text{const.}$, where n is the "group number" and is equal to the number of "shared electrons," usually the sum of the valency electrons in the component atoms. Since such a formula fails to distinguish between isotopes, an attempt is made to find a modification which will fit in with isotope theory. The formula suggested is $\omega_e r_e^3\sqrt{\mu}=\text{const.}$, where μ is the reduced mass in gm. This constant varies for the molecular periods, and for most non-hydride molecules is found to be proportional to the number of completed shells. The average value for the KK period (molecules containing atoms each having a completed K shell) is found to be $10{\cdot}602\times10^{-33}$ gm.$^{\frac{1}{2}}$ cm.^{2}

LXXXVI. *Synthesis of X-ray Filtration Curves from Kramers's Emission Law.* *By* L. SILBERSTEIN, *Ph.D.* (Communication No 541 from the Kodak Research Laboratories *.)

IN a previous paper on continuous X-radiation † a method of determining the spectral composition $I_\lambda = f(\lambda)$ of such a radiation from its observed filtration or absorption curve, *i. e.*, from the total transmission $I(x)$ as a function of the filter thickness x, has been devised. This method was based upon the fact that all observed filtration curves can be approximately represented by the empirical formula

$$I(x) = I(o)e^{-Ax - B\sqrt{x}}, \quad . \quad . \quad . \quad . \quad . \quad (a)$$

where A, B are constant coefficients whose numerical values vary from case to case.

If $\mu = \mu(\lambda)$ be the absorption coefficient of the filter and, in particular, $\mu(o) = \alpha$, the integral equation

$$\int_0^\infty e^{-x\mu} f(\lambda) d\lambda = \int_a^\infty e^{-x\mu} f \frac{d\lambda}{d\mu} d\mu = I(x)$$

can in this case be rigorously solved (*l. c.* p. 385). If λ_0 be the wave-length for which the absorption coefficient of the filter is just A, *i. e.*,

$$\mu(\lambda_0) = A, \quad . \quad . \quad . \quad . \quad . \quad . \quad . \quad (b)$$

then the solution, representing the spectral curve of the analyzed radiation sample is

$$f(\lambda) = \frac{I_0 B}{2\sqrt{\pi}} \frac{e^{-B^2/4(\mu - A)}}{(\mu - A)^{3/2}} \cdot \frac{d\mu}{d\lambda}, \text{ for } \lambda \geqq \lambda_0, \quad . \quad . \quad (c)$$

and

$$f(\lambda) = 0 \text{ for } \lambda < \lambda_0. \quad . \quad . \quad . \quad . \quad . \quad (c')$$

In fine, the inferred spectral curve would start or have its *lower limit* at a wave-length λ_0 determined by (*b*), which in general turned out to differ considerably from the quantum limit

$$\frac{hc}{eV} = \frac{12{\cdot}34}{V}$$

* Communicated by the Eastman Kodak Research Laboratories.
† Phil. Mag. xv. pp. 375–394 (Feb. 1933).

(Å.U., if V be the potential in kilovolts). Thus, *e. g.*, for X-rays emitted by the tube Media at 100 kv. and with aluminium as filter (*l. c.* p. 392) $A=0{\cdot}92$ cm.$^{-1}$, which corresponds to $\lambda_0=0{\cdot}230$, while the quantum limit is $0{\cdot}123$. Similarly, at $V=50$ kv., we have had $A=3{\cdot}20$ cm.$^{-1}$ or $\lambda_0=0{\cdot}417$ instead of the quantum limit $0{\cdot}246$, and so on. In most cases, however, our limit λ_0 was too low.

It is true that this difference, especially in the latter case, has not seriously affected the ultimate spectral location of energy. Yet, since the said quantum limit has been excellently established by William Duane and others *, it has seemed desirable to modify our method so that the inferred spectral curve shall start precisely at the quantum limit; in other words, to prescribe the value of the coefficient A beforehand, in accordance with the given excitation potential, by claiming

$$A=\mu\left(\frac{12{\cdot}34}{V}\right), \quad . \quad . \quad . \quad . \quad . \quad . \quad (d)$$

and thus leaving only one adjustable parameter B. Thus, *e. g.*, for 100 kv., and aluminium filter, $A=\mu(0{\cdot}123)=0{\cdot}48$ cm.$^{-1}$, for 70 kv., $A=\mu(0{\cdot}176)=0{\cdot}63$, and so on.

The filtration curve, *i. e.*, a set of observed transmissions $I(x)$, being given, it is, in general, manifestly not in our power to represent it by formula (a) with A thus predetermined. Given that set of $I(x)$, the least square method, say, gives the best values of both A and B. But it is possible to obtain the desired end, to satisfy the quantum requirement (d), by a simple artifice, namely, by inquiring into the spectral composition not of the original radiation of total intensity $I(o)$, but of the radiation modified by a prefiltration through an appropriate layer a of the filter, *i. e.*, by trying to represent the observed transmissions, for $x>a$, by

$$I(x)=I(a)\,.\,e^{-A(x-a)-B\sqrt{x-a}} \quad . \quad . \quad . \quad . \quad . \quad (e)$$

Since the exponent is not linear in $x-a$, the values of A and B belonging to (e) will manifestly differ from those in (a), and will vary with the prefiltration a. It is thus

* Duane and his collaborators have not only confirmed the inverse proportionality of the λ-limit to the potential, but carefully determined the coefficient of proportionality and thus (using the known c/e) found $h=6{\cdot}556\,.\,10^{-27}$, agreeing remarkably well with the best determinations of Planck's constant.

possible to determine a so as to secure the desired quantic value of A. It remains to be seen, of course, whether the formula (e) thus constructed does actually represent the observed transmissions with fair accuracy. Such, however, turned out to be the case; nay, in all cases so far tried the representation was on the whole much closer than that given by the narrower formula (a).

The coefficients A, B being thus determined, to suit (d) and (e), the formula (c), with I (o) replaced by I (a), will give the spectral composition of the prefiltered radiation. To find the spectral curve of the original radiation it is enough to multiply each ordinate $f(\lambda)$ by the corresponding factor $e^{a\mu(\lambda)}$. The details concerning the whole procedure and the resulting spectral curves for numerous X-ray samples were given in the writer's internal report to these Laboratories. What interests us, however, in the present connexion is only one feature of those spectral curves, namely, the position λ_m of their peaks (max. f), and it will suffice to quote here from that report some relevant results concerning them.

The absorption coefficient μ_m of the filter corresponding to the wave-length λ_m locating the peak of the spectral curve is readily evaluated in terms of A, B, a. The potential V being given, and the filter, say aluminium or copper, being chosen, A is directly given by (d), while a and B are determined (alongside with I(a)) by suiting (e) to the observed transmissions. It may be worth while to mention how the "prefiltration" a is computed. Let x_1, x_2, x_3 be a triad of thicknesses and I_1, I_2, I_3 the corresponding observed transmissions. Put

$$c_{12}=\log\frac{I_1}{I_2}+A(x_1-x_2),$$

and let c_{23}, c_{31} have similar meanings. Then the equation for a is

$$c_{12}\sqrt{x_3-a}+c_{23}\sqrt{x_1-a}+c_{31}\sqrt{x_2-a}=0, \quad . \quad (f)$$

where, by the very definition of the numbers $c_{\iota\kappa}$,

$$c_{12}+c_{23}+c_{31}=0.$$

Owing to this identical relation, one root of the quadratic is obviously $a=\infty$, which leads, however, to the trivial result I(a)=0. Discarding this, and transferring a term and squaring, the terms in a^2 cancel, and the quadratic (f)

reduces to a linear equation for the only available root *. This can be written, symmetrically,

$$a=\frac{(x_1c_{23}^2+\text{etc.})^2-4(x_1x_2c_{23}^2c_{31}^2+\text{etc.}}{4c_{23}c_{31}c_{12}(x_1c_{23}+\text{etc.})},$$

where "etc." stands for "two more terms by cyclic permutation." With a thus determined the evaluation of B, along with I(a), is immediate. All coefficients entering into the expression for the spectral curve are thus numerically known and μ_m is then readily found; whence the required position λ_m of the maximum or peak of the spectral curve belonging to the original radiation.

In this manner λ_m has been determined for twelve samples of X-rays (emitted at various constant potentials, ranging from 60 to 150 kv.) from their aluminium- and copper-filtration curves as given by Taylor and Singer of the Washington Bureau of Standards ('Radiology,' xxii. pp. 445–460, April 1934, tables iii. and iv.). It will be enough to quote here the final results for six of these, with Cu as filter, the remaining six being of much the same nature. The auxiliary magnitudes a, B, etc. need not be quoted; it may suffice to mention that the "prefiltrations" a were all around 0·3 mm. of copper. The results are :—

V.....	100	110	120	130	140	150	kv.
$\lambda_0=\frac{12\cdot34}{V}$.	0·123	0·112	0·103	0·095	0·088	0·082	Å.U.
μ_m	10·02	8·23	7·73	6·87	5·69	4·91	cm.$^{-1}$
λ_m.....	0·176	0·162	0·157	0·150	0·138	0·130	Å.U.
$\therefore\ \lambda_m/\lambda_0=$	1·43	1·45	1·52	1·58	1·57	1·59	

What has seemed remarkable about these figures is that the ratio of the wave-length of maximum intensity I_λ to that of the starting-point of the spectral curve, though

* If the "quadratic" had actually two finite roots, it would give rise to an embarrassing situation, namely, leading to two different spectral curves, while by a known theorem the integral equation

$$\int_0^\infty e^{-x\mu}f(\lambda)d\lambda=\mathrm{I}(x)$$

can have but one (continuous) solution $f(\lambda)$ corresponding to any given I(x).

showing a slight systematic increase with potential does not differ much from

$$\frac{\lambda_m}{\lambda_0}=\frac{3}{2}.$$

Now, it has occurred to me that precisely such a ratio of the two wave-lengths would follow from my friend Kramers's theoretical emission law, derived by him in a masterly way from sound principles *, yet by no means sufficiently tested experimentally. In fact, Kramers's law for constant excitation potential V and a fixed current intensity can be written, in terms of frequencies ν,

$$I_\nu=C(\nu_0-\nu),\ h\nu_0=eV,$$

where C=const., for $\nu\leqq\nu_0$ of course, and $I_\nu=0$ for $\nu>\nu_0$, or in terms of λ, throwing a universal constant upon C,

$$f(\lambda)\equiv I_\lambda=\frac{C}{\lambda^2}\left(\frac{1}{\lambda_0}-\frac{1}{\lambda}\right),\ \lambda_0=\frac{12{\cdot}34}{V}. \quad . \quad . \quad (1)$$

The derivative $f'(\lambda)$ vanishes for

$$\frac{1}{\lambda^3}\left(\frac{3}{\lambda}-\frac{2}{\lambda_0}\right)=0.$$

One root, $\lambda=\infty$, expresses the obvious asymptotic tendency to the λ-axis, and the other gives the position of the peak, $\lambda_m=\frac{3}{2}\lambda_0$, as announced.

Thus, having, through the restriction (*d*) of the coefficient A, imposed upon our inferred spectral curves Kramers's starting-points λ_0, we have found from filtration data a location λ_m of their peaks agreeing closely enough with his law. And since the starting-point and the maximum of a continuous spectrum are certainly its two most characteristic features, it was likely that Kramers's law would hold also *in toto*. At any rate it has, in view of this coincidence, seemed well worth while to try to construct from Kramers's law a formula for the total transmissions, *i. e.*, the filtration curves, and to compare them with the observed ones. In doing so, I have, as a matter of fact, expected nothing but a bare parallelism between the calculated and the observed transmissions, but the results have greatly exceeded my expectations.

* Phil. Mag. xlvi. p. 836 (1923).

Let us, then, assume Kramers's law (1) for $f(\lambda)$ normalized so as to give

$$\int_{\lambda_0}^{\infty} f(\lambda)d\lambda = I(o) = 1.$$

This calls for $C = 2\lambda_0^2$. At the same time let us assume for μ the "cube-law"

$$\mu = \alpha + \beta\lambda^3, \quad \ldots\ldots \quad (2)$$

although it certainly disagrees with the table of observed $\mu(\lambda)$ for small λ, *e. g.*, for aluminium up to about 0·25 Å.U. Fortunately, it fits in well enough in the most relevant interval, from 0·3 to 1·2 or 1·3 Å.U. * It is, of course, well known that also this cube-law, originally empirical, has been derived by Kramers (*l. c.*) theoretically. While adopting the law (2), however, we need not commit ourselves as to any particular value of β. This coefficient, in fact, will be seen to drop out from the final result, leaving, apart from α, only $\mu(\lambda_0)$ which can be taken from the table of observed μ's.

The problem in hand thus amounts to evaluating the integral on the right hand of the equation

$$I(x) = \int_{\lambda_0}^{\infty} e^{-x\mu} f(\lambda)d\lambda = 2\lambda_0^2 e^{-\alpha x} \int_{\lambda_0}^{\infty} e^{-\beta x \lambda^3} \left(\frac{1}{\lambda_0 \lambda^2} - \frac{1}{\lambda^3} \right) d\lambda, \quad (3)$$

defining the transmission through a layer x of the filter.

Introduce a new integration variable through

$$\beta x \lambda^3 = u,$$

and write in particular

$$u_0 = x\beta\lambda_0^3 = x(\mu_0 - \alpha),$$

where $\mu_0 = \mu(\lambda_0)$. Then the integral in question will become

$$\frac{e^{\alpha x}}{2\lambda_0^2} I(x) = \frac{(\beta x)^{1/3}}{3\lambda_0} \int_{u_0}^{\infty} e^{-u} u^{-4/3} du - \frac{(\beta x)^{2/3}}{3} \int_{u_0}^{\infty} e^{-u} u^{-5/3} du,$$

and since $(\beta x)^{1/3} = \frac{1}{\lambda_0} u_0^{1/3}$,

* It is generally known that μ experiences a sudden jump at the K-limit, then another at the L-limit, and so on. But the K-limit, say for Al, is placed much beyond $\lambda = 1{\cdot}76$, where the absorption coefficient attains already the very high value $\mu = 200$ cm.$^{-1}$, so that the corresponding contributions, $f \cdot e^{-\mu x}$ are, even for 1 mm. of aluminium, evanescent, whether with or without the μ-jumps.

$$\tfrac{3}{2}e^{\alpha x}\,\mathrm{I}(x)=u_0^{1/3}\int_{u_0}^{\infty}e^{-u}\,u^{-4/3}\,du-u_0^{2/3}\int_{u_0}^{\infty}e^{-u}\,u^{-5/3}\,du.$$

To raise the exponents of u apply an integration by parts. Then

$$e^{\alpha x}\mathrm{I}(x)=e^{-u_0}-2u_0^{1/3}\int_{u_0}^{\infty}e^{-u}\,u^{-1/3}\,du+u_0^{2/3}\int_{u_0}^{\infty}e^{-u}\,u^{-2/3}\,du.$$

Here each of the two integrals is, so to speak, a truncated gamma function, $\Gamma(2/3)$ and $\Gamma(1/3)$ respectively, the missing parts being $\int_0^{u_0}$. Thus, and remembering that

$$u_0=(\mu_0-\alpha)x,$$

$$\mathrm{I}(x)=e^{-\mu_0 x}-e^{-\alpha x}\left\{2u_0^{1/3}\left[\Gamma\left(\frac{2}{3}\right)-\int_0^{u_0}e^{-u}\,u^{-1/3}\,du\right]\right.$$
$$\left.-u_0^{2/3}\left[\Gamma\left(\frac{1}{3}\right)-\int_0^{u}e^{-u}\,u^{-2/3}\,du\right]\right\}.$$

Now, by Legendre's table, to three decimal places,

$$2\,\Gamma(2/3)=2{\cdot}709\quad\text{and}\quad\Gamma(1/3)=2{\cdot}680,$$

while the two integrals are not reducible in finite form to known or tabulated functions. But they are, at any rate, functions of u_0 alone for which we will henceforth write u, and so, therefore, is also the whole bracketed factor of $e^{-\alpha x}$. Call it $\mathrm{R}(u)$, perhaps to commemorate Roentgen, defining it, that is, by

$$\mathrm{R}(u)=2{\cdot}709\,u^{1/3}-2{\cdot}680\,u^{2/3}-2\,u^{1/3}\int_0^{u}e^{-u}\,u^{-1/3}\,du$$
$$+u^{2/3}\int_0^{u}e^{-u}\,u^{-2/3}du\quad\ldots\quad(4)$$

Notice for the sequel that this function of u, a pure number, contains no adjustable parameters whatever, very much like the sine or cosine or what not.

Our synthetic formula for the transmission or the "filtration curve" of a continuous X-radiation emitted at a potential V will now become

$$\left.\begin{aligned}&\mathrm{I}(x)=e^{-\mu_0 x}-e^{-\alpha x}\,\mathrm{R}(u),\\ \text{where}\quad&\mu_0=\mu(\lambda_0)=\mu\left(\frac{12{\cdot}34}{\mathrm{V}}\right),\ \alpha=\mu(\lambda=0),\end{aligned}\right\}\quad\ldots\quad(5)$$

μ being the absorption coefficient of the filter and x its thickness. Manifestly, $R(u)=0$, so that $I(o)=1$, as it should be, the total incident intensity being taken as unit. The first term by itself is such as if the whole radiation were of one wave-length, λ_0, and the exponential in the second term is such as if it were of vanishing wave-length, but this is tempered by the factor $R(u)$ which takes care of the composite spectral quality of the radiation.

It remains to "legalize" the Roentgen function, that is to say, to study its properties and to construct its table. But before doing so, let us see what the transmission formula gives for small values of u. Consider $u^{1.3}$ as a magnitude of "the first order." The second term in (4) will be of the second order, the last two terms taken jointly will be shown presently to start with u^2 and thus give only terms of the sixth and higher orders; $\mu_0 x$ in (5) is itself of the third order (being but little greater than u, even at 100 kv.), and αx is still smaller, so that, up to terms of third order, $e^{-\mu_0 x}$ and $e^{-\alpha x} \doteqdot 1$, and we are left with

$$I(x)=1-2{\cdot}71(\mu_0-\alpha)^{1/3}\,x^{1/3}. \quad . \quad . \quad . \quad (5_0)$$

In words, the fraction absorbed by a (comparatively) thin layer of the filter is proportional to *the cube-root* of its thickness. Again, the derivative of $x^{1/3}$ being ∞ for $x=0$, $I'(o)=-\infty$ and thus also

$$\left(\frac{d \log I}{dx}\right)_0 = -\infty .$$

The initial gradient of our theoretical curves is negatively infinite. This is very reassuring. In fact, a characteristic property of all observed filtration curves is that they start sloping down precipitously (*cf.* especially Taylor and Singer's curves on fig. 1, p. 449, *loc. cit.*). To evaluate (5_0) numerically, take the case of X-rays emitted at $V=100$ kv. and filtered through aluminium. Then $\lambda_0=0{\cdot}123$, $\mu_0=0{\cdot}480$, while $\alpha=0{\cdot}15$ cm.$^{-1}$ (*cf. infra*), and (5_0) becomes

$$I(x)=1-1{\cdot}87x^{1/3},$$

where x is to be taken in cm. Obviously, this approximate formula cannot be used for thicknesses exceeding one-hundredth of a millimetre ($x^{1.3}=0{\cdot}1$). For 0·01 mm. it will give $I(x)=0{\cdot}81$, but no data are available for such thin filters. (For 1/2 mm. it gives the transmission

0·31, which does not much exceed Neeff's value 0·25 for a 100 kv. radiation from a Metalix tube. But Neeff's value is certainly much too low, and so is 0·31, since for $x=0{\cdot}05$ the higher terms can no longer be neglected.)

In order to compare our result with the best available observations, which do not extend below 1 mm. of aluminium, the complete formula (5) has to be used, and for this purpose the function $R(u)$ must be evaluated up to about $u=0{\cdot}75$, which will be seen to cover the whole range of practical applications.

The only way of accomplishing this is a power-series development of the two integrals appearing in the definition (4) of this function. Now, developing e^{-u} and integrating term by term,

$$S_1 \equiv \int_0 e^{-u} u^{-1/3} du = \frac{3}{2} u^{2/3} - \frac{3}{5} u^{5/3} + \frac{3}{16} u^{8/3} - \frac{1}{22} u^{11/3} + \ldots,$$

$$S_2 \equiv \int_0^u e^{-u} u^{-2/3} du = 3u^{1/3} - \frac{3}{4} u^{4/3} + \frac{3}{14} u^{7/3} - \frac{1}{20} u^{10/3} + \ldots,$$

so that the sum of the last two terms in (4) is

$$-2S_1 u^{1/3} + S_2 u^{2/3} = \frac{9}{20} u^2 - \frac{9}{56} u^3 + \frac{9}{220} u^4 \ldots,$$

the first powers of u having cancelled themselves, and the required series becomes

$$R(u) = 2{\cdot}709 u^{1/3} - 2{\cdot}680 u^{2/3} + \frac{9}{4}\left(\frac{u^2}{5} - \frac{u^3}{14} + \frac{u^4}{55} - \ldots\right). \quad (6)$$

The terms written down are sufficient for ensuring an accuracy to four decimal places for u-values up to 0·75. By means of this development a sufficiently dense set of R-values, to four decimal places, has been calculated and these, being rounded off to three figures, are collected in the following table.

The function attains a maximum, $R=0{\cdot}693$, at about $u=0{\cdot}14$, beyond which it soon acquires an almost constant gradient within the range of practical interest.

With the aid of this little table, sufficient even for 20 mm. of aluminium, say, and a 100 kv.-radiation, the application of formula (5) will be found to require but little labour.

Let us now see how it compares with the experimental findings.

It will be enough to consider *aluminium* as filter (for which the best transmission data are available) and X-rays emitted at several widely differing potentials.

u.	R.	Δ.	u.	R.	Δ.
0·00	0·000		0·14	$0{\cdot}692_8$	
·01	459	179	·15	692_6	
·02	538	45			
·03	583	31	0·20	0·684	—
·04	614	21	·25	·670	14
·05	635	16	·30	·649	21
·06	·651	12	·35	·627	22
·07	663	9	·40	·604	23
·08	672	7	·45	·580	24
			·50	·557	23
·09	0·679	5	·55	·534	23
·10	·684	4	·60	·511	22
·11	·688	2	·65	·489	21
·12	·690	2	·70	·468	20
·13	·692	1	·75	·448	

We need for this purpose the limiting value α of the absorption coefficient of aluminium. The lowest μ-value observed is *

$$\mu=0{\cdot}157 \text{ cm.}^{-1}, \text{ for } \lambda=0{\cdot}017 \text{ Å.U.}$$

In absence of better knowledge it seems reasonable to adopt, tentatively, for the limiting value,

$$\alpha=0{\cdot}15 \text{ cm.}^{-1}. \quad . \quad . \quad . \quad . \quad . \quad . \quad \text{(Al)}$$

Let us consider X-rays emitted at the constant potentials 60, 80, 100, and 110 kv. To these potentials correspond the λ_0-values 0·206, 0·154, 0·123, 0·112, and the absorption coefficients

$$\mu_0=0{\cdot}759,\ 0{\cdot}556,\ 0{\cdot}479,\ 0{\cdot}461 \text{ cm.}^{-1}.$$

Thus, by (5), the filtration curves of these X-radiations become with x taken in centimetres,

$$\text{I}(x)=e^{-0{\cdot}759\,x}-e^{-0{\cdot}15\,x}\,\text{R}(0{\cdot}609\,x), \ldots \quad \text{(60 kv.)}.$$
$$\text{I}(x)=e^{-0{\cdot}556\,x}-e^{-0{\cdot}15\,x}\,\text{R}(0{\cdot}406\,x), \ldots \quad \text{(80 kv.)}.$$
$$\text{I}(x)=e^{-0{\cdot}479\,x}-e^{-0{\cdot}15\,x}\,\text{R}(0{\cdot}329\,x), \ldots \quad \text{(100 kv.)}.$$
$$\text{I}(x)=e^{-0{\cdot}461\,x}-e^{-0{\cdot}15\,x}\,\text{R}(0{\cdot}311\,x). \ldots \quad \text{(110 kv.)}.$$

* According to a table given in A. H. Compton's 'X-Rays and Electrons,' New York, 1928, p. 185,—with 2·70 as the density of Al. (That table gives the mass-absorption coefficients, *i. e.*, μ/density.)

These formulæ, aided by the R-table, give for 1, 2, etc., up to 20 mm. of aluminium the percentage transmissions, 100 I(x), arrayed in the columns superscribed "calc." of the following table. The adjacent columns, "obs.", contain the percentage transmissions of "general X-radiation" which has traversed 1·29 mm. of cerium glass (tube wall), as determined ionometrically by Taylor and Singer *.

The graphs (continuous curves; "filtration curves") corresponding to the calculated transmissions for the

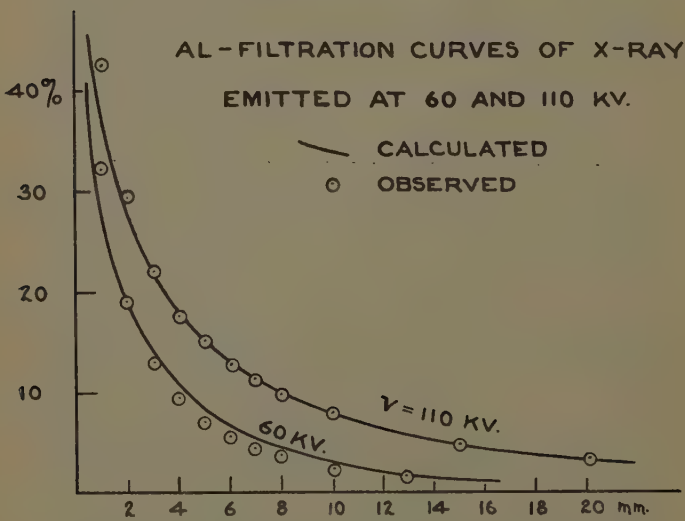

two extreme X-radiations, namely, those emitted at 60 and 110 kv., are drawn in the attached figure. The observed transmissions are marked by eyelets. The agreement of theory and experiment is better than one would ever be entitled to expect, in view of the fact that the calculated values refer to X-rays as produced at the anticathode, inside the tube, while the observed ones belong to radiation that has traversed 1·29 mm.

* 'Radiology,' xxii. 1934, p. 45, table iii. Here, by the way, the superscription of the 1st column "copperfilter" is an obvious misprint for "aluminium filter."

Comparison of calc. and obs. Transmissions through Al.

Al filter in mm.	60 kv.			80 kv.			100 kv.			110 kv.		
	calc.	obs.	Δ.	calc.	obs.	Δ.	calc.	obs.	Δ.	calc.	obs.	Δ.
1	28·5	32·1	−3·6	34·0	36·0	−2·0	37·0	40·0	−3·4	37·8	42·4	−4·6
2	18·9	19·0	−0·1	24·2	22·9	+1·3	27·0	27·2	−0·2	27·8	29·4	−1·6
3	13·9	12·9	+1·0	18·6	16·5	+2·1	21·3	20·4	+0·9	22·0	22·4	−0·4
4	10·7	9·3	+1·4	15·0	12·6	+2·4	17·4	16·2	+1·2	18·1	18·0	+0·1
5	8·4	7·0	+1·4	12·3	10·1	+2·2	14·7	13·4	+1·3	15·2	15·0	+0·2
6	6·7	5·4	+1·3	10·3	8·3	+2·0	12·5	11·3	+1·2	13·1	12·9	+0·2
7	5·3	4·4	0·9	8·9	6·9	+2·0	10·6	9·8	+0·8	11·3	11·2	+0·1
8	4·6	3·6	1·0	7·6	5·8	+1·8	9·4	8·6	+0·8	9·8	9·9	−0·1
10	3·2	2·4	0·8	5·5	4·4	+1·1	7·1	6·6	+0·5	7·7	7·9	−0·2
15	1·0	1·2	−0·2	2·9	2·4	+0·5	4·1	4·1	0·0	4·4	4·8	−0·4
20	—	—	—	1·4	1·4	0·0	2·4	2·6	−0·2	2·7	3·2	−0·5

of cerium glass, and again, in view of the circumstance that our $I(x)$-values are proportional to the total intensity or energy of the transmitted X-rays, whereas the observed $I(x)$ have been obtained ionometrically, and at least some slight deviations from proportionality of the ionometric and the energetic I-values can be expected. Taylor and Singer think that 1·29 mm. of cerium glass is "equivalent" to about 1 mm. of aluminium. No such "equivalence," of course, in all respects can have place. According to our formula (5) the effect of the tube wall can in this case be "equivalent" to much less than 1 mm. of Al, as the reader may easily verify. It is quite possible that 1·29 mm. of cerium glass absorb, *in toto*, as much as 1 mm. of aluminium, but the deformation of the spectral curve (spectral composition) of the X-rays by such layers of glass and of aluminium are, no doubt, very different from each other. If the absorption coefficient $\mu(\lambda)$ of cerium glass for various λ were known, the effect of the tube walls could readily be computed by our formula (5). So far as I know, however, no such determinations have been made. But the calculated transmissions of the last table, even as they stand, show—apart from hair splitting niceties—a remarkably close agreement with the observed ones.

The moral of this result is twofold. *First*, there is no longer any need of determining the filtration curves by actual measurements (some of the sets of Taylor cost several months of hard work), because they can be reliably calculated by means of (5), provided the tube walls are as thin as (or, *a fortiori*, thinner than) those indicated. *Second*, the good agreement shown by our last table, and still more by the graph, can be considered as a very convincing proof of the correctness of Kramers's radiation law. Thus also the "filtration curves" become wholly superfluous. Their purpose was only to serve as a (very indirect) means of qualifying an X-radiation, but this is certainly done much better, directly, by the spectral composition itself as expressed by Kramers's formula with $\lambda_0 = 12{\cdot}34/V$, and—if need be—by computing the corrections of I_λ due to absorption in the tube wall.

Rochester, N.Y.
September 29, 1934.

LXXXVII. *Concerning the Meaning of Time in Lorentz Tranformation.* *By* F. Tavani *.

IN the generalized Lorentz transformation for the case of the origin moving in a space of two dimensions there appear two expressions of time†, for the case of the origin moving in a space of three dimensions there are three expressions of time. The question arises whether to these three expressions corresponds one and same entity. It is a new problem in the theory of relativity, quite unforeseen before the idea of extending the theory to the case of the origin moving in a space of two or three dimensions. It demands a solution, and the consequences whatever they may be, must be applied to the theory. The solution is at the same time strictly connected with the meaning of time in the original Lorentz transformation. In this, time is a coordinate of an event, and the dimension in which such coordinate is determined is considered as a fourth dimension. If the dimension along which the origin moves is indicated with the axis X of the frame the expression of time is $\beta_1\left(t_1' + \frac{u_1 X'}{c^2}\right)$. This time we call t_1. In the generalized transformation the origin moves also along the axis Y, and for this motion we have another expression of time : $t_2 = \beta_2\left(t_2' + \frac{u_2 Y'}{c^2}\right)$ ‡. They are both coordinates of the same event, referred to a frame whose origin moves in a space of two dimensions, and their values are, in general, different. In fact, in order that a clock may indicate the time when attached to a moving frame it is necessary that its hands should have a motion uniform relatively to the origin of the frame—that is to say, that the centre of the clock should be at rest relatively to the frame, and for this reason it should have the same motion of the origin itself.

In the original Lorentz transformation the origin moves along the axis X, therefore the clock is also supposed to

* Communicated by the Author.

† F. Tavani, "Generalization of Lorentz Transformation," Phil. Mag. xviii. p. 191 (July 1934).

‡ Phil. Mag. *loc. cit.*

move along X. In the generalized transformation the origin moves, simultaneously along X and Y therefore the centre of the clock must move also along X and Y. So along these two axes the hands of the clock, besides having a motion of their own uniform relatively to the centre, possess also the motion of the centre or, what is the same, of the origin along the two said axes, and since the two motions of the origin along them are in general different one from the other, so also the times indicated by the clocks are in general different, and they would appear so if they could be observed. Therefore

$$t_1=\beta_1\left(t_1'+\frac{Xu_1}{c^2}\right) \text{ is different from } t_2=\beta_2\left(t_2'+\frac{Yu_2}{c^2}\right),$$

and to the same instant of the motion of the origin along its path would correspond on the clock of time t_1 an indication different from that given by the clock of time, t_2. If instead of instants we consider intervals of time, to an interval of the time of motion of the origin correspond two equal intervals, one of time t_1 and the other of time t_2. In conformity with the view of relativity about assuming time as a fourth dimension in determining an event, this fourth dimension is the time of a clock moving with the origin along the axis of X—that is to say, the time indicated with t_1—and if the origin moves in a space of two dimensions, then two elementary motions of the clock equal to those of the origin are given, and t_2 acts as a coordinate in a space of five dimensions. If the origin moves in a space of three dimensions the different times of its motion are t_1, t_2, t_3, corresponding to the motion of the origin along the three axes X, Y, Z, and an event is determined by six coordinates taken in a space of six dimensions.

Whenever the motion of a point P is referred to a moving frame, whose origin moves in a space of three dimensions, the time of the motion of P referred to the axis X is t_1, that of the motion of P referred to the axis Y is t_2, and that of the motion referred to Z is t_3; and it is on time thus classified that depend the quantities, functions of time, whose components are distributed along the reference axes.

In the generalization of Lorentz transformation, as well as in this note which is a consequence of it, we have considered O′ as the origin moving in a space of two

dimensions ; the whole reasoning remains valid when the rôle between the two origins O and O′ is inverted.

61 Burton Road,
London, S.W. 9.

LXXXVIII. *Notices respecting New Books.*

Reports on Progress in Physics. [Pp. 371]. Published by the Physical Society of London and printed at the University Press, Cambridge, 1934. (Price to non-Fellows of the Society, 12*s.* 6*d.* net.)

THIS is the first volume of a new series. It contains no editorial preface ; but we gather from the first contributor (Prof. Temple) that the series is intended to consist of *annual* reports of contemporary progress in Physics. It is obvious, however, that contributors could not start off in empty space (or space-time) ; it appears to have been left to individuals to introduce their subject as best they might, so as to indicate the initial position from which developments have taken place. An editorial preface would have been a great advantage, indicating the scope of the present volume. One contributor states definitely that his report covers the years 1932–33 ; but he is singular in that respect, and some extend into 1934. It would have been better to call the present an Introductory Volume instead of labelling it 1934, since it is the year that is being reported on that the reader will specially desire to know. The question whether an index (particularly a *name* index) should be provided may also be borne in mind, especially for those who wish to turn up important references to a particular author's publications. Such questions as these will no doubt be satisfactorily dealt with by the editorial committee.

Professor G. Temple leads off with an expository and critical account of the quantum theory and wave-mechanics. He frankly admits that there is really no compelling argument for identifying the values obtained in actual experiments with the average values obtained by the quantum theory. However, we may say (what he himself says of Eddington's special form) that the theory is so promising and fascinating in its unification of philosophical principles that one naturally hopes for further developments in this field. The whole paper should be read by every physics student (and teacher).

The second article, by G. C. McVittie, travels amongst the spiral nebulæ and the question of the possible expansion of the Universe. Here speculation is less trammelled by hard facts ; out of the 75,000 recorded nebulæ only ten are able

to give evidence. The outcome appears to be that it is impossible at the present stage to discriminate between the relativistic and non-relativistic interpretations of the expansion.

Later in the volume, E. N. da C. Andrade brings us back to the almost infinitely small in the "physics of the atom," in connexion with which 140 published papers are discussed. This is a valuable contribution, since it deals with the experimental data in a critical manner.

Professor J. C. McLennan discusses modern work, which is revolutionizing our knowledge of the electrical properties of bodies at exceedingly low temperatures.

We turn next to what may be called laboratory physics, dealing mainly with methods of measurement. In thirty-nine pages E. G. Richardson summarizes the work of two years on such subjects as supersonics, piano playing, conical diaphragms, vibrations in fluids, acoustic impedance, and subjective aspects of sound. Dr. A. Ferguson discusses recent attempts at facilitating the reduction of surface-tension measurements. Thirty pages are devoted to reports on spectroscopy (H. Dingle, R. W. Pearse, E. Gwynne Jones, C. V. Jackson, and A. Hunter); another thirty to optics (T. Smith, J. S. Anderson, J. Guild, and H. F. Buckley); forty pages to X-rays by the X-ray staff of the National Physical Laboratory (General Editor, G. W. C. Kaye); separate articles are given on electric and magnetic measurements (L. Hartshorn) and on heat (J. H. Awbery). We notice in the last of these papers a much needed criticism of the current misuse (in certain quarters) of the term *free energy*.

We regret that it is quite impossible to epitomize these summaries. The whole work appears to have been very well done, and the volume should be in every physicist's possession.

Atomic Structure and Spectral Lines. By ARNOLD SOMMERFELD. 3rd English Edition, translated from the 5th German Edition by H. L. BROSE.—Vol. I. [Pp. xi+675.[(Methuen: London, 1934. Price 35*s*.)

SOMMERFELD'S 'Atombau' has been accepted since its first appearance (1919) as a masterly exposition of quantum atomic physics, and the successive editions, the latest being that of 1931, have reflected faithfully the course of subsequent progress. As a text-book, 'Atombau' is almost in a class by itself; it has been invaluable to the specialist research worker no less than to the student. No small part of the advance that has been made has been due to Sommerfeld himself; but the great service conferred on physicists by Sommerfeld in his book has been through the lucidity of his exposition of the subject as a whole—a lucidity by no means

common to all those who have shared in making the advances of the last fifteen years.

The rapidity of advance soon made the previous English edition (based on the 1922 German edition) too out of date for those requiring the latest accounts, and the present edition will be welcome to all those physicists who find the reading of German a laborious task. This volume deals with the earlier phase of the quantum theory. The stage has been reached at which it may reasonably be expected that it will have a long useful life. It is now, perhaps, seldom fully appreciated how far it was possible to go on the basis of the Rutherford-Bohr theory with the addition of the conception of the spinning electron. The simplicity of the postulates, and the remarkable range of successful correlation to which they led are such that it seems doubtful whether the older mode of presentation can be conveniently abandoned. In the earlier editions of 'Atombau' there was, perhaps, a tendency to stress the numerical triumphs rather than the inherent inconsistencies of the first form of the quantum theory. In this volume the weaknesses and gaps in the scheme are pointed out as they occur, results are given in their corrected form, and where necessary forward reference is made to a second volume. This volume (which will be a revised and enlarged version of the 'Wellenmechanischer Ergänzungsband') will provide the necessary supplement to complete the presentation as a whole.

The present volume consists of nine chapters, dealing with introductory facts, the hydrogen spectrum, the natural system of elements, X-ray spectra, the theory of fine structure, series laws, complex structure of series terms and band spectra. As compared with the 1924 German edition, the first part is somewhat shortened. Hamiltonian methods have been incorporated in the text, and the treatment of multiplets and complex spectra is much more complete, full use having been made of the conception of the spinning electron and of the Pauli principle. It is unnecessary to refer in detail to the treatment of the various topics. It will be sufficient to remark on the detailed and comprehensive, but always straightforward, discussion of the intricacies of term structure arising from many electron configurations.

In the English edition there has been added a section on hyperfine structure by E. Gwynne-Jones, and a short appendix on recent work on cosmic rays, nuclear disintegration, and heavy hydrogen by the translator.

The index is somewhat inadequate for a book of this character, and it contains the surprising item, "differentiation of X-rays," apparently investigated by the Braggs.

The translator has carried out a formidable task with uniform excellence, and both he and the publishers are to be

congratulated on making this work available to a wider circle of physicists.

Thermionic Emission. By A. L. Reimann. [Pp. 324+xi+figs. 64.] (Chapman and Hall. Price 21*s.*)

The subject of thermionic emission has become of increasingly great practical importance during the past twenty years, during which time a vast amount of experimental and theoretical work has been carried out all over the world.

In view of the special practical applications of the subject it is by no means amiss that a book should be written by a member of the research staff of the General Electric Company.

Other *résumés* have, of course, been produced in recent years—a brief but nevertheless valuable report, for example, was published in 1932 under the heading 'Thermionic Emission' by Dr. W. S. Stiles—a special report of the Department of Scientific and Industrial Research. This valuable little book summarized our knowledge up to 1930. It is of interest to note—as a rough indication of the rate of advance—that, whereas some 310 original papers were included in the earlier bibliography, Dr. Reimann lists more than 360. Of the fifty-five new papers (post 1930) cited in the new book it is to be noticed that only ten have appeared in English periodicals—the majority being of American origin. It is interesting, too, to note that the latest paper cited in the chapter on "modern theory" is dated 1932.

The author in his preface draws attention to the considerable advances made during the past fifteen years in our knowledge of thermionic phenomena, and refers to the "quite fundamental nature" of the advances on the theoretical side which have emerged from quantum statistics and wave mechanics. The main stress in this book, however, is definitely on the experimental side.

Leading off with a general survey of just a few pages, Chapters II. and III. follow, dealing with electron emission from clean and contaminated metals respectively. Chapter IV. is devoted to oxide cathodes, and Chapter V. to modern theory of electron emission. So far as the main body of the book is concerned this is the last section, but a final short chapter has been added on the emission of ions from electrolytes and metals.

Some may find the style a little too free and easy in places, and possibly some of the descriptive sections tiresome in their length, but taken as a whole the book is to be recommended. It should be of special value to those interested in the special thermionic properties of clean, coated, and contaminated metal surfaces.

[*The Editors do not hold themselves responsible for the views expressed by their correspondents.*]